

Aus der Abteilung Humangenetik
(Prof. Dr. med. Dr. h. c. W. Engel)
im Zentrum Hygiene und Humangenetik
der Medizinischen Fakultät der Universität Göttingen

The molecular role of the heat shock protein family110 (HSP110)

Inaugural-Dissertation
zur Erlangung des Doktorgrades
der Medizinischen Fakultät
der Georg-August-Universität zu Göttingen

vorgelegt von
Belal A. Mohamed
aus
Kalyoubia, Ägypten

Göttingen 2012

Dekan : Prof. Dr. rer. nat. H. K. Kroemer

I. Berichterstatter : Prof. Dr. sc. agr. Adham

II. Berichterstatter : Prof. Dr. rer. nat. mansouri

III. Berichterstatter : Prof. Dr. med. Oppermann

Tag der mündlichen Prüfung : 11/12/2012

Table of Contents

1. Introduction	
1.1. The heat shock proteins (HSPs).....	1
1.2. HSP110 family.....	2
1.3. Structure of HSP110 family.....	3
1.4. The co-chaperoning activity of HSP110 family.....	4
1.5. Molecular function of HSP110 family.....	5
1.5.1. Molecular function of HSPA4.....	6
1.5.2. Molecular function of HSPA4L.....	7
1.5.3. Molecular function of HSPH1.....	8
1.6. Aims of the study.....	8
2. Materials and Methods.....	10
3. Results and Discussion.....	13
3.1. Consequences of HSPA4 ablation on male germ cells development.....	13
3.2. Cardioprotective role of HSPA4.....	18
3.3. Elucidating the consequence of cardiac HSPA4 overexpression.....	23
3.3.1. Generation of recombinant <i>Hspa4</i> adenovirus (Ad- <i>Hspa4</i>).....	23
3.3.2. Generation of cardiac specific <i>Hspa4</i> transgenic mouse model.....	26
3.4. Simultaneous deletion of murine <i>Hspa4l</i> and <i>Hspa4</i> genes causes pulmonary immaturity and early neonatal lethality in mouse.....	27
3.5. Generation of <i>Hsph1</i> conditional KO and <i>Hspa4/Hsph1</i> DKO mice.....	41
4. References.....	44
5. Publications.....	61
5.1. Publication I.....	62
5.2. Publication II.....	75
6. List of Publications.....	86

1. Introduction

1. 1. The heat shock proteins (HSPs)

HSPs were first identified in *Drosophila* in 1962 as proteins that accumulate in the cell after exposure to elevated temperature (Ritossa, 1962). Later studies demonstrated that HSPs are a conserved set of proteins that are expressed in all prokaryotes and eukaryotes (Ritossa, 1996). The HSPs are a set of highly conserved proteins that are expressed constitutively and/or induced in response to a wide variety of stress conditions (Collins and Hightower, 1982; Khandjian and Türlér, 1983; Li GC, 1985; Li GC and Laszlo, 1985; La Thangue and Latchman, 1988; Norton PM and Latchman, 1989). Induction of HSPs is mediated by the nuclear translocation of heat shock transcription factors (HSFs) and subsequent binding to heat shock elements (HSEs) in the promoter regions of *Hsp* genes (Tonkiss and Calderwood, 2005; Morimoto, 2011).

HSPs act as molecular chaperones by assisting the folding of nascent and misfolded proteins thereby preventing their aggregation (Hartl, 1991; Gething and Sambrook, 1992). Protein quality control (PQC) in the cells facilitates proper folding of nascent proteins and refolding of misfolded proteins by molecular chaperones and promotes degradation of aggregated proteins by ubiquitin-proteasome system (UPS) and to less extent by autophagy (Wang X et al., 2008). Functional defects in chaperones result in an accumulation of misfolded proteins (Patterson, 2006). Recent reports demonstrated that increased accumulation of misfolded proteins above the threshold levels impairs the functional capacity of the proteasome leading to proteasome functional insufficiency (PFI), which is thought to be involved in up to half of all human morbidities (Thomas et

al., 1995; Bradbury, 2003; Bennett et al., 2005). These diseases include Amyotrophic Lateral Sclerosis (ALS), Alzheimer's, Huntington's, Parkinson's disease and cardiomyopathy (Ross, 1995; Taylor et al., 2002; Wong et al., 2002; Bates, 2003; Berke and Paulson, 2003; Caughey and Lansbury, 2003; Kostin et al., 2003; Nussbaum and Ellis, 2003; Weekes et al., 2003; Ross and Pickart, 2004; Sanbe et al., 2004; Selkoe, 2004; Powell, 2006; Tsukamoto et al., 2006; Birks et al., 2008).

According to molecular mass and degree of structural homology, mammalian HSPs are classified into several families including: small HSPs (25-28 kDa), HSP40 (40kDa), HSP60, HSP70 (68-80 kDa), HSP90 (83-99 kDa), and HSP110 (110 kDa) (Tomasovic et al., 1983; Welch et al., 1983; Li GC and Laszlo, 1985; Vos et al., 2008).

1. 2. HSP110 family

HSP110 family members have been cloned from a wide range of organisms including human, mouse, Arabidopsis and yeast (Foltz et al., 1993; Mukai et al., 1993; Morozov et al., 1995; Yasuda et al., 1995; Kojima et al., 1996; Storozhenko et al., 1996; Kaneko et al., 1997a, b; Mauk et al., 1997).

The constitutive expression and stress inducibility of HSP110 family members in a wide variety of cell types leads to suggest that the HSP110 members play a protective role not only in stressed cells but also in unstressed through helping in successful folding, assembly, intracellular localization, secretion, regulation, and degradation of other proteins (Levinson et al., 1980; Landry et al., 1982; Gething, 1997).

1. 3. Structure of HSP110 family

The HSP110 sequence was found to share an around 30-33% amino acid homology with members of the HSP70 family, most of which occurs in the conserved ATP-binding domain of these molecules (Lee-Yoon et al., 1995). HSP110 family contains four domains: the highly conserved N-terminal nucleotide-binding domain (NBD) (domain A in Fig. 1), which binds ATP/ADP and mediates ATP hydrolysis, the central β -sheet peptide binding domain (PBD) that binds the peptide substrate (domain B in Fig. 1), the loop domain (domain L in Fig. 1) and the C-terminal α -helix domain that regulates substrate binding (domain H in Fig. 1). The C-terminal domain exhibits a high degree of sequence homology among HSP110 members, thereby providing features specific for this family (McCarty et al., 1995; Fung et al., 1996; Zhu et al., 1996).

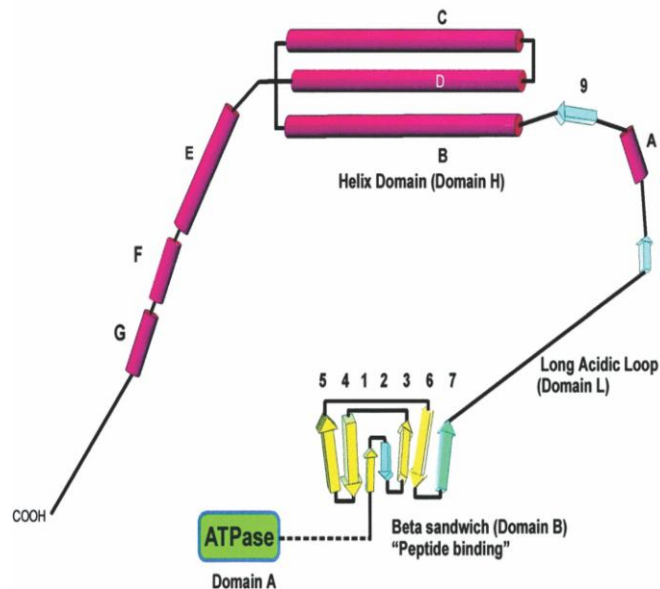


Figure 1. Predicted folding pattern for HSP110. HSP110 family contains four domains: the N-terminal ATPase (domain A), the central β -sheet peptide binding domain (PBD) (domain B), the loop domain (domain L) and the C-terminal α -helix domain (domain H) (adapted from Oh et al., 1999, pp. 15714).

1. 4. The co-chaperoning activity of HSP110 family

Biochemical analyses illustrated that HSP110 family serves as co-chaperone of mammalian and yeast HSP70 chaperones, where they act as nucleotide exchange factors (NEF) during the ATP-hydrolysis cycle (Steel et al., 2004; Dragovic et al., 2006; Raviol et al., 2006; Shaner et al., 2006; Polier et al., 2008). Binding of newly synthesized polypeptides to HSP70 chaperones and the subsequent release of folded proteins is regulated by continuous cycles of adenosine triphosphate (ATP) hydrolysis and the exchange adenosine diphosphate (ADP) for ATP (Fig. 2). It is believed that the chaperones containing HSP70, HSP40 and HSP110 proteins represent the major protein folding machinery in the eukaryotic cytosol (Polier et al., 2008). In the ATP-bound state, PBD of HSP70 chaperone binds to polypeptides with low affinity. However, ATP hydrolysis to ADP by HSP40 co-chaperone leads to conformational changes that result in high affinity substrate binding by HSP70 (Fig. 2, step 1). To complete the protein folding cycle, binding of HSP110 to HSP70 in the ADP-state stimulates the release of ADP (Fig. 2, step 2). Subsequent binding of ATP induces the dissociation of HSP70-HSP110 complexes and the folded protein substrate is released (Fig. 2, step 3). HSP70 in the ATP-bound state will be ready for another cycle of protein folding (Dragovic et al., 2006; Raviol et al., 2006; Polier et al., 2008; Schuermann et al., 2008).

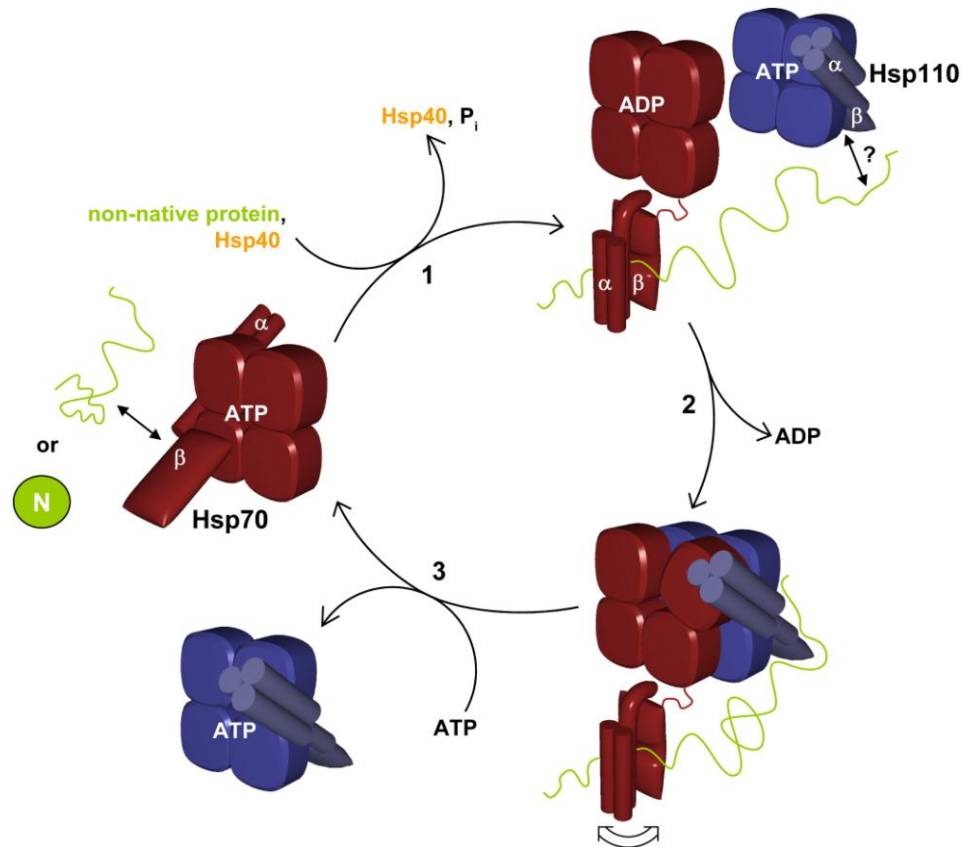


Figure 2. Schematic representation of the collaboration between HSPs for proper protein folding. HSP70 in ATP-bound state (left side). HSP40 facilitates ATP hydrolysis and subsequent binding of HSP70 to unfolded protein substrate (Step 1). HSP70 in ADP-bound state is recognized by HSP110, which binds to HSP70 mediating liberation of ADP from HSP70 (Step 2). Finally, upon binding of ATP to HSP70, the HSP70-HSP110 complex dissociates and the folded protein substrate is released (step 3). HSP70 will be ready for another cycle of folding (adapted from Polier et al., 2008, pp. 1077).

1. 5. Molecular function of HSP110 family

The HSP110 gene family includes two genes in *Saccharomyces cerevisiae* known as *Sse1* and *Sse2* (Mukai, et al., 1993; Shirayama et al., 1993) and four genes in the mammalian genome, namely *Hspa4/Apg2*, *Hspa4l/Apg1*, *Hsph1/Hsp105* and *Hyou1/Grp175/orp150* (Lee-Yoon et al., 1995; Yasuda et al., 1995; Kojima et al., 1996; Kaneko et al., 1997a, b; Nonoguchi et al., 1999; Yagita et al., 1999). Apart from HYOU1, which is present in the endoplasmic reticulum (ER), all other mammalian and yeast HSP110 members are found in the cytoplasm (Chen X et al., 1996; Vos et al., 2008).

To gain insights into the molecular function of mammalian HSP110 family members, genetic targeted disruption in mice by homologous recombination was undertaken.

1. 5. 1. Molecular function of HSPA4

The *Hspa4* gene was cloned from a mouse testis cDNA library (Kaneko et al., 1997a). Murine *Hspa4* mRNA is ubiquitously expressed in all tissues, with the highest expression in testis, ovary and spleen (Kaneko et al., 1997a). In brain, HSPA4 protein was found to be expressed constitutively in rat neuronal tissues throughout entire embryonic and postnatal period, suggesting an important role of HSPA4 in these tissues under non-stress conditions (Okui et al., 2000). *Hspa4* is expressed in cells of various origins, including embryonic fibroblasts, myelomonocytic leukemia, mastocytoma, Sertoli cells, bone marrow stromal cells and primary human articular chondrocytes (Kaneko et al., 1997a; Dehne et al., 2010). Strikingly, *Hspa4* gene has been found among 250 genes, which are highly upregulated in pluripotent stem cells (Ramalho-Santos et al., 2002).

In contrast to most of HSPs, the expression level of *Hspa4* is not induced by heat shock conditions (Kaneko et al., 1997a; Nonoguchi et al., 1999). *Hspa4* expression is induced by acidic pH and is involved in the radioadaptive response (Kang et al., 2002; Rafiee et al., 2006). In addition, in rat transient forebrain ischemia leads to increased *Hspa4* expression in cerebral cortex and hippocampus (Yagita et al., 1999; Koh et al., 2000; Lee et al., 2002). *Hspa4* Overexpression in cancer BaF3-BCR/ABL cell line leads to increased cell proliferation and protection against oxidative damage suggesting an important role of HSPA4 in carcinogenesis and progression of chronic myeloid leukemia (Li C et al., 2010). Furthermore, HSPA4 has been found to be overexpressed in

hepatocellular carcinoma (Gotoh et al., 2004). SiRNA mediated repression of HSPA4 *in vitro* causes a significant decrease in migration, invasion, and transformation activity in lung cancer H1299 cell line (Wu et al., 2011). It was shown that HSPA4 is involved in the progression of enterocolitis in a zebrafish model of inflammatory bowel disease, which suggests that *Hspa4* expression can be used as effective read-out for genetic, chemical and environmental factors that might influence intestinal inflammation (Crawford et al., 2011).

1. 5. 2. Molecular function of HSPA4L

Murine *Hspa4l* genomic sequence has been firstly determined from adult mouse testis cDNA library (Kaneko et al., 1997b). Nonoguchi et al. (2001) reported that HSPA4L is expressed in human testicular germ cells and in sperm supporting its role in spermatogenesis and fertilization. Expression level of murine *Hspa4l* is highly increased in spermatogenic cells from late pachytene spermatocytes to late spermatids and in kidney where it is restricted to epithelial cells of distal convoluted tubules (Held et al., 2006). Noteworthy, *Hspa4l* is highly expressed in leukemia cells, and was found to elicit humoral immune responses in leukemia patients (Takahashi et al., 2007).

Murine *Hspa4l* expression has been shown to be induced upon osmotic stress, heat shock and cerebral ischemia (Kojima et al., 1996; Kaneko et al., 1997b; Xue et al., 1998). Analysis of the promoter region of *Hspa4l* gene revealed the presence of functional tonicity (TonE) and heat shock-responsive elements that mediate independently the induction of *Hspa4l* expression upon hypertonicity and heat shock, respectively (Kojima et al., 2004).

Held et al. (2006) have generated *Hspa4l* knockout (KO) mice through gene targeting in embryonic stem cells. *Hspa4l* KO mice were viable and born at expected Mendelian ratio with no overt phenotypes. Adult *Hspa4l* KO male but not female mice were infertile due to increased apoptotic cell death of spermatocytes together with impaired sperm motility. Moreover, *Hspa4l* KO mice developed hydronephrosis due to upper urinary tract obstruction.

1. 5. 3. Molecular function of HSPH1

The *Hsph1* genomic sequence from mouse has been isolated and characterized (Yasuda et al., 1995, 1999). Murine *Hsph1* is ubiquitously expressed in all tissues (Yasuda et al., 1995). HSPH1 exists as complexes associated with HSP70 and its cognate protein HSC70 (HSP70/HSC70) in mammalian cells (Hatayama et al., 1998; Wakatsuki and Hatayama, 1998).

Treatment of 3T3 fibroblast cells with DNA virus oncoprotein leads to induction of *Hsph1* transcript (Morozov et al., 1995). It has been reported that *Hsph1* is induced in neurons of the cerebral cortex and hippocampus upon exposure to cerebral ischemia (Kim H et al., 2001; Yagita et al., 2001).

1. 6. Aims of the study

Hspa4 KO mice model was generated in the Institute of Human Genetics, Göttingen. Two lines of *Hspa4* KO mice were generated in hybrid C57BL/6J x 129/SV and in inbred 129/Sv genetic background. Analysis of *Hspa4* KO mice in hybrid genetic background revealed that approximately 60% of *Hspa4* KO males were infertile. Analysis of *Hspa4*

KO mice in the inbred background showed that *Hspa4* KO mice displayed growth retardation and 65% of the KO mice died during the 1st 4 weeks after birth. *Hspa4* KO mice which overcame the early lethality displayed impaired fertility, skeletal muscle myopathy and cardiac hypertrophy.

To definitively rule out the possibility that *Hspa4l* expression is able to compensate for the loss of *Hspa4* in *Hspa4* KO mice, *Hspa4l/Hspa4* double KO (DKO) mouse model was generated. Strikingly, the DKO mice did not survive and died immediately after birth.

The aims of the experiments were the following:

1. Analysis of the expression patterns of HSPA4 in different tissues and in testis during prenatal and postnatal germ cells development together with identification of possible underlying causes of impaired male fertility in *Hspa4* KO mice.
2. Characterization of the development of hypertrophic cardiomyopathy in *Hspa4* KO mice at the histological and molecular levels together with identification of possible underlying causes
3. Determination of the possible underlying causes of early postnatal lethality encountered in *Hspa4l/Hspa4* DKO pups.
4. Finally, generation and characterization of *Hsph1* KO and *Hspa4/Hsph1* DKO mouse models were undertaken to elucidate the consequences of *Hsph1* deletion and simultaneous *Hspa4* and *Hsph1* deletion.

2. Materials and Methods

The following methods were used to analyze the expression pattern and role of HSPA4 during spermatogenesis. We analyzed the expression pattern of HSPA4 in the gonads during different prenatal and postnatal developmental stages and in different mutant testes by immunohistochemical analyses and Western blotting. To evaluate the role of HSPA4 in vivo, a loss of function mouse model was generated. We characterized the impact of HSPA4 ablation on the progression of spermatogenesis by histological and immunohistochemical analyses of *Hspa4* KO testes. To determine the different sperm parameters, we used CEROS Computer assisted semen analysis system. The expression levels of some meiotic and post-meiotic marker genes were estimated by Northern blotting. To detect apoptotic cells in testes, we performed TUNEL assay (**Publication I**).

We performed the following methods to determine the cardioprotective role of HSPA4. Western blotting and immunofluorescence analyses were performed to elucidate the expression levels and cellular distribution of HSPA4 in the sham- and transaortic constriction (TAC) - operated hearts. We analyzed the cardiac hypertrophy and fibrosis in *Hspa4* KO mice by staining of the heart sections with Hematoxylin & eosin (H&E) and Masson's trichrome, respectively. Cardiomyocyte diameter and cross sectional area were measured by NIH Image J software. The expression levels of hypertrophy related gene markers (*Nppa*, *Nppb*, *Myh7* and *Acta1*) and fibrosis related gene markers (*Col3a1* and *Colla1* and *Tgfb1*) were measured using quantitative real time PCR (qRT-PCR). The different parameters of heart dimension and function were measured using Two-

dimensional directed M-mode echocardiogram. Identification of signaling pathways which mediate the development of cardiac hypertrophy was done by Western blotting and qRT-PCR analyses. To test the effects of HSPA4 loss on cardiac responses to hemodynamic stress condition, *Hspa4* KO and WT mice were exposed to TAC. TAC was performed as previously described (Müller et al., 2008). The hypertrophic response was evaluated by histological analyses, qRT-PCR and echocardiography. To probe the ubiquitination status and the proteasome enzyme activity in *Hspa4* KO mice, we determined the levels of ubiquitinated proteins by Western blotting, immunofluorescence analyses and 20S Proteasome Assay Kit. In order to identify the differentially expressed genes in *Hspa4* KO hearts, global gene expression analysis was applied using the Gene-Chip® Mouse Gene 1.0 ST arrays (Affymetrix) (**Publication II**).

We did the following methods to elucidate the expression patterns and the role of HSPA4L/HSPA4 during lung morphogenesis. The expression pattern of HSPA4L and HSPA4 in the lung during different developmental stages was investigated by Western blotting and immunofluorescence analyses. To examine the effect of dual deletion of *Hspa4l* and *Hspa4* on the lung development, we intercrossed *Hspa4l* KO and *Hspa4* KO mice to obtain *Hspa4l*^{-/-} *Hspa4*^{-/-} mice. The embryonic lungs were histologically examined by staining of sections with H&E and periodic acid Schiff (PAS). The saccular spaces and the mesenchymal thickness were measured using NIH Image J software. The expression levels of alveolar type I (ATI) and alveolar type II (ATII) pneumocytes related markers were evaluated by immunohistochemistry and Western blotting. To probe the ubiquitination status in the lung of *Hspa4l*^{-/-} *Hspa4*^{-/-} mice, we determined the

level of ubiquitinated proteins by Western blotting analysis. The ultrastructure of the lung alveoli was examined by electron microscopy as described previously (Peng et al., 2006). In order to determine the cell proliferation, BrdU labeling was carried out. *In situ* TUNEL assay and cleaved Caspase 3 immunofluorescence analysis were performed to assess apoptosis.

3. Results and Discussion

The HSPs function as molecular chaperones. The Chaperones are multifunctional antistress proteins, which regulate diverse biological processes to maintain cellular homeostasis (Gething and Sambrook, 1992; Morimoto et al., 1994; Hartl, 1996; Gething, 1997). Under pathological conditions, inducible or constitutively expressed molecular chaperones protect cells from different environmental stressors (Hishiya and Takayama, 2008).

3.1. Consequences of HSPA4 ablation on male germ cells development

The spermatogenesis progresses through three distinct phases, namely mitotic proliferation of spermatogonia, meiotic division of spermatocytes and postmeiotic differentiation of haploid spermatids into spermatozoa (Eddy et al., 1991). All these developmental stages represent situations where dramatic transformations, cellular proliferation and differentiation take place. The expression of different HSPs is enhanced during spermatogenesis to facilitate proper folding, transport and assembly of protein complexes required for completion of different phases of spermatogenesis (Dix et al., 1997; Dix and Hong, 1998; Meinhardt et al., 1999). Previous reports demonstrated that decreased expression of the some HSPs is associated with the pathogenesis of male infertility in human (Werner et al., 1997; Son et al., 1999; Huszar et al., 2000; Son et al., 2000; Feng et al., 2001; Adly et al., 2008). The protective role of HSPs in testis was confirmed by data showing development of overt male infertility in mutant mice with

targeted gene disruption of different HSPs (Allen JW et al., 1996; Dix et al., 1996; Ikawa et al., 1997; Mori et al., 1997; Terada et al., 2005; Held et al., 2006).

HSPA4 is ubiquitously expressed in different tissues (Kaneko et al, 1997a; Nonoguchi et al., 1999). In the **publication I**, elucidation of the expression pattern and the physiological function of HSPA4 in male germ cell development were undertaken. We demonstrated that HSPA4 was ubiquitously expressed during prenatal and postnatal development in both somatic and germ cells of testis, with high enrichment in gonocytes, which represent the fetal/neonatal precursors of the undifferentiated spermatogonial stem cells (Culty, 2009). Expression of HSPA4 in male gonocytes was gradually decreased after their differentiation to spermatogonia (Fig. 1 and 2, pp. 134-135 in the Publication I). The enrichment of HSPA4 expression in the gonocytes is in accordance with previous reports, which revealed that *Hspa4* is highly expressed in different tissue-specific stem cells and its expression is downregulated upon differentiation (Ramalho-Santos et al., 2002; Bhattacharya et al., 2004). The high expression of HSPA4 in gonocytes suggests an important role of HSPA4 in germ stem cells development. It is believed that molecular chaperones may protect stem cells from oxidative stress-induced aging (Ramalho-Santos et al., 2002). *Caenorhabditis elegans*, with extended life span, have elevated levels of molecular chaperones, which function to eliminate oxidative free radicals and consequently extend longevity (Finkel and Holbrook, 2000).

The preferential HSPA4 expression in the germ cell forced us to study the impact of *Hspa4* ablation on germ cell development. Analyses of *Hspa4* KO mice revealed that all *Hspa4* KO mice of the hybrid 129Sv X C57Bl/6J background were born at expected Mendelian ratio. Phenotype analyses showed the *Hspa4* KO mice were indistinguishable

from WT mice with the exception of testes, which were significantly smaller. Some of *Hspa4* KO mice were infertile. Male infertility was manifested by decreased number and reduced motility of spermatozoa. To identify the cause of the reduced number of spermatozoa, histological sections of *Hspa4* WT and KO adult testes were analyzed. In contrast to WT control, KO testis showed diverse defects. Most of seminiferous tubules were smaller in size, vacuolated, devoid of round and elongated spermatids and contained an increased number of multinucleated abnormal spermatids. Remarkably, many pachytene spermatocytes were degenerated. Consequently, epididymidis contained less number of sperms compared to WT controls (Fig. 4, pp. 138 in the publication I).

To identify the timing of onset of spermatogenic distortion in *Hspa4* KO mice, testicular sections from different postnatal days (P) were histologically analyzed. At P5 and P10, no apparent difference between *Hspa4* WT and KO testes could be detected. Beginning from P15, we found few pachytene spermatocytes in the seminiferous tubules of KO compared to WT testis. These data were confirmed by immunohistochemical staining with anti-HSPA4L, which is highly expressed in germ cells from pachytene spermatocytes (Held et al. 2006). Number of HSPA4L expressing cells was significantly decreased in KO compared to WT testis. At P20, round spermatids were present in the majority of WT tubules, whereas *Hspa4* KO tubules were almost devoid of spermatids and contained a reduced number of pachytene spermatocytes. At day 25, *Hspa4* KO tubules showed severe depletion of germ cells (Fig. 5, pp. 139 in the Publication I). These results suggest that the *Hspa4* deficiency results in either developmental delay or partial arrest of the first wave of spermatogenesis.

To investigate whether the depletion of germ cells is due to exaggerated cell death by apoptosis, TUNEL assay was performed. A significant increase of TUNEL-positive spermatocytes was found in *Hspa4* KO testis (Fig. 6, pp 140 in the Publication I). Numerous proteins, which are required for the development of male germ cells during meiotic and post-meiotic stages, are mostly translated in pachytene spermatocytes (Messina et al., 2010). Failure of molecular chaperones to direct correct folding of newly synthesized proteins in pachytene spermatocytes might lead to accumulation of misfolded and damaged proteins, which would trigger spermatocytes to release meiotic division and initiate apoptosis. Based on the high sequence similarity of HSP110 family members, we expected that the molecular chaperones that include the NEF members of HSP110 family would be abnormal or partially affected in *Hspa4* KO mice.

Spermatogenic arrest was confirmed at the molecular level by analyzing the expression levels of some meiotic and postmeiotic gene markers in testis of WT, fertile- and infertile- KO mice. Expression of synaptonemal complex protein-3 (*Sycp3*) is restricted to leptotene and zygotene spermatocytes (Lammers et al., 1994). Phosphoglycerate kinase-2 (*Pgk2*) and acrosin (*Acr*) were reported to be expressed in pachytene spermatocytes (Goto et al. 1990, Kashiwabara et al., 1990; Kremling et al., 1991). *Hsc70t* (*Hsp70* homolog gene) and transition nuclear protein 2 (*Tnp2*) are post-meiotic genes (Kleene and Flynn, 1987; Tsunekawa et al., 1999). While the expression level of *Sycp3* showed no significant difference between WT and KO testes, the expression levels of late meiotic (*Pgk2* and *Acr*) and postmeiotic gene markers (*Hsc70t* and *Tnp2*) were significantly reduced in infertile KO testes as compared to WT and fertile KO testes (Fig. 7, pp. 141 in the Publication I). These results further confirm that spermatogenesis in

infertile KO mice is arrested at late stages of meiotic prophase I. Taken together; these data indicate that HSPA4 is required for successful completion of spermatogenesis in mouse.

The relatively leaky phenotype of *Hspa4* KO mice led us to suggest that *Hspa4* ablation could be compensated by other members of the HSP110 family. To address this hypothesis, we have determined the protein levels of HSPA4L, HSPH1 in the testes of *Hspa4* WT and KO mice. Protein levels of HSPA4L, HSPH1 were not markedly different between *Hspa4* KO and WT testes, suggesting that the depletion of HSPA4 is not compensated by an increased expression of studied HSPs in *Hspa4* KO testes (Fig. 7, pp. 141 in the Publication I).

Partial penetrance of male infertility, encountered in *Hspa4* KO mice, was also reported in other genetically modified mouse models (Bitgood et al., 1996; Pearse et al., 1997; Robertson et al., 1999; Yu et al., 2000; Adham et al., 2001; Nayernia et al., 2002; Froment et al., 2004; Burnicka-Turek et al., 2009). The causes of partial penetrance of the phenotype are often attributed to the mixed genetic background of mice used in KO studies, although the involvement of additional nongenetic factors cannot be excluded. A high incidence of male infertility was found among *Hspa4* KO mice in F2 generation, which contains a high level of inter-individual genetic variability. The decline in the incidence of infertility phenotype in subsequent generations would point to a selection bias against that genotype.

The spermatogenic defects in *Hspa4* KO mice resemble those of the *Hsp70-2* mutants. *HSP70-2* is a member of the HSP70 family which is expressed at high levels in pachytene spermatocytes during the meiotic phase of spermatogenesis (Allen RL et al.,

1988; Zakeri et al., 1988). Targeted disruption of *Hsp70-2* resulted in male infertility associated with arrested meiosis and germ cell apoptosis (Dix et al., 1997). The possibility that HSPA4 and HSP70-2 are involved in the same pathway remains to be investigated.

3.2. Cardioprotective role of HSPA4

Abnormal cardiac remodeling, which includes cardiac hypertrophy and fibrosis, plays a fundamental role in the pathogenesis of cardiovascular diseases such as hypertensive heart disease and chronic heart failure (Kuwahara et al., 2003; Mann and Bristow, 2005). Several lines of evidence demonstrated the protective role of HSPs against cardiac hypertrophy (Hayashi et al., 2006; Kim YK et al., 2006; Kumarapeli et al., 2008; Cai et al., 2010; Willis and Patterson, 2010; Norton N et al., 2011; Zhang et al., 2011; Zou et al., 2011).

In the **Publication II**, we have determined the cardioprotective role of HSPA4. We demonstrated that HSPA4 protein levels were significantly increased in the heart of WT mice subjected to pressure overload. Consistent with the data from the animal model, expression levels of human HSPA4 were significantly elevated in cardiac samples of patients with aortic stenosis. Immunofluorescence staining of murine heart sections showed cytoplasmic localization of HSPA4 in the cardiomyocytes, while the intensity of HSPA4 fluorescence staining in TAC-operated heart was stronger (Fig. 1, pp. 462 in the Publication II). These data indicate that the heart responds to hemodynamic stress by increasing HSPA4 expression. These results point to a potentially protective role of HSPA4 against pressure overload-induced cardiac hypertrophy. To elucidate the

cardioprotective role of HSPA4, we characterized the cardiac remodeling in *Hspa4* KO mice. Histological analyses revealed the development of hypertrophic cardiomyopathy and fibrosis in *Hspa4* KO mice (Fig. 2, pp. 463 in the Publication II). Expression profiling of the hypertrophy- and fibrosis- related gene markers revealed a significant upregulation of the studied genes in *Hspa4* KO compared with WT hearts. Two-dimensional directed M-mode echocardiogram analysis was performed to assess the cardiac dimension and function. Left ventricular mass (LVM), Interventricular septum dimension (IVSD), left ventricle posterior wall thickness (LVPWT) and ratio of wall thickness to heart radius (h/r) were significantly increased in *Hspa4* KO hearts compared to that of control littermates (Fig. 2, pp. 463 and Supplemental Table 2 in the Publication II). Taken together, these results indicate that the deficiency of HSPA4 leads to development of baseline cardiac hypertrophy and fibrosis.

To further confirm the cardioprotective role of HSPA4, we determined the responses of *Hspa4* KO animals to pressure overload by exposing *Hspa4* WT and KO mice to TAC. After 2 weeks of TAC, *Hspa4* KO mice exhibited exaggerated cardiac hypertrophy compared with WT controls (Fig. 3, pp. 464 and Supplemental Table 3 in the Publication II). These data reveal that HSPA4 ablation aggravates pathological cardiac hypertrophy in response to pressure overload.

Our results are consistent with previous reports showing that other members of the HSP family, such as HSP90, HSP70, HSP20, and α B-crystallin, attenuate the development of cardiac hypertrophy induced either by angiotensin II, isoproterenol stimulation, or pressure overload (Hayashi et al., 2006; Kumarapeli et al., 2008; Willis and Patterson, 2010; Zhang et al., 2011). These findings further support the idea that the members of

HSP family may be involved in mechanisms that protect against pathological cardiac remodeling and may be effective therapeutic candidates for cardiac hypertrophy and heart failure.

To determine the signaling pathways that were affected in the heart of *Hspa4* KO mice and might be responsible for the development of cardiac hypertrophy, we investigated the expression levels of some genes and proteins, which are suggested to be involved in development of cardiac hypertrophy. These analyses demonstrated that the transcriptional activity of NFAT and the expression levels of activated CaMKII were significantly elevated in *Hspa4* KO heart (Fig. 4B-D, pp. 465 in the Publication II). Both proteins participate in signaling pathways that play critical roles in regulating hypertrophic growth of the heart (Wilkins and Molkentin, 2002). In collaboration with GATA4, activated NFAT induces the expression of fetal genes (Molkentin et al., 1998; Olson and Williams, 2000). Similarly, activated CaMKII promotes MEF2 transcriptional activity, which induces the expression of prohypertrophic genes (Passier et al., 2000). The increased activity of gp130-STAT3 signaling in response to extracellular stress was reported to induce myocardial hypertrophy (Kunisada et al., 1998; Kunisada et al., 2000). In this study, we also found a marked increase in protein level of phosphorylated STAT3 (Fig. 4A, pp. 465 in the Publication II). This result suggests that gp130-STAT3 signaling also participates in cardiac remodeling in *Hspa4* KO mice. It remains to be determined whether the observed increase in the activity of these prohypertrophic signaling pathways is, on the one hand, the result of the development of cardiac hypertrophy in *Hspa4* KO hearts. On the other hand, it might also have resulted from an increase of misfolded

proteins in cardiomyocytes, causing intracellular stress and the activation of stress-induced signaling pathways.

PQC depends on sophisticated collaboration between molecular chaperones and targeted proteolysis. When PQC is impaired or overloaded, abnormal proteins accumulate and cause aberrant aggregation in the cell, thereby injuring the cell and ultimately leading to cell death (Rutkowski and Kaufman, 2004). This can be quite detrimental to post-mitotic organs such as heart and brain due to their very limited self-renewal capacity (Wang X and Robbins, 2006). Emerging data suggest that protein misfolding and aberrant aggregation are common causes of heart diseases (Heling et al., 2000; Hein et al., 2003; Kostin et al., 2003; Sanbe et al., 2004; Chen Q et al., 2005; Liu J et al., 2006; Wang X and Robbins, 2006; Wang X et al., 2008).

Given the role of HSPA4 as a co-chaperone, which functions to maintain proper protein folding, we speculated that HSPA4 ablation may impair the cardiac PQC. To address this hypothesis, we checked the level of ubiquitinated proteins in the *Hspa4* KO heart. As expected, we showed an accumulation of ubiquitinated proteins in the *Hspa4* KO heart compared to WT controls (Fig. 5, pp. 466 in the Publication II). These results suggest that the accumulation of ubiquitinated proteins resulting from impaired chaperone activity is possibly responsible for myocardial remodeling in *Hspa4* KO mice.

To rule out systemic causes of the cardiac hypertrophy seen in *Hspa4* KO mice, we characterized neonatal cardiomyocyte cultures, which were established from *Hspa4* WT and KO mice. Morphometric analyses demonstrated a high ratio of cardiomyocytes with increased cross sectional area (CSA) in KO culture compared to that in WT control. At the molecular level, expression levels of hypertrophic markers, *Nppa* and *Nppb*, were

significantly increased in neonatal *Hspa4* KO cardiomyocyte compared to WT control (Fig. 6, pp. 466 in the Publication II). These data indicate that hypertrophic cardiomyocyte phenotype in *Hspa4* KO mice is due to an intrinsic heart defect.

Microarray analysis was performed to identify gene expression profiles and expand the knowledge of pathways regulating the development of cardiac hypertrophy in *Hspa4* KO mice. RNA from the hearts of 3.5-week-old *Hspa4* WT and KO mice were isolated, labeled and subjected to microarray screening. We selected 3.5 week-old-mice for identification of differentially expressed genes because this time largely precedes any pathological manifestations in *Hspa4* KO heart, so that secondary alterations in gene expression were less likely. Results of microarray analysis identified 97 differentially expressed genes in *Hspa4* KO heart (Fig. 7, pp. 467 and Supplemental Tables 4, 5 in the Publication II). Among the differentially expressed genes, several of them encode for proteins that are involved in ion channel signaling, including the voltage-gated potassium channels KCNE1 and KCND2, the potassium/sodium hyperpolarization-activated cyclic nucleotide-gated channel 1 (HCN1), sodium channel-gated, type IV, alpha subunit (SCN4A) and leucine glioma inactivation 1 (LGI1) that regulates the activity of voltage-gated potassium channels (Schulte et al., 2006). It remains to be addressed whether the observed alterations in the expression of these genes could lead to electric remodeling in *Hspa4* KO hearts; and further, if this is responsible for development of cardiac hypertrophy. Interestingly, *Maplc3a*, *Dub2a* and *Dcun1d1* genes, which their coded proteins play a potential role in PQC machinery (Baek et al., 2001; Kouroku et al., 2007; Kim AY et al., 2008), were significantly altered in the *Hspa4* KO hearts compared with WT controls. However, verification of these results by qRT-PCR and immunoblot

analyses is required. These might provide mechanistic insights into the function of HSPA4 in chaperone mediated protein folding and give explanation for development of cardiac hypertrophy upon HSPA4 ablation.

In conclusion, we have demonstrated that lack of HSPA4 led to cardiac hypertrophy and fibrosis. Moreover, our data revealed the distinct, non-redundant role of HSPA4 in the PQC that maintains the proper protein folding and homeostasis in the cardiomyocytes.

3.3. Elucidating the consequence of cardiac HSPA4 overexpression

We have shown that deficiency of HSPA4 led to baseline cardiac hypertrophy and an exaggerated hypertrophic response to TAC-induced pressure overload. To investigate whether forced expression of HSPA4 in the heart will be sufficient to protect against cardiac hypertrophy, we performed gain-of-function experiments *in vitro* and *in vivo*.

3.3.1. Generation of recombinant *Hspa4* adenovirus (Ad-*Hspa4*)

To evaluate the ability of HSPA4 to attenuate cardiomyocyte hypertrophy *in vitro*, recombinant adenovirus was generated in collaboration with Dr. S. Lutz (Department of Pharmacology, Medical Faculty, Göttingen). Briefly, we have constructed an Ad-*Hspa4* by cloning the full-length murine *Hspa4* cDNA into the shuttle vector pAdTrack-CMV and subsequent cotransformation of this vector and pAdEasy-1 into electrocompetent AdEasier bacteria (Stratagene) as described previously (He et al., 1998). Expression of *Hspa4* in the Ad-*Hspa4* is driven by the constitutive active CMV promoter. The virus also encodes the enhanced green fluorescent protein (EGFP) as a reporter gene. The EGFP is under the control of a separate CMV promoter (Fig. 3). The

EGFP adenovirus (Ad-EGFP) was used as the appropriate control adenovirus. Recombinant viral backbones from transformed AdEasier bacteria were collected and used for transfection of human embryonic kidney cells (HEK-293). After three weeks of transfection, Ad-*Hspa4* adenovirus was harvested and used for transfection of neonatal rat cardiomyocytes (NRCMs).

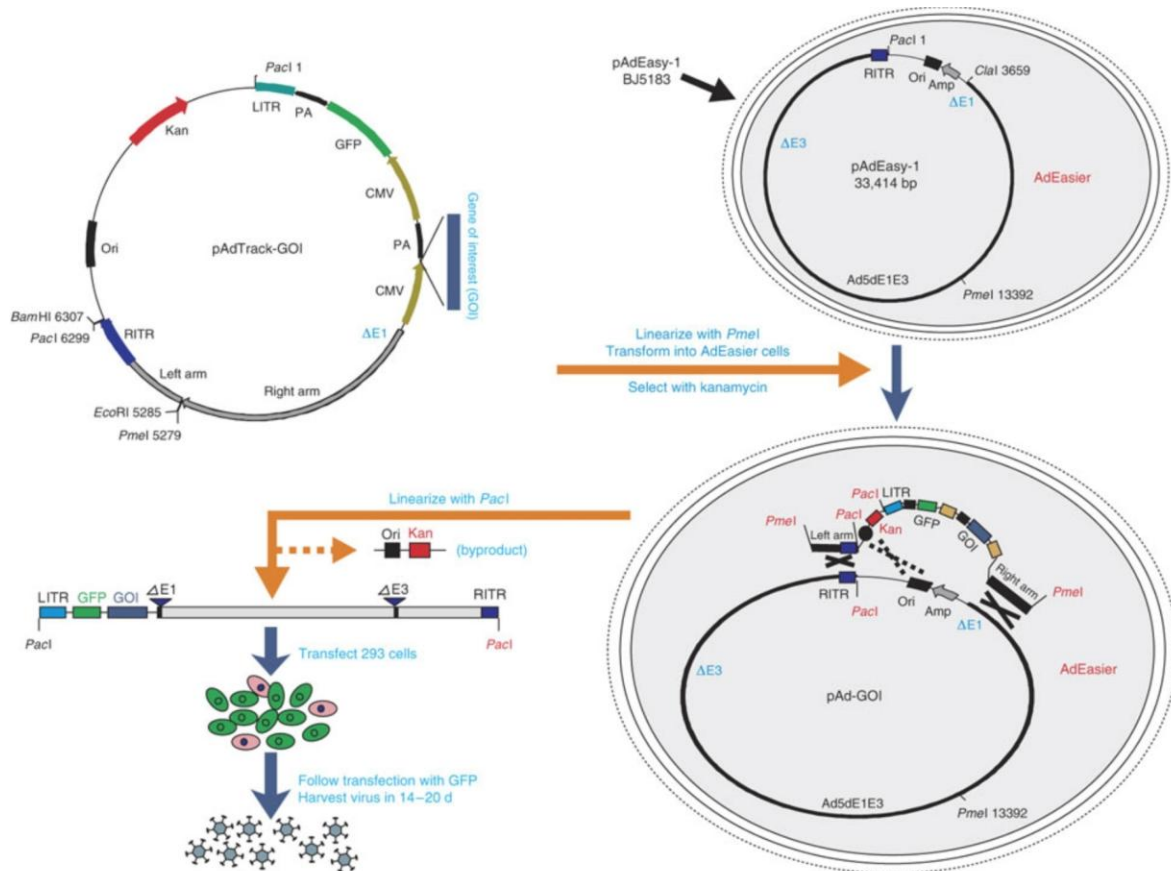


Figure 3. Schematic representation of the AdEasy technology. The *Hspa4* cDNA was cloned into a pAdTrack-CMV shuttle vector and subsequently transformed into competent AdEasier cells, which are BJ5183 derivatives containing the adenoviral backbone plasmid pAdEasy-1. The confirmed recombinant adenovirus plasmids were digested with *PacI* to liberate both inverted terminal repeats (ITRs) and transfected into HEK-293 cells. HEK-293 cells express recombinant adenovirus E1, allowing them to produce adenoviruses from backbone vectors without the E1 gene. Recombinant adenoviruses are typically generated within 14–20 d. The 'left arm' and 'right arm' represent the regions mediating homologous recombination between the shuttle vector and the adenoviral backbone vector. Alternative homologous recombination between two Ori sites is shown with dotted lines. PA: polyadenylation site; LITR: left-hand ITR and packaging signal; RITR: right-hand ITR (Adapted from He et al., 1998, pp. 2511).

The efficiency of gene transfer was evaluated by confocal fluorescence microscopy of EGFP expression in cardiac myocytes 24 hrs after infection. The number of cells infected was more than 95% of the cultured NRCMs (Fig. 4A). To confirm the overexpression of HSPA4 in infected NRCMs, protein lysates from Ad-*Hspa4*- and control Ad-EGFP-infected NRCMs were isolated and subjected to Western blotting. As shown in Figure 4B, the protein level of HSPA4 was significantly increased in Ad-*Hspa4*- infected NRCMs compared to control.

To elucidate the impact of forced HSPA4 expression on cardiomyocyte hypertrophy, Ad-*Hspa4*- infected NRCMs will be treated with phenylephrine (PE), an agonist for cardiac hypertrophy. The hypertrophic response will be evaluated by morphometric analysis of cardiomyocytes areas, sarcomeric rearrangement by immunostaining with α -actinin antibody, measurement of the expression levels of hypertrophic markers (*Nppa* and *Nppb*) and quantification of EGFP synthesis as a surrogate for overall protein synthesis in Ad-*Hspa4*- and control Ad-EGFP- infected cells.

We have demonstrated that ablation of HSPA4 leads to impaired folding capacity of chaperones with subsequent accumulation of ubiquitinated proteins in the myocardium (Publication II). To test whether HSPA4 overexpression could enhance the chaperone mediated folding machinery and reduce ubiquitinated proteins accumulation, protein lysates from Ad-*Hspa4*- and control Ad-EGFP-infected NRCMs were isolated and subjected to immunoblotting. Interestingly, the total ubiquitinated proteins were significantly decreased in infected Ad-*Hspa4* cells compared to that in Ad-EGFP control (Fig. 4C). This result suggests that HSPA4 plays a fundamental role in the chaperone mediated protein folding.

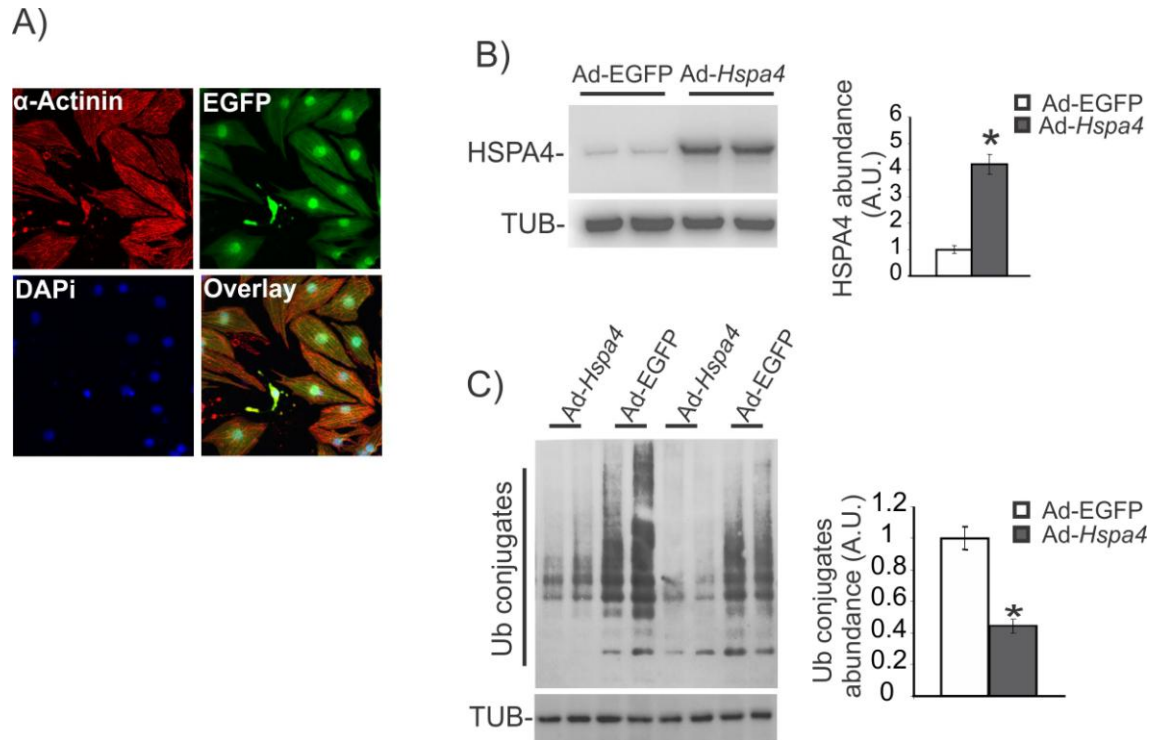


Figure 4. Analysis of *Ad-Hspa4*- infected NRCMs. A, Cultured NRCMs were infected with *Ad-Hspa4*. Co-expression of the green fluorescent protein (EGFP) tracer and α -actinin indicates efficient infection of more than 95% of the cardiomyocytes. B, Immunoblotting shows increasing HSPA4 protein levels in *Ad-Hspa4*- infected cardiomyocytes. Western blots were probed with antibodies directed against HSPA4 and α -tubulin (TUB). In the bar graph presenting in the right panel, expression levels of HSPA4 were normalized to that of α -tubulin. Values are expressed as mean \pm SD. HSPA4 protein levels in Ad-EGFP control culture serve as reference. * $P < 0.05$ vs control, A.U. indicates arbitrary units. C, Western blot analyses of total ubiquitinated proteins in *Ad-Hspa4*- and Ad-EGFP- infected NRCMs. Representative image and pooled densitometry data are shown. Values are expressed as mean \pm SD. HSPA4 protein levels in Ad-EGFP control culture serve as reference. * $P < 0.05$ vs control, A.U. indicates arbitrary units.

3.3.2. Generation of cardiac specific *Hspa4* transgenic mouse model

To investigate the cardioprotective effect of HSPA4 overexpression against pressure overload-induced cardiac hypertrophy *in vivo*, we decided to generate a mouse model with cardiac-specific overexpression of HSPA4. Towards this end, murine *Hspa4* cDNA was generated by PCR, cloned into pGEM-T Easy vector (Promega, Madison WI, USA) and verified by DNA sequencing. The *Hspa4* cDNA was then cloned downstream of the cardiac specific α -MHC promoter. The plasmid containing the α -MHC promoter was

provided by Prof. Dr. W.-H. Zimmermann (Department of Pharmacology, Medical Faculty, Göttingen). The cardiac α -MHC promoter is exclusively transactivated in cardiomyocytes (Fig. 5).

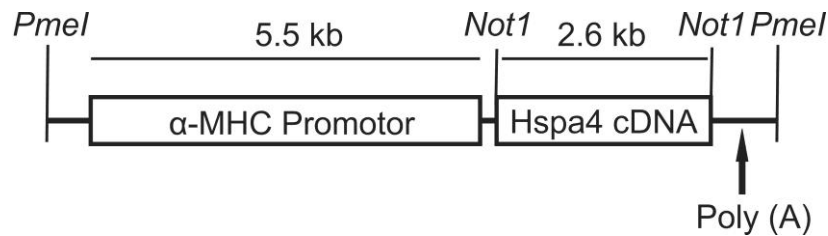


Figure 5. Schematic diagram of the transgene construct used for the generation of *Hspa4* transgenic mice. The construct contains the α -MHC gene promoter, the full-length mouse *Hspa4* cDNA clone, and a polyadenylation sequence (poly A).

In future experiments, the recombinant α -MHC-*Hspa4* fragment will be microinjected into nuclei of fertilized oocytes collected from mice of FVB strain. The microinjected oocytes will be transferred into oviducts of pseudopregnant females. Genomic integration, copy number and expression of transgenic allele in the transgenic founders will be determined by qRT-PCR analysis and Western blotting. To evaluate the cardioprotective effect of forced HSPA4 expression against pressure overload-induced cardiac hypertrophy, *Hspa4* transgenic and WT mice will be subjected to TAC operation. After two weeks, we will determine the extent of cardiac hypertrophy by echocardiogram, histology, expression levels of hypertrophy and fibrosis related markers in both genotypes.

3.4. Simultaneous deletion of murine *Hspa4l* and *Hspa4* genes causes pulmonary immaturity and early neonatal lethality in mouse

The HSP110 gene family includes two genes in *Saccharomyces cerevisiae* known as *Sse1* and *Sse2* (Mukai, et al., 1993; Shirayama et al., 1993). Ablation of *Sse1* resulted in growth defect and temperature sensitivity, whereas *Sse2* loss had no overt phenotype (Mukai, et al., 1993). However, deletion of both *Sse1* and *Sse2* genes was lethal, indicating a unique important cellular function of both proteins in yeast (Shaner et al., 2005; Trott et al., 2005). Given the ubiquitous patterns of *Hspa4l* and *Hspa4* expression and their high sequence homology (Kaneko et al., 1997a, b), it is conceivable that mutual functional compensation could confound the phenotype of *Hspa4l*^{-/-} and *Hspa4*^{-/-} KO mice. To address this hypothesis, we have generated and analyzed the *Hspa4l/Hspa4* DKO mice. *Hspa4l*^{-/-} *Hspa4*^{-/-} mice died shortly after birth. To get insight into the underlying cause of death, we closely monitored the fate of E18.5 embryos, which was just prior to the delivery day, delivered by Caesarean section (C-section). Inactivation of HSPA4L and HSPA4 in lung of *Hspa4l*^{-/-} *Hspa4*^{-/-} embryos was confirmed by Western blotting (Fig. 6A).

At E18.5 the body weight of *Hspa4l*^{-/-} *Hspa4*^{-/-} embryos was significantly smaller than that of controls (WT, *Hspa4l*^{-/-} and *Hspa4*^{-/-} embryos) (Fig. 6B, C). *Hspa4l*^{-/-} *Hspa4*^{-/-} embryos made visible effort to breath. However, in contrast to control embryos, *Hspa4l*^{-/-} *Hspa4*^{-/-} embryos were less active and became cyanotic and died of respiratory distress during 1 hr after revival. These observations suggest that HSPA4L and HSPA4 are essential for embryonic development and that simultaneous ablation of both genes leads to embryonic growth retardation and early neonatal death. Histological analyses revealed no overt abnormalities in other tissues including heart (data not shown) in *Hspa4l*^{-/-} *Hspa4*^{-/-} embryos, raising the possibility that the pulmonary defect is responsible for

neonatal lethality. While organ weights of heart, kidney and liver were similar between genotypes (data not shown), we observed that the lung of *Hspa4l^{-/-} Hspa4^{-/-}* embryos at E18.5 were significantly smaller compared with controls (Fig. 6D). This finding indicates that the *Hspa4l^{-/-} Hspa4^{-/-}* embryos develop pulmonary hypoplasia. Lungs dissected from *Hspa4l^{-/-} Hspa4^{-/-}* embryos did not float on water, indicating that the lungs are not inflated with air (Fig. 6E).

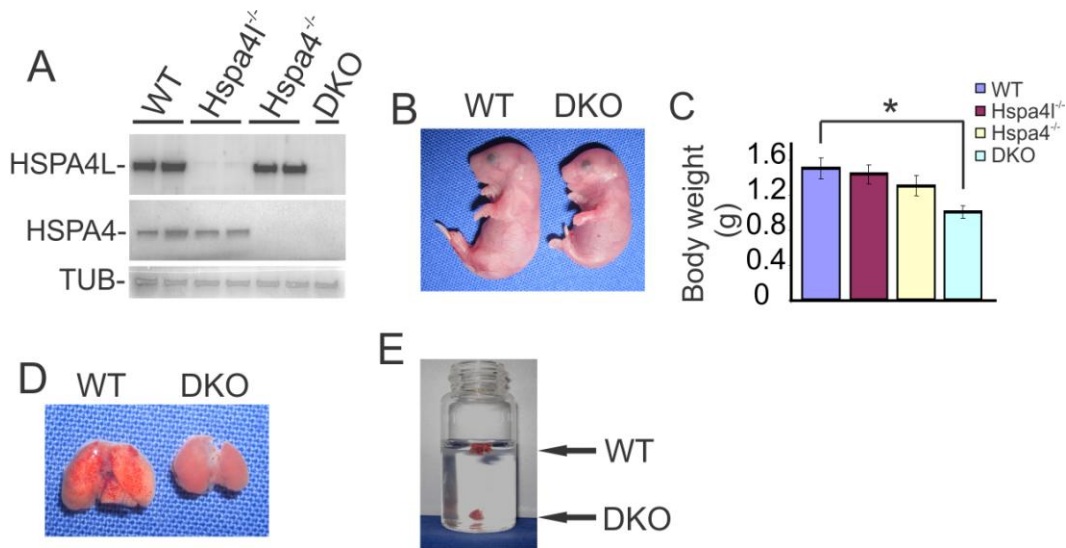


Figure 6. Simultaneous ablation of HSPA4L and HSPA4 led to pulmonary hypoplasia. (A) Western blotting for the expression of HSPA4L and HSPA4 proteins in extracts of lungs from wild type (WT), *Hspa4l^{-/-}*, *Hspa4^{-/-}* and *Hspa4l^{-/-} Hspa4^{-/-}* (DKO) embryos at E18.5. Expression of α -tubulin (TUB) was used as a loading control. (B) Representative image of WT and DKO embryos at E18.5. (C) The body weight of E18.5 WT, *Hspa4l^{-/-}*, *Hspa4^{-/-}* and DKO embryos. Five to seven embryos per genotype were used in this analysis. Value is presented as mean \pm SD, * $P < 0.05$ vs WT. (D) Gross images of the lung tissue isolated from WT and DKO embryos at E18.5. (E) The floating lung assay for WT and DKO embryos. DKO lung (the lower one) has sunk, while the WT lung is floating in the PBS. DKO, double knockout.

Prior to investigation of the pulmonary phenotype of DKO embryos, the expression level and distribution pattern of HSPA4L and HSPA4 during lung development were studied. Immunoblot analysis showed that both HSPA4L and HSPA4 proteins were ubiquitously

expressed in lung during the embryonic (E12.5-E18.5) and postnatal days (P1, P2, P45) (Fig. 7A).

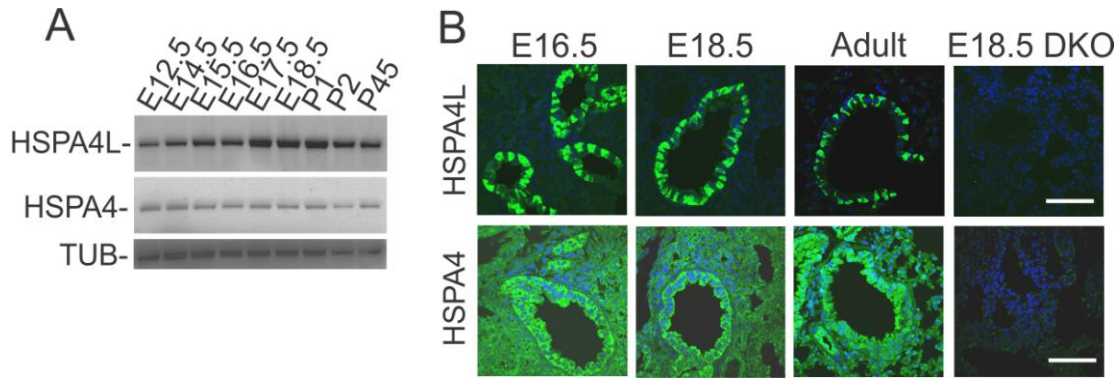


Figure 7. Expression of HSPA4L and HSPA4 in embryonic and adult murine lung. (A) Western blot analysis for the expression of HSPA4L and HSPA4 in WT lung at different developmental stages. Expression of α -tubulin (TUB) was used as a loading control. (B) Cellular distribution of HSPA4L- and HSPA4-positive cells in the lung. Immunofluorescence study of HSPA4L and HSPA4 in lung sections from WT mice of E16.5, E18.5- and of adult- stage and from *Hspa4l*^{-/-} *Hspa4*^{-/-} (DKO) embryos at E18.5. Nuclei were stained blue with DAPI. Bar = 30 μ m. DKO, double knockout.

Multiple cell types are present in the lung, including epithelial, mesenchymal and endothelial cells. To elucidate the cellular distribution of HSPA4L and HSPA4 proteins in the lung, paraffin sections of lungs isolated from embryonic and adult WT mice were subjected to immunofluorescence analysis. HSPA4L immunoreactivity was identified exclusively in a subpopulation of bronchial and bronchiolar epithelial cells in both embryonic and adult lung sections (Fig. 7B). Detectable HSPA4 immunoreactivity was ubiquitously distributed in all pulmonary cells with stronger signals identified in bronchial and bronchiolar epithelial cells (Fig. 7B). No immunoreactivity was observed for HSPA4L and HSPA4 in the lung sections derived from E18.5 *Hspa4l*^{-/-} *Hspa4*^{-/-} embryos (Fig. 7B) confirming the specificity of the antibodies used. These data demonstrate an extensive overlap in the expression pattern of HSPA4L and HSPA4 in bronchial epithelium.

In the mouse, lung development is divided into four stages (Maeda et al., 2007). During the pseudoglandular stage (E9.5–E16.5) branching morphogenesis generates the respiratory tree, and the pulmonary vasculature starts to develop. At the canalicular stage (E16.5–E17.5) the terminal bronchioles expand to form the respiratory ducts and sacs. The saccular stage (E17.5–PN5) is characterized by thinning of the mesenchyme and the differentiation of ATI and ATII pneumocytes, which are responsible for gas exchange and surfactant synthesis, respectively (Williams and Mason, 1977; Weaver TE and Conkright, 2001; Boggaram, 2003). The alveolar stage occurs after birth and is characterized by the remodeling of saccules into alveoli.

In the lung of *Hspa4l^{-/-} Hspa4^{-/-}* embryos at E15.5, branching morphogenesis and canalicular stages occurred normally compared to age matched controls (Fig. 8A). These data suggest that early signaling events including, mesenchymal FGF-10, endodermally derived FGF-R2, SHH/GLI 2,3 and retinoic acid receptors, which transpire between foregut endoderm and surrounding splanchnic mesoderm (Mendelsohn et al., 1994; Bellusci et al., 1997; Litington et al., 1998; Min et al., 1998; De Moerlooze et al., 2000) are unaffected in the *Hspa4l^{-/-} Hspa4^{-/-}* lung.

Diminished saccular expansions with concomitant increased mesenchymal tissue, which are consistent with pulmonary immaturity, were evident in the lung at E17.5 and became exaggerated at E18.5 and E19.5 stages (Fig. 8A). Morphometric analysis demonstrated a significant decrease of saccular size and increased thickness of mesenchymal septa in the *Hspa4l^{-/-} Hspa4^{-/-}* lung compared with controls (Fig. 8B, C).

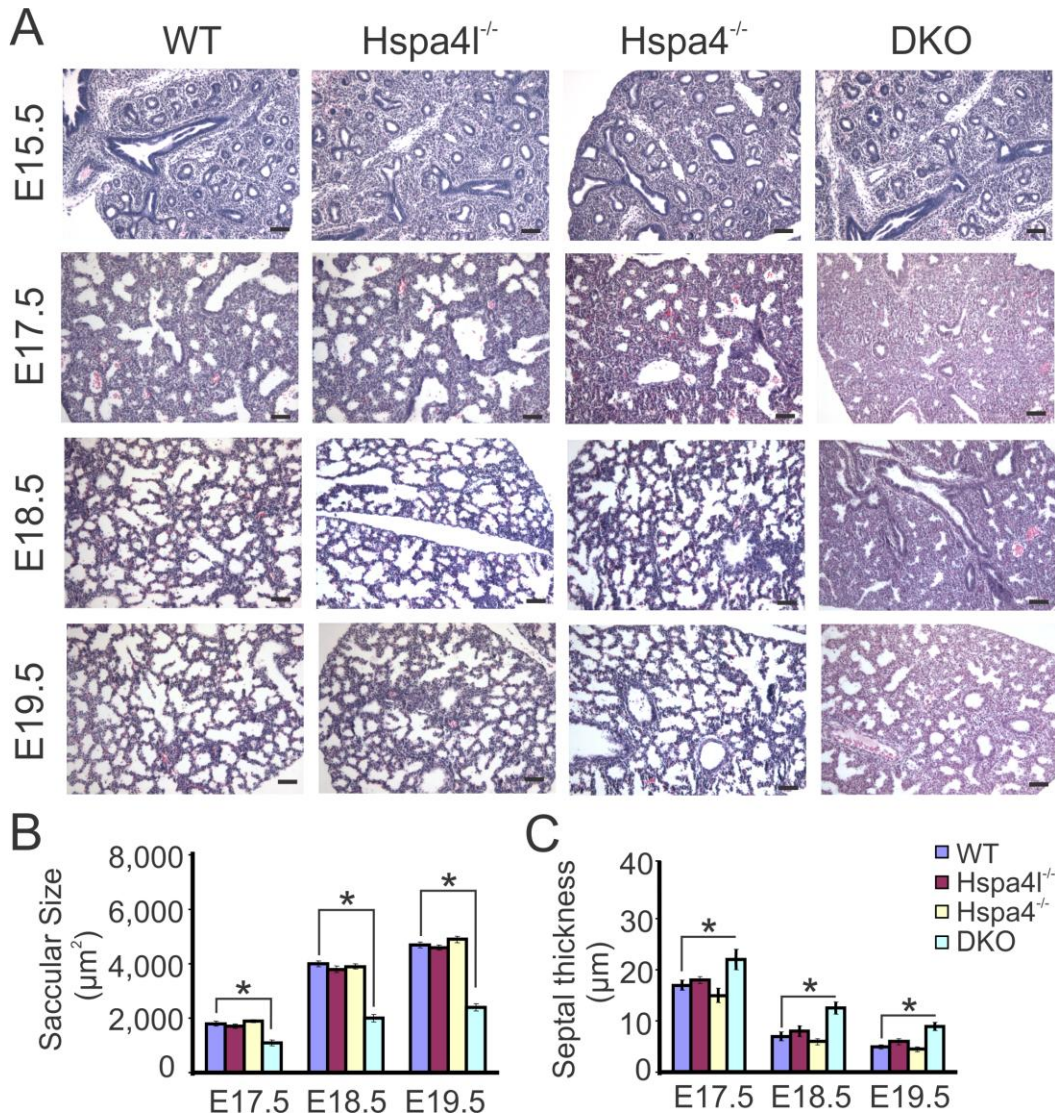


Figure 8. Delayed maturation of distal pulmonary epithelium in *Hspa4l*^{-/-} *Hspa4*^{-/-} embryos. (A) Lung sections from embryos were prepared at the indicated developmental stages and stained with H&E. Representative sections revealed no apparent phenotypic differences between wild type (WT), *Hspa4l*^{-/-}, *Hspa4*^{-/-} and *Hspa4l*^{-/-} *Hspa4*^{-/-} (DKO) lungs at E15.5. At E17.5, E18.5 and E19.5, WT, *Hspa4l*^{-/-} and *Hspa4*^{-/-} lungs have dilated terminal sacs and a thinned mesenchyme. In contrast, DKO lung has reduced terminal sacs with thickened intervening mesenchyme. Bar = 50 μm. (B and C) Morphometric analysis of lung saccular airspace (B) and mesenchymal septal thickness (C) in E17.5, E18.5 and E19.5 embryos. **P* < 0.05 vs WT, *n* = 5 per genotype per embryonic stage. DKO, double knockout.

The limited saccular expansion in the lung at the end of gestation forced us to investigate the maturation status of ATII pneumocytes. Immature ATII cells are glycogen-rich and when they differentiate, glycogen is converted into phospholipids, which are mixed with surfactant-associated proteins (SPs) to form the surfactant complexes (Ronney et al.,

1994; Ridsdale and Post, 2004). In ATII pneumocytes, synthesized surfactant is stored in the cytoplasmic lamellar bodies. Immaturity of type II pneumocytes, which is associated with high glycogen content and decreased surfactant production, leads to respiratory distress and poor neonatal survival (Whitsett and Weaver, 2002). Thus, we stained E18.5 lung sections with PAS to assess intracellular glycogen in the ATII cells. Indeed, the proportion of glycogen-rich cells in the alveolar epithelium of the *Hspa4l^{-/-} Hspa4^{-/-}* lung was more than fivefold higher than that in the WT, *Hspa4l^{-/-}* and *Hspa4^{-/-}* control lungs (Fig. 9A, B). To further substantiate this result, we examined the morphology of ATII cells using transmission electron microscopy. As illustrated in Figure 9C, ATII pneumocytes from *Hspa4l^{-/-} Hspa4^{-/-}* embryos contained abundant glycogen, smaller and less number of lamellar bodies when compared to WT littermates. These findings suggest that maturation of ATII cells is impaired in the *Hspa4l^{-/-} Hspa4^{-/-}* lung.

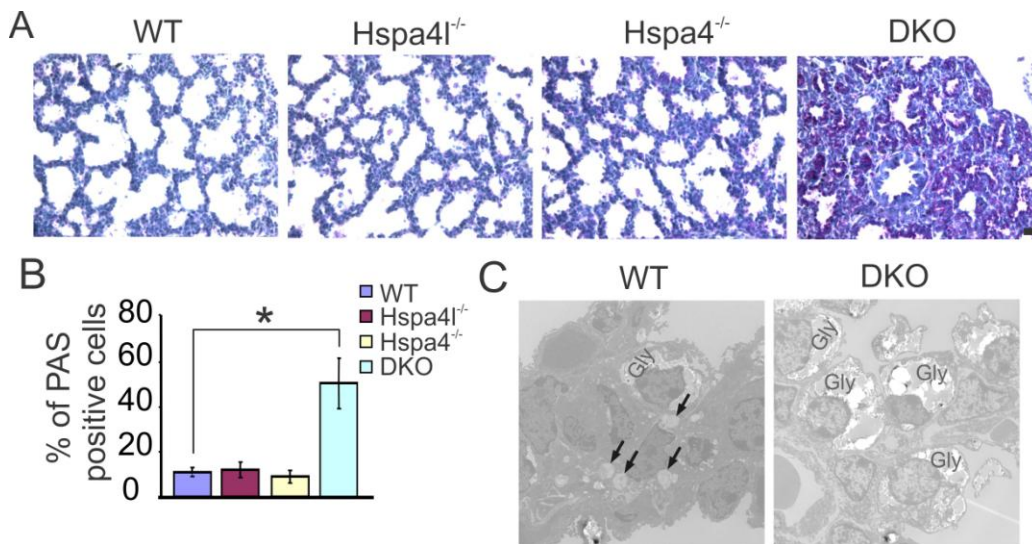


Figure 9. Glycogen accumulation and poor lamellar bodies in ATII pneumocytes of *Hspa4l^{-/-} Hspa4^{-/-}* lung. (A) PAS stains indicating cytoplasmic glycogen in lung sections from E18.5 wild type (WT), *Hspa4l^{-/-}*, *Hspa4^{-/-}* and *Hspa4l^{-/-} Hspa4^{-/-}* (DKO) embryos. Bar= 20 μ m. (B) Quantitation of PAS-positive cells. More than 800 alveolar epithelial cells were randomly examined for each genotype for the statistical comparison. * $P < 0.05$ vs WT, $n = 3-4$ per genotype. (C) Electron microscopy of E18.5 WT and DKO lungs demonstrates ultrastructure immaturity of the ATII cells in the peripheral lung saccules of DKO lung.

Cuboidal ATII cells of WT lung were found to contain numerous lamellar bodies (arrows). In ATII cells of DKO lung, lamellar bodies are scanty and the cytoplasm is occupied by glycogen (Gly). DKO, double knockout.

To confirm impaired maturation of ATII pneumocytes, we then directly assessed the ability of ATII cells to synthesize SPs in the lung of *Hspa4l^{-/-} Hspa4^{-/-}* embryos at E18.5. The SPs include SP-A, SP-B, SP-C, and SP-D (Rooney et al., 1994). Immunofluorescence analyses were performed using antibodies against mature SP-B and proSP-C. In comparison to WT, *Hspa4l^{-/-}* and *Hspa4^{-/-}* control lungs, the number of proSP-C- and SP-B-positive cells was significantly reduced in *Hspa4l^{-/-} Hspa4^{-/-}* lung (Fig. 10A). In agreement with the immunofluorescence results, Western blotting revealed that protein levels of mature SP-B and proSP-C were significantly decreased in *Hspa4l^{-/-} Hspa4^{-/-}* compared to control lungs (Fig. 10B). These reduced levels of SPs together with abnormal accumulation of intracellular glycogen in the pulmonary epithelial cells denote that the maturation of pulmonary ATII cells is severely impaired in embryonic lung of *Hspa4l^{-/-} Hspa4^{-/-}* embryos.

Expression of SPs in ATII epithelial cells normally increases prior to birth (Randell and Young, 2004). Of these, SP-B and SP-C play pivotal roles in surfactant function and homeostasis (Clark et al., 1995; Clark et al., 2001; Ikegami et al., 2003; Shulenin et al., 2004). Mutations in SP-B cause lethal respiratory distress in human and mouse (Nogee et al., 1994; Clark et al., 1995; Nogee et al., 2000). Targeted disruption of SP-B in mouse perturbed formation of lamellar bodies, causing respiratory failure shortly after birth (Clark et al., 1995). Reduction of SP-B was also found to be associated with surfactant dysfunction and respiratory failure in the perinatal and postnatal periods (Gregory et al., 1991). The reduced expression of SP-B and proSP-C may be responsible for the alveolar

collapse, which leads to respiratory failure and neonatal lethality in *Hspa4l^{-/-} Hspa4^{-/-}* embryos.

Because ATI cells differentiate from ATII cells (Warburton et al., 2000; Bhaskaran et al., 2007), it is reasonable to hypothesize that immature ATII cells will impair maturity of ATI cells. To address this hypothesis, we performed immunofluorescence analysis with antibody against Aquaporin 5 (AQP5). AQP5 is a water channel protein and its expression is restricted to ATI pneumocytes (Verkman et al., 2000; Williams, 2003). AQP5 immunostaining was widespread in cells lining the distal airspaces in E18.5 lung of WT, *Hspa4l^{-/-}* and *Hspa4^{-/-}* embryos. In contrast, AQP5 displayed a differential pattern of expression in the *Hspa4l^{-/-} Hspa4^{-/-}* lung. In some areas of the lung, AQP5 immunostaining was present in the apical membrane of ATI cells, while AQP5-positive cells were lacked in other regions of the lung (Fig. 10A). Consistent with this finding, Western blot analysis demonstrated a significant reduction in the expression levels of AQP5 protein in the lung of *Hspa4l^{-/-} Hspa4^{-/-}* embryos (Fig. 10B). These results suggest that the respiratory distress seen in *Hspa4l^{-/-} Hspa4^{-/-}* embryos could be also due to an impaired gas exchange resulting from decreased numbers of mature ATI cells. Taken together, these data indicate that dual deletion of HSPA4L and HSPA4 leads to delayed maturation of alveolar epithelium.

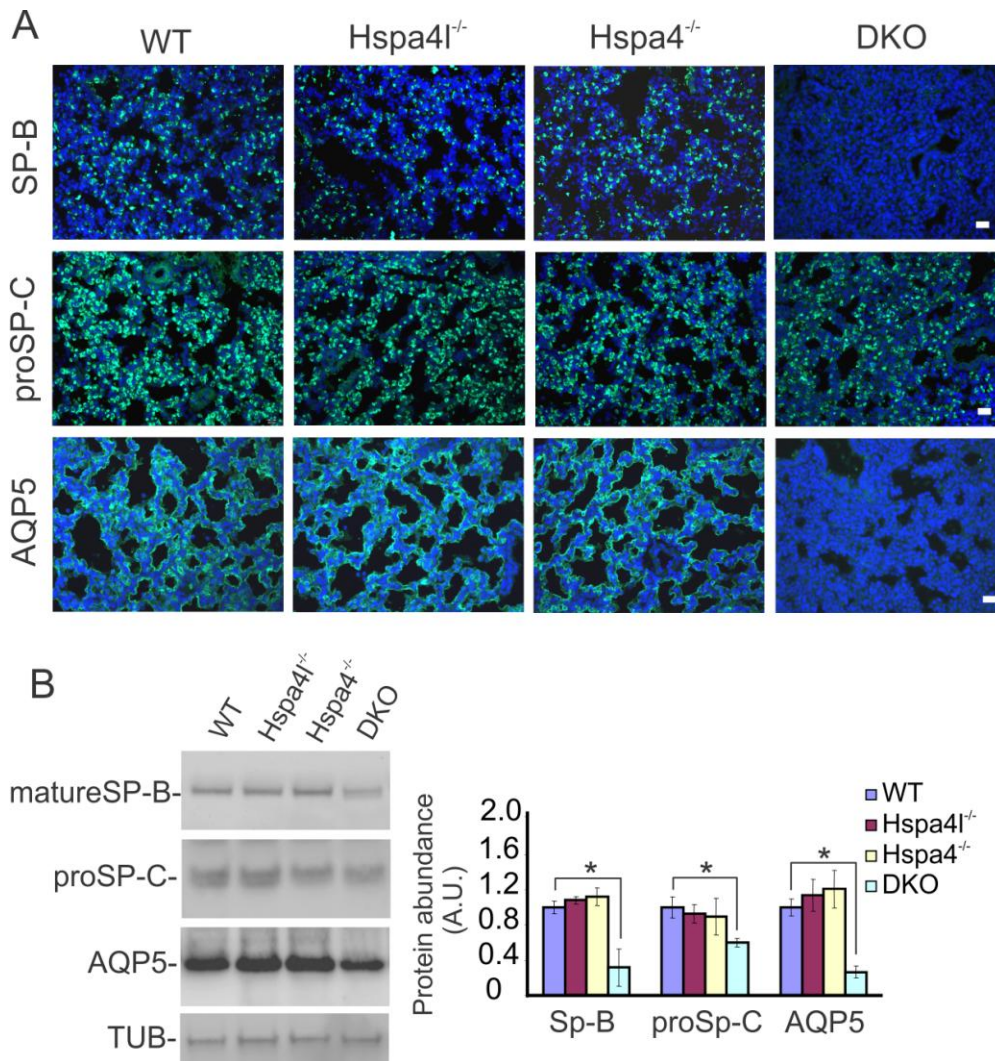


Figure 10. Diminished expression of SP-B, proSP-C and AQP5 in the lung of *Hspa4l*^{-/-} *Hspa4*^{-/-} embryos. (A) Histological sections of lungs from wild type (WT), *Hspa4l*^{-/-}, *Hspa4*^{-/-} and *Hspa4l*^{-/-} *Hspa4*^{-/-} (DKO) embryos at E18.5 were immunostained with antibodies against SP-B, proSP-C and AQP5. Scale bars: 20 μ m. (B) Immunoblotting of lung homogenates from different genotypes was probed with antibodies directed against SP-B, proSP-C, AQP5 and α -tubulin. In the bar graph presented in the right panel, expression levels of SP-B, proSP-C and AQP5 proteins were normalized to that of α -tubulin. Values are expressed as mean \pm SD. protein levels in WT lung served as reference. * P < 0.05 vs control, n = 3-4 per genotype. A.U. indicates arbitrary units. DKO, double knockout.

Normal growth of an organ depends on precise control of cell proliferation and cell death.

Cell proliferation not only sustains overall lung growth in the embryo, but also influences lung remodeling during stages of gestation (Weaver M et al., 2000). Many genes and signaling pathways critical to these processes have been described (Chinoy et al., 2001;

Compernelle et al., 2002; Wan et al., 2005; Martis et al., 2006; Ban et al., 2007; Shu et al., 2007). *Hspa4l* and *Hspa4* expressions are induced in carcinomas and are thought to play a role during proliferation (Kaneko et al., 1997a, b; Nakatsura et al., 2001; Gotoh et al., 2004; Tsapara et al., 2006; Takahashi et al., 2007; Li C et al., 2010). We assessed cell proliferation in the E18.5 lung of WT, *Hspa4l*^{-/-}, *Hspa4*^{-/-} and *Hspa4l*^{-/-} *Hspa4*^{-/-} embryos. Relative to WT, *Hspa4l*^{-/-} and *Hspa4*^{-/-} lungs, increased cell proliferation was demonstrated in *Hspa4l*^{-/-} *Hspa4*^{-/-} lungs as quantified by increased number of BrdU-positive cells and a significant upregulation of Cyclin D1 that is considered as one of the key factors regulating progression through the G1/S transition of the cell cycle (Hansen and Albrecht, 1999; Ciemerych and Sicinski, 2005; Golsteyn, 2005; Harper and Brooks, 2005).

It has been reported that alveolar and mesenchymal cells undergo apoptosis during normal lung development and maturation (Kresch et al., 1998; Scavo et al., 1998; Stiles et al., 2001; Sutherland et al., 2001). Precise control of the cell deletion by apoptosis is essential during normal lung development (De Paepe et al., 1999). A combination of *in situ* TUNEL assay and immunostaining for cleaved Caspase 3 was performed. As shown in Figure 11C and D, there was a significant decrease in the number of cleaved Caspase 3- and TUNEL-positive cells in the lung of E18.5 *Hspa4l*^{-/-} *Hspa4*^{-/-} embryos.

Taken together, increased cell proliferation and diminished cell apoptosis could be a potential mechanism contributing to increased mesenchymal thickness observed in the lung of *Hspa4l*^{-/-} *Hspa4*^{-/-} embryos.

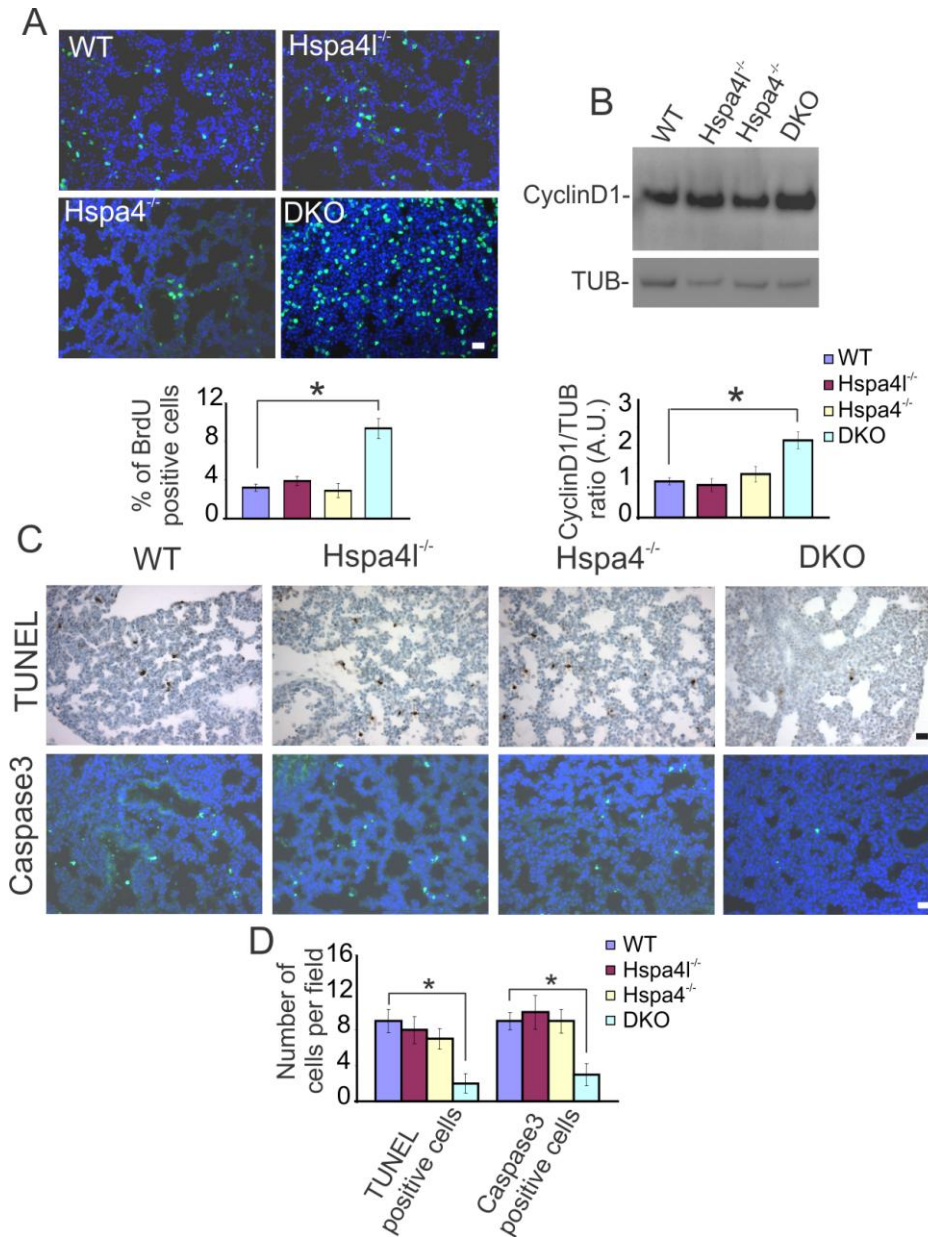


Figure 11. Increased proliferation and diminished apoptosis in the *Hspa4l*^{-/-} *Hspa4*^{-/-} lungs. (A) Immunofluorescence staining was performed using antibodies against BrdU in lung sections of wild type (WT), *Hspa4l*^{-/-}, *Hspa4*^{-/-} and *Hspa4l*^{-/-} *Hspa4*^{-/-} (DKO) embryos (upper panel). Bar= 20 μ m. Quantitation of BrdU-positive cells (lower panel). More than 1000 alveolar epithelial cells were randomly examined for each genotype for the statistical comparison. * $P < 0.05$ vs WT, $n = 3-4$ per genotype. (B) Western blotting was probed with antibodies directed against Cyclin D1 and α -tubulin (TUB). In the bar graph presented in the lower panel, expression levels of Cyclin D1 were normalized to that of α -tubulin. Values are expressed as mean \pm SD. Cyclin D1 protein levels in WT lung served as reference. * $P < 0.05$ vs control, $n = 3-4$ per genotype. A.U. indicates arbitrary units. (C) *In situ* TUNEL assay and cleaved Caspase 3 immunostaining. Bar= 20 μ m. (D) Quantitation of TUNEL- and Caspase 3-positive cells. * $P < 0.05$ vs WT, $n = 3-4$ per genotype. DKO, double knockout.

To verify whether simultaneous depletion of HSPA4L and HSPA4 impaired the chaperone activity in the lung, Western blotting with protein extracts from lung of WT, *Hspa4l*^{-/-}, *Hspa4*^{-/-} and *Hspa4l*^{-/-} *Hspa4*^{-/-} embryos at E18.5 was immunostained with anti-Ubiquitin antibody. As shown in Figure 12A, levels of ubiquitinated proteins were significantly increased in extract of *Hspa4l*^{-/-} *Hspa4*^{-/-} lung compared to that in lung extracts of other genotypes. Although, we have shown an increased accumulation of ubiquitinated proteins in the heart of postnatal *Hspa4*^{-/-} mice (Publication II), Western blot analysis did not show elevated levels of ubiquitinated proteins in the myocardial lysates derived from E18.5 *Hspa4l*^{-/-} *Hspa4*^{-/-} embryos (Fig. 12B). These results suggest that dual depletion of HSPA4L/HSPA4 affects the folding capacity of chaperones in the embryonic lung.

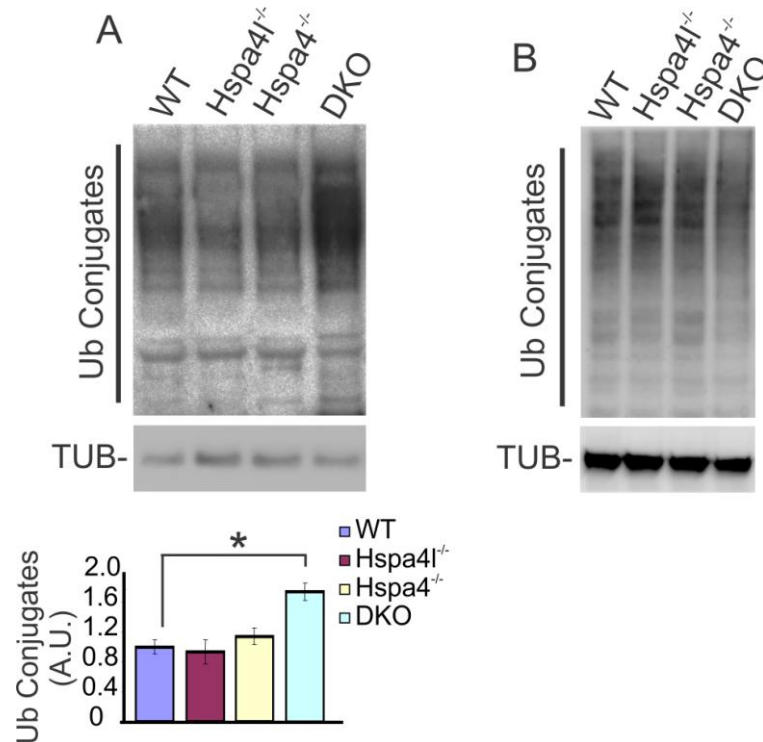


Figure 12. Increased accumulation of ubiquitinated proteins in *Hspa4l*^{-/-} *Hspa4*^{-/-} lungs. (A) Total ubiquitinated proteins in pulmonary protein extracts from E18.5 wild type (WT), *Hspa4l*^{-/-}, *Hspa4*^{-/-} and

Hspa4l^{-/-} Hspa4^{-/-} (DKO) embryos were analyzed by immunoblots (left panel). Histograms show relative abundance of ubiquitinated proteins in protein extracts (right panel). Expression of α -tubulin (TUB) was used as a loading control. Values are expressed in mean \pm SD. Ubiquitinated proteins in WT samples were expressed as 1.0. * $P < 0.05$ vs WT, $n = 4$ per group. A.U. indicates arbitrary units. (B) Western blotting for the abundance of ubiquitinated proteins in the heart of E18.5 WT, *Hspa4l^{-/-}*, *Hspa4^{-/-}* and DKO embryos. DKO, double knockout.

Increased accumulation of misfolded proteins above the threshold level impairs the functional capacity of the proteasome (Bennett et al., 2005). The ubiquitin- proteasome system (UPS) is also responsible for the degradation of the majority of cellular proteins that are no longer needed. Dysfunctional protein degradation will affect not only PQC but also many other cellular processes (Carrier et al., 2010; Fasanaro et al., 2010; Hedhli and Depre, 2010; Luo et al., 2010). Previous study has addressed the link between SPs synthesis and the efficient proteasomal activity. The result of this study revealed that impaired activity of proteasome in lung cell lines leads to inhibition of SPs synthesis, in particular SP-B and SP-C (Das and Boggaram, 2007). Moreover, mutations in SP-C *in vivo* and *in vitro* especially in BRICHOS domain are associated with accumulation of misfolded proteins and proteasomal dysfunction, which lead to deterioration of lung development (Bridges et al., 2003; Mulugeta et al., 2005). It will be important to deeply assess the proteasomal function in the lung of *Hspa4l^{-/-} Hspa4^{-/-}* mice to determine whether the proteasome is indeed defective. This will give a solid proof that the surfactant deficiency and neonatal lethality exhibited by *Hspa4l^{-/-} Hspa4^{-/-}* pups is indeed a consequence of proteasomal dysfunction. Taken together, our data suggest that ablation of deficiency of HSPA4L/HSPA4 leads to accumulation of misfolded and ubiquitinated proteins, which overwhelm and distort the capacity of proteasome in the lung of *Hspa4l^{-/-} Hspa4^{-/-}* pups.

We have demonstrated that HSPA4L and HSPA4 were ubiquitously expressed in the lung during prenatal and postnatal development. However, targeted disruption of either *Hspa4l* or *Hspa4* did not impair embryonic development. Growth retardation and impaired lung maturation demonstrated in *Hspa4l*^{-/-} *Hspa4*^{-/-} embryos suggest that a possible functional redundancy might exist between HSPA4L and HSPA4 during embryonic development.

In conclusion, our *in vivo* data provide novel molecular evidence of previously unknown contribution of both HSPA4L and HSPA4 to the maturation of alveolar epithelium.

3.5. Generation of *Hsph1* conditional KO and *Hspa4/Hsph1* DKO mice

In order to determine the physiological function of the third member of *Hsp110* family, namely *Hsph1* gene, we generated *Hsph1* deficient mice. To generate *Hsph1* chimeric mice, we used commercial *Hsph1* recombinant embryonic stem cells (ESCs) produced by European Conditional Mouse Mutagenesis Program (EUCOMM). The genome of homologous recombinant ES cells contains 2 loxP sites, which flank exons 9 and 10 of *Hsph1* gene (Fig. 13A). To verify the correct homologous recombination in *Hsph1* gene, Southern hybridization was performed. The external probe detected a 15.5-kb *Bam*HI fragment of the WT allele and a 11.5-kb *Bam*HI recombinant fragment of the floxed allele (Fig. 13B). The recombinant ESCs were injected into C57BL/6J blastocysts. The microinjected blastocysts were transferred into uteri of pseudopregnant females. We obtained two germ-line transmitting chimeras, which were mated with C57Bl/6J females to produce heterozygous mice (*Hsph1*^{F/+}). To delete the floxed sequence, heterozygous mice were intercrossed with *CreEII* transgenic mice. The *CreEII* transgenic mice have the Cre-recombinase gene under the control of the *EII* promoter, which directs transcription

of Cre-recombinase in oocyte and 1-cell stage of embryonic development. Expression of *CreEII* results in deletion of floxed *Hsph1* sequences in all cells of the developing embryo including the germ cells (Lakso et al., 1996). To determine whether Cre-mediated recombination was successful, we analyzed genomic DNA of the progeny using PCR with oligonucleotide primers F1, F2 and R. The PCR amplifies a 322-bp fragment of WT, a 350-bp fragment of floxed and a 420-bp fragment of deleted *Hsph1* alleles (Fig. 13C). RT-PCR with RNA isolated from the brain confirmed the absence of *Hsph1* transcript in *Hsph1*^{Δ/Δ} mice (Fig. 13D).

Breeding of *Hsph1*^{Δ/+} animals produced *Hsph1*^{+/+}, *Hsph1*^{Δ/+}, and *Hsph1*^{Δ/Δ} litters. Of 220 pups born and examined at the age of 3 to 4 weeks, 56 were *Hsph1*^{+/+}, 111 were *Hsph1*^{Δ/+}, and 53 were *Hsph1*^{Δ/Δ}. These numbers are compatible with Mendelian ratios expected for nondeleterious alleles. Thus, *Hsph1* is not essential for embryonic development or viability of adult animals. The *Hsph1*^{Δ/Δ} mice did not show overt abnormalities. Histological analysis of various tissues failed to detect any significant differences between *Hsph1*^{Δ/Δ} and WT mice (data not shown). During our work to generate *Hsph1* KO mice, two reports have described the consequence of targeted disruption of *Hsph1* gene (Nakamura et al., 2008; Eroglu et al., 2010). Nakamura et al. (2008) have reported that the HSPH1 deletion did not affect the embryonic development, viability and fertility of mutant mice. However, *Hsph1* KO mice are resistant to ischemic injury and that the protective effects of HSPH1 deficiency in cerebral ischemia may be mediated by an increase in the chaperone activity of HSP70. Results of other group have demonstrated that lack of HSPH1 in mice is associated with tauopathy and neurodegeneration, which suggests that HSPH1 plays a protective role against

neurodegenerative diseases such as Alzheimer's disease and other tauopathies (Eroglu et al., 2010).

To address whether there is a functional redundancy between HSPA4 and HSPH1, we decided to generate *Hspa4/Hsph1* DKO mice. Toward this end, *Hspa4*^{+/-} mice were bred with *Hsph1*^{Δ/Δ} mice to obtain *Hspa4*^{+/-} *Hsph1*^{Δ/+}, which will be intercrossed in order to have *Hspa4*^{-/-} *Hsph1*^{Δ/Δ} mice. Analysis and characterization of the *Hspa4*^{-/-} *Hsph1*^{Δ/Δ} mice will be undertaken.

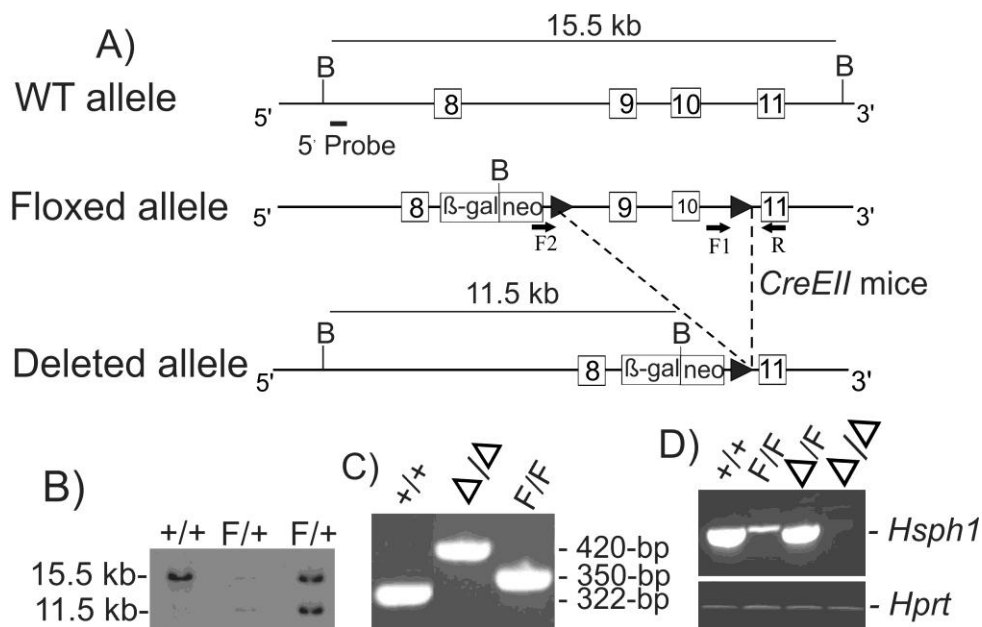


Figure 13. Generation of *Hsph1* conditional KO mice and analysis of genotypes. A, Schematic diagram of targeting strategy. Arrows indicate the primers used for genotyping. Black triangles indicate loxP sites. Exons 9 and 10 (open boxed 9 and 10) were flanked by loxP sites and can be excised by Cre recombinase. Abbreviations: B, *Bam*HI; neo, neomycin resistant cassette; β-gal, β-galactosidase cassette. B, Southern blot analysis of WT and targeted ESCs DNA using a 5' external probe. Genomic DNA extracted from ESCs was digested with *Bam*HI and probed with an external probe, which detected a 15.5-kb *Bam*HI fragment in the WT allele and a 11.5-kb *Bam*HI recombinant fragment in conditional allele. Locations of the probes are indicated in A. C, Genotyping of various *Hsph1* alleles by PCR of DNA isolated from mice tail. Primers are designed to distinguish WT (+/+, 322-bp), floxed (F/F, 350-bp), and deleted (Δ/Δ, 420-bp) *Hsph1* alleles. D, RT-PCR analysis was performed with RNA of brain from *Hsph1*^{+/+}, *Hsph1*^{F/F}, *Hsph1*^{Δ/F} and *Hsph1*^{Δ/Δ} animals. A 450-bp product of *Hsph1* gene was obtained from RNA of *Hsph1*^{+/+}, *Hsph1*^{F/F} and *Hsph1*^{Δ/F} animals, but no band was visible in case of *Hsph1*^{Δ/Δ} mice. The integrity of the RNA was verified by using *Hprt* primers.

4. References

Adham IM, Nayernia K, Burkhardt-Göttges E, Topaloglu O, Dixkens C, Holstein AF, Engel W (2001): Teratozoospermia in mice lacking the transition protein 2 (Tnp2). *Mol Hum Reprod* 7, 513-520

Adly MA, Assaf HA, Hussein MR (2008): Heat shock protein 27 expression in the human testis showing normal and abnormal spermatogenesis. *Cell Biol Int* 32, 1247-1255

Allen JW, Dix DJ, Collins BW, Merrick BA, He C, Selkirk JK, Poorman-Allen P, Dresser ME, Eddy EM (1996): HSP70-2 is part of the synaptonemal complex in mouse and hamster spermatocytes. *Chromosoma* 104, 414-421

Allen RL, O'Brien DA, Jones CC, Rockett DL, Eddy EM (1988): Expression of heat shock proteins by isolated mouse spermatogenic cells. *Mol Cell Biol* 8, 3260-3266

Baek KH, Mondoux MA, Jaster R, Fire-Levin E, D'Andrea AD (2001): DUB-2A, a new member of the DUB subfamily of hematopoietic deubiquitinating enzymes. *Blood* 98, 636-642

Ban N, Matsumura Y, Sakai H, Takanezawa Y, Sasaki M, Arai H, Inagaki N (2007): ABCA3 as a lipid transporter in pulmonary surfactant biogenesis. *J Biol Chem* 282, 9628-9634

Bates G (2003): Huntingtin aggregation and toxicity in Huntington's disease. *Lancet* 361, 1642-1644

Bellusci S, Furuta Y, Rush MG, Henderson R, Winnier G, Hogan BL (1997): Involvement of Sonic hedgehog (Shh) in mouse embryonic lung growth and morphogenesis. *Development* 124, 53-63

Bennett EJ, Bence NF, Jayakumar R, Kopito RR (2005): Global impairment of the ubiquitin-proteasome system by nuclear or cytoplasmic protein aggregates precedes inclusion body formation. *Mol Cell* 17, 351-365

Berke SJ, Paulson HL (2003): Protein aggregation and the ubiquitin proteasome pathway: gaining the UPPER hand on neurodegeneration. *Curr Opin Genet Dev* 13, 253-261

Bhaskaran M, Kolliputi N, Wang Y, Gou D, Chintagari NR, Liu L (2007): Trans-differentiation of alveolar epithelial type II cells to type I cells involves autocrine signaling by transforming growth factor beta 1 through the Smad pathway. *J Biol Chem* 282, 3968-3976

- Bhattacharya B, Miura T, Brandenberger R, Mejido J, Luo Y, Yang AX, Joshi BH, Ginis I, Thies RS, Amit M et al. (2004): Gene expression in human embryonic stem cell lines: unique molecular signature. *Blood* 103, 2956-2964
- Birks EJ, Latif N, Enesa K, Folkvang T, Luong le A, Sarathchandra P, Khan M, Ovaa H, Terracciano CM, Barton PJ et al. (2008): Elevated p53 expression is associated with dysregulation of the ubiquitin-proteasome system in dilated cardiomyopathy. *Cardiovasc Res* 79, 472-480
- Bitgood MJ, Shen L, McMahon AP (1996): Sertoli cell signaling by Desert hedgehog regulates the male germline. *Curr Biol* 6, 298-304
- Boggaram V (2003): Regulation of lung surfactant protein gene expression. *Front Biosci* 8, d751-764
- Bradbury J (2003): Alpha-synuclein gene triplication discovered in Parkinson's disease. *Lancet Neurol* 2, 715
- Bridges JP, Wert SE, Noguee LM, Weaver TE (2003): Expression of a human surfactant protein C mutation associated with interstitial lung disease disrupts lung development in transgenic mice. *J Biol Chem* 278, 52739-52746
- Burnicka-Turek O, Shirneshan K, Paprotta I, Grzmil P, Meinhardt A, Engel W, Adham IM (2009): Inactivation of insulin-like factor 6 disrupts the progression of spermatogenesis at late meiotic prophase. *Endocrinology* 150, 4348-4357
- Cai WF, Zhang XW, Yan HM, Ma YG, Wang XX, Yan J, Xin BM, Lv XX, Wang QQ, Wang ZY et al. (2010): Intracellular or extracellular heat shock protein 70 differentially regulates cardiac remodelling in pressure overload mice. *Cardiovasc Res* 88, 140-149
- Carrier L, Schlossarek S, Willis MS, Eschenhagen T (2010): The ubiquitin-proteasome system and nonsense-mediated mRNA decay in hypertrophic cardiomyopathy. *Cardiovasc Res* 85, 330-338
- Caughey B, Lansbury PT (2003): Protofibrils, pores, fibrils, and neurodegeneration: separating the responsible protein aggregates from the innocent bystanders. *Annu Rev Neurosci* 26, 267-298
- Chen Q, Liu JB, Horak KM, Zheng H, Kumarapeli AR, Li J, Li F, Gerdes AM, Wawrousek EF, Wang X (2005): Intracellular amyloidosis impairs proteolytic function of proteasomes in cardiomyocytes by compromising substrate uptake. *Circ Res* 97, 1018-1026

Chen X, Easton D, Oh HJ, Lee-Yoon DS, Liu X, Subjeck J (1996): The 170 kDa glucose regulated stress protein is a large HSP70-, HSP110-like protein of the endoplasmic reticulum. *FEBS Lett* 380, 68–72

Chinoy MR, Chi X, Cilley RE (2001): Down-regulation of regulatory proteins for differentiation and proliferation in murine fetal hypoplastic lungs: altered mesenchymal-epithelial interactions. *Pediatr Pulmonol* 32, 129-141

Ciemerych MA, Sicinski P (2005): Cell cycle in mouse development. *Oncogene* 24, 2877-2898

Clark JC, Wert SE, Bachurski CJ, Stahlman MT, Stripp BR, Weaver TE, Whitsett JA (1995): Targeted disruption of the surfactant protein B gene disrupts surfactant homeostasis, causing respiratory failure in newborn mice. *Proc Natl Acad Sci USA* 92, 7794-7798

Clark JC, Tichelaar JW, Wert SE, Itoh N, Perl AK, Stahlman MT, Whitsett JA (2001): FGF-10 disrupts lung morphogenesis and causes pulmonary adenomas in vivo. *Am J Physiol Lung Cell Mol Physiol* 280, L705-715

Collins PL, Hightower LE (1982): Newcastle disease virus stimulates the cellular accumulation of stress (heat shock) mRNAs and proteins. *J Virol* 44, 703-707

Compernelle V, Brusselmans K, Acker T, Hoet P, Tjwa M, Beck H, Plaisance S, Dor Y, Keshet E, Lupu F et al. (2002): Loss of HIF-2alpha and inhibition of VEGF impair fetal lung maturation, whereas treatment with VEGF prevents fatal respiratory distress in premature mice. *Nat Med* 8, 702-710

Crawford KC, Vega Flores M, Oehlers SH, Hall CJ, Crosier KE, Crosier PS (2011): Zebrafish heat shock protein a4 genes in the intestinal epithelium are up-regulated during inflammation. *Genesis* 49, 905-911

Culty M (2009): Gonocytes, the forgotten cells of the germ cell lineage. *Birth Defects Res C Embryo Today* 87, 1-26

Das A, Boggaram V (2007): Proteasome dysfunction inhibits surfactant protein gene expression in lung epithelial cells: mechanism of inhibition of SP-B gene expression. *Am J Physiol Lung Cell Mol Physiol* 292, L74-84

Dehne T, Schenk R, Perka C, Morawietz L, Pruss A, Sittlinger M, Kaps C, Ringe J (2010): Gene expression profiling of primary human articular chondrocytes in high-density micromasses reveals patterns of recovery, maintenance, re- and dedifferentiation. *Gene* 462, 8-17

De Moerlooze L, Spencer-Dene B, Revest JM, Hajihosseini M, Rosewell I, Dickson C (2000): An important role for the IIIb isoform of fibroblast growth factor receptor 2

(FGFR2) in mesenchymal-epithelial signalling during mouse organogenesis. *Development* 127, 483-492

De Paepe ME, Sardesai MP, Johnson BD, Lesieur-Brooks AM, Papadakis K, Luks FI (1999): The role of apoptosis in normal and accelerated lung development in fetal rabbits. *J Pediatr Surg* 34, 863-870

Dix DJ, Allen JW, Collins BW, Mori C, Nakamura N, Poorman-Allen P, Goulding EH, Eddy EM (1996): Targeted gene disruption of Hsp70-2 results in failed meiosis, germ cell apoptosis, and male infertility. *Proc Natl Acad Sci USA* 93, 3264-3268

Dix DJ, Allen JW, Collins BW, Poorman-Allen P, Mori C, Blizard DR, Brown PR, Goulding EH, Strong BD, Eddy EM (1997): HSP70-2 is required for desynapsis of synaptonemal complexes during meiotic prophase in juvenile and adult mouse spermatocytes. *Development* 124, 4595-4603

Dix DJ, Hong RL (1998): Protective mechanisms in germ cells: stress proteins in spermatogenesis. *Adv Exp Med Biol* 444, 137-143

Dragovic Z, Broadley SA, Shomura Y, Bracher A, Hartl FU (2006): Molecular chaperones of the Hsp110 family act as nucleotide exchange factors of Hsp70s. *EMBO J* 25, 2519-2528

Eddy EM, McGee RS, Willis WD, O'Brien DA (1991): Immunodissection of sperm surface modifications during epididymal maturation. *Bull Assoc Anat (Nancy)* 75, 139-144

Eroglu B, Moskophidis D, Mivechi NF (2010): Loss of Hsp110 leads to age-dependent tau hyperphosphorylation and early accumulation of insoluble amyloid beta. *Mol Cell Biol* 30, 4626-4643

Fasanaro P, Capogrossi MC, Martelli F (2010): Regulation of the endothelial cell cycle by the ubiquitin-proteasome system. *Cardiovasc Res* 85, 272-280

Feng HL, Sandlow JI, Sparks AE (2001): Decreased expression of the heat shock protein hsp70-2 is associated with the pathogenesis of male infertility. *Fertil Steril* 76, 1136-1139

Finkel T, Holbrook NJ (2000): Oxidants, oxidative stress and the biology of ageing. *Nature* 408, 239-247

Foltz KR, Partin JS, Lennarz WJ (1993): Sea urchin egg receptor for sperm: sequence similarity of binding domain and hsp70. *Science* 259, 1421-1425

Froment P, Staub C, Hembert S, Pisselet C, Magistrini M, Delaleu B, Seurin D, Levine JE, Johnson L, Binoux M et al. (2004): Reproductive abnormalities in human insulin-like growth factor-binding protein-1 transgenic male mice. *Endocrinology* 145, 2080-2091

Fung KL, Hilgenberg L, Wang NM, Chirico WJ (1996): Conformations of the nucleotide and polypeptide binding domains of a cytosolic Hsp70 molecular chaperone are coupled. *J Biol Chem* 271, 21559-21565

Gething MJ (1997): Protein folding. The difference with prokaryotes. *Nature* 388, 329-331

Gething MJ, Sambrook J (1992): Protein folding in the cell. *Nature* 355, 33-45

Golsteyn RM (2005): Cdk1 and Cdk2 complexes (cyclin dependent kinases) in apoptosis: a role beyond the cell cycle. *Cancer Lett* 217, 129-138

Goto M, Koji T, Mizuno K, Tamaru M, Koikeda S, Nakane PK, Mori N, Masamune Y, Nakanishi Y (1990): Transcription switch of two phosphoglycerate kinase genes during spermatogenesis as determined with mouse testis sections in situ. *Exp Cell Res* 186, 273-278

Gotoh K, Nonoguchi K, Higashitsuji H, Kaneko Y, Sakurai T, Sumitomo Y, Itoh K, Subjeck JR, Fujita J (2004): Apg-2 has a chaperone-like activity similar to Hsp110 and is overexpressed in hepatocellular carcinomas. *FEBS Lett* 560, 19-24

Gregory TJ, Longmore WJ, Moxley MA, Whitsett JA, Reed CR, Fowler AA 3rd, Hudson LD, Maunder RJ, Crim C, Hyers TM (1991): Surfactant chemical composition and biophysical activity in acute respiratory distress syndrome. *J Clin Invest* 88, 1976-1981

Hansen LK, Albrecht JH (1999): Regulation of the hepatocyte cell cycle by type I collagen matrix: role of cyclin D1. *J Cell Sci* 112, 2971-2981

Harper JV, Brooks G (2005): The mammalian cell cycle: an overview. *Methods Mol Biol* 296, 113-153

Hartl FU (1991): Heat shock proteins in protein folding and membrane translocation. *Semin Immunol* 3, 5-16

Hartl FU (1996): Molecular chaperones in cellular protein folding. *Nature* 381, 571-580

Hatayama T, Yasuda K, Yasuda K (1998): Association of HSP105 with HSC70 in high molecular mass complexes in mouse FM3A cells. *Biochem Biophys Res Commun* 248, 395-401

Hayashi M, Imanaka-Yoshida K, Yoshida T, Wood M, Fearn C, Tatake RJ, Lee JD (2006): A crucial role of mitochondrial Hsp40 in preventing dilated cardiomyopathy. *Nat Med* 12, 128-132

- He TC, Zhou S, da Costa LT, Yu J, Kinzler KW, Vogelstein B (1998): A simplified system for generating recombinant adenoviruses. *Proc Natl Acad Sci USA* 95, 2509-2514
- Hedhli N, Depre C (2010): Proteasome inhibitors and cardiac cell growth. *Cardiovasc Res* 85, 321-329
- Hein S, Arnon E, Kostin S, Schönburg M, Elsässer A, Polyakova V, Bauer EP, Klövekorn WP, Schaper J (2003): Progression from compensated hypertrophy to failure in the pressure-overloaded human heart: structural deterioration and compensatory mechanisms. *Circulation* 107, 984-991
- Held T, Paprotta I, Khulan J, Hemmerlein B, Binder L, Wolf S, Schubert S, Meinhardt A, Engel W, Adham IM (2006): Hspa4l-deficient mice display increased incidence of male infertility and hydronephrosis development. *Mol Cell Biol* 26, 8099-8108
- Heling A, Zimmermann R, Kostin S, Maeno Y, Hein S, Devaux B, Bauer E, Klövekorn WP, Schlepper M, Schaper W et al. (2000): Increased expression of cytoskeletal, linkage, and extracellular proteins in failing human myocardium. *Circ Res* 86, 846-853
- Hishiya A, Takayama S (2008): Molecular chaperones as regulators of cell death. *Oncogene* 27, 6489-6506
- Huszar G, Stone K, Dix D, Vigue L (2000): Putative creatine kinase M-isoform in human sperm is identified as the 70-kilodalton heat shock protein HspA2. *Biol Reprod* 63, 925-932
- Ikawa M, Wada I, Kominami K, Watanabe D, Toshimori K, Nishimune Y, Okabe M (1997): The putative chaperone calmeglin is required for sperm fertility. *Nature* 387, 607-611
- Ikegami M, Dhami R, Schuchman EH (2003): Alveolar lipoproteinosis in an acid sphingomyelinase-deficient mouse model of Niemann-Pick disease. *Am J Physiol Lung Cell Mol Physiol* 284, L518-525
- Kaneko Y, Kimura T, Kishishita M, Noda Y, Fujita J (1997a): Cloning of apg-2 encoding a novel member of heat shock protein 110 family. *Gene* 189, 19-24
- Kaneko Y, Nishiyama H, Nonoguchi K, Higashitsuji H, Kishishita M, Fujita J (1997b): A novel hsp110-related gene, apg-1, that is abundantly expressed in the testis responds to a low temperature heat shock rather than the traditional elevated temperatures. *Biol Chem* 272, 2640-2645
- Kang CM, Park KP, Cho CK, Seo JS, Park WY, Lee SJ, Lee YS (2002): Hspa4 (HSP70) is involved in the radioadaptive response: results from mouse splenocytes. *Radiat Res* 157, 650-655

Kashiwabara S, Arai Y, Kodaira K, Baba T (1990): Acrosin biosynthesis in meiotic and postmeiotic spermatogenic cells. *Biochem Biophys Res Commun* 173, 240-245

Khandjian EW, Türlér H (1983): Simian virus 40 and polyoma virus induce synthesis of heat shock proteins in permissive cells. *Mol Cell Biol* 3, 1-8

Kim AY, Bommeljé CC, Lee BE, Yonekawa Y, Choi L, Morris LG, Huang G, Kaufman A, Ryan RJ, Hao B et al. (2008): SCCRO (DCUN1D1) is an essential component of the E3 complex for neddylation. *J Biol Chem* 283, 33211-33220

Kim H, Huh PW, Kim C, Kim YJ, Park EM, Park YM (2001): Cerebral activation and distribution of inducible hsp110 and hsp70 mRNAs following focal ischemia in rat. *Toxicology* 167, 135-144

Kim YK, Suarez J, Hu Y, McDonough PM, Boer C, Dix DJ, Dillmann WH (2006): Deletion of the inducible 70-kDa heat shock protein genes in mice impairs cardiac contractile function and calcium handling associated with hypertrophy. *Circulation* 113, 2589-2597

Kleene KC, Flynn JF (1987): Characterization of a cDNA clone encoding a basic protein, TP2, involved in chromatin condensation during spermiogenesis in the mouse. *J Biol Chem* 262, 17272-17277

Koh HS, Moon IS, Lee YH, Shong M, Kwon OY (2000): Expression of an HSP110 family, ischemia-responsive protein (irp94), in the rat brain after transient forebrain ischemia. *Z Naturforsch C* 55, 449-454

Kojima R, Randall J, Brenner BM, Gullans SR. Osmotic stress protein 94 (Osp94) (1996): A new member of the Hsp110/SSE gene subfamily. *J Biol Chem* 271, 12327-12332

Kojima R, Randall JD, Ito E, Manshio H, Suzuki Y, Gullans SR (2004): Regulation of expression of the stress response gene, Osp94: identification of the tonicity response element and intracellular signalling pathways. *Biochem J* 380, 783-794

Kostin S, Pool L, Elsässer A, Hein S, Drexler HC, Arnon E, Hayakawa Y, Zimmermann R, Bauer E, Klövekorn WP et al. (2003): Myocytes die by multiple mechanisms in failing human hearts. *Circ Res* 92, 715-724

Kourokou Y, Fujita E, Tanida I, Ueno T, Isoai A, Kumagai H, Ogawa S, Kaufman RJ, Kominami E, Momoi T (2007): ER stress (PERK/eIF2alpha phosphorylation) mediates the polyglutamine-induced LC3 conversion, an essential step for autophagy formation. *Cell Death Differ* 14, 230-239

Kremling H, Keime S, Wilhelm K, Adham IM, Hameister H, Engel W (1991): Mouse proacrosin gene: nucleotide sequence, diploid expression, and chromosomal localization. *Genomics* 11, 828-834

Kresch MJ, Christian C, Wu F, Hussain N (1998): Ontogeny of apoptosis during lung development. *Pediatr Res* 43, 426-431

Kumarapeli AR, Su H, Huang W, Tang M, Zheng H, Horak KM, Li M, Wang X (2008): Alpha B-crystallin suppresses pressure overload cardiac hypertrophy. *Circ Res* 103, 1473-1482

Kunisada K, Tone E, Fujio Y, Matsui H, Yamauchi-Takahara K, Kishimoto T (1998): Activation of gp130 transduces hypertrophic signals via STAT3 in cardiac myocytes. *Circulation* 98, 346-352

Kunisada K, Negoro S, Tone E, Funamoto M, Osugi T, Yamada S, Okabe M, Kishimoto T, Yamauchi-Takahara K (2000): Signal transducer and activator of transcription 3 in the heart transduces not only a hypertrophic signal but a protective signal against doxorubicin-induced cardiomyopathy. *Proc Natl Acad Sci USA* 97, 315-319

Kuwahara K, Saito Y, Takano M, Arai Y, Yasuno S, Nakagawa Y, Takahashi N, Adachi Y, Takemura G, Horie M et al. (2003): NRSF regulates the fetal cardiac gene program and maintains normal cardiac structure and function. *EMBO J* 22, 6310-6321

Lakso M, Pichel JG, Gorman JR, Sauer B, Okamoto Y, Lee E, Alt FW, Westphal H (1996): Efficient in vivo manipulation of mouse genomic sequences at the zygote stage. *Proc Natl Acad Sci USA* 93, 5860-5865

Lammers JH, Offenberger HH, van Aalderen M, Vink AC, Dietrich AJ, Heyting C (1994): The gene encoding a major component of the lateral elements of synaptonemal complexes of the rat is related to X-linked lymphocyte-regulated genes. *Mol Cell Biol* 14, 1137-1146

Landry J, Bernier D, Chrétien P, Nicole LM, Tanguay RM, Marceau N (1982): Synthesis and degradation of heat shock proteins during development and decay of thermotolerance. *Cancer Res* 42, 2457-2461

La Thangue NB, Latchman DS (1988): A cellular protein related to heat-shock protein 90 accumulates during herpes simplex virus infection and is overexpressed in transformed cells. *Exp Cell Res* 178, 169-179

Lee MY, Choi YS, Choi JS, Min DS, Chun MH, Kim ON, Lee SB, Kim SY (2002): An immunohistochemical study of APG-2 protein in the rat hippocampus after transient forebrain ischemia. *Brain Res* 924, 237-241

- Lee-Yoon D, Easton D, Murawski M, Burd R, Subject JR (1995): Identification of a major subfamily of large hsp70-like proteins through the cloning of the mammalian 110-kDa heat shock protein. *J Biol Chem* 270, 15725-15733
- Levinson W, Oppermann H, Jackson J (1980): Transition series metals and sulfhydryl reagents induce the synthesis of four proteins in eukaryotic cells. *Biochim Biophys Acta* 606, 170-180
- Li C, Liu D, Yuan Y, Huang S, Shi M, Tao K, Feng W (2010): Overexpression of Apg-2 increases cell proliferation and protects from oxidative damage in BaF3-BCR/ABL cells. *Int J Oncol* 36, 899-904
- Li GC (1985): Elevated levels of 70,000 dalton heat shock protein in transiently thermotolerant Chinese hamster fibroblasts and in their stable heat resistant variants. *Int J Radiat Oncol Biol Phys* 11, 165-177
- Li GC, Laszlo A (1985): Amino acid analogs while inducing heat shock proteins sensitize CHO cells to thermal damage. *J Cell Physiol* 122, 91-97
- Litingtung Y, Lei L, Westphal H, Chiang C (1998): Sonic hedgehog is essential to foregut development. *Nat Genet* 20, 58-61
- Liu J, Chen Q, Huang W, Horak KM, Zheng H, Mestrlil R, Wang X (2006): Impairment of the ubiquitin- proteasome system in desminopathy mouse hearts. *FASEB J* 20, 362-364
- Luo W, Zhong J, Chang R, Hu H, Pandey A, Semenza GL (2010): Hsp70 and CHIP selectively mediate ubiquitination and degradation of hypoxia-inducible factor (HIF)-1alpha but Not HIF-2alpha. *J Biol Chem* 285, 3651-3663
- Maeda Y, Davé V, Whitsett JA (2007): Transcriptional control of lung morphogenesis. *Physiol Rev* 87, 219-244
- Mann DL, Bristow MR (2005): Mechanisms and models in heart failure: the biomechanical model and beyond. *Circulation* 111, 2837-2849
- Martis PC, Whitsett JA, Xu Y, Perl AK, Wan H, Ikegami M (2006): C/EBPalpha is required for lung maturation at birth. *Development* 133, 1155-1164
- Mauk R, Jaworski D, Kamei N, Glabe CG (1997): Identification of a 97-kDa heat shock protein from *S. franciscanus* ovaries with 94% amino acid identity to the *S. purpuratus* egg surface receptor for sperm. *Dev Biol* 184, 31-37
- McCarty JS, Buchberger A, Reinstein J, Bukau B (1995): The role of ATP in the functional cycle of the DnaK chaperone system. *J Mol Biol* 249, 126-137

- Meinhardt A, Wilhelm B, Seitz J (1999): Expression of mitochondrial marker proteins during spermatogenesis. *Hum Reprod Update* 5, 108-119
- Mendelsohn C, Lohnes D, Décimo D, Lufkin T, LeMeur M, Chambon P, Mark M (1994): Function of the retinoic acid receptors (RARs) during development (II). Multiple abnormalities at various stages of organogenesis in RAR double mutants. *Development* 120, 2749-2771
- Messina V, Di Sauro A, Pedrotti S, Adesso L, Latina A, Geremia R, Rossi P, Sette C (2010): Differential contribution of the MTOR and MNK pathways to the regulation of mRNA translation in meiotic and postmeiotic mouse male germ cells. *Biol Reprod* 83, 607-615
- Min H, Danilenko DM, Scully SA, Bolon B, Ring BD, Tarpley JE, DeRose M, Simonet WS (1998): Fgf-10 is required for both limb and lung development and exhibits striking functional similarity to *Drosophila* branchless. *Genes Dev* 12, 3156-3161
- Molkentin JD, Lu JR, Antos CL, Markham B, Richardson J, Robbins J, Grant SR, Olson EN (1998): A calcineurin-dependent transcriptional pathway for cardiac hypertrophy. *Cell* 93, 215-228
- Mori C, Nakamura N, Dix DJ, Fujioka M, Nakagawa S, Shiota K, Eddy EM (1997): Morphological analysis of germ cell apoptosis during postnatal testis development in normal and Hsp 70-2 knockout mice. *Dev Dyn* 208, 125-136
- Morimoto RI (2011): The heat shock response: systems biology of proteotoxic stress in aging and disease. *Cold Spring Harb Symp Quant Biol* 76, 91-99
- Morimoto RI, Tissieres A, Georgopoulos C, eds.: *Heat Shock Proteins: Structure, Function and Regulation*. Cold Spring Harbor Lab. Press. Cold Spring Harbor, NY. 1994
- Morozov A, Subject J, Raychaudhuri P (1995): HPV16 E7 oncoprotein induces expression of a 110 kDa heat shock protein. *FEBS Lett* 371, 214-218
- Müller P, Kazakov A, Semenov A, Böhm M, Laufs U (2008): Pressure-induced cardiac overload induces upregulation of endothelial and myocardial progenitor cells. *Cardiovasc Res* 77, 151-159
- Mukai H, Kuno T, Tanaka H, Hirata D, Miyakawa T, Tanaka C (1993): Isolation and characterization of SSE1 and SSE2, new members of the yeast HSP70 multigene family. *Gene* 132, 57-66
- Mulugeta S, Nguyen V, Russo SJ, Muniswamy M, Beers MF (2005): A surfactant protein C precursor protein BRICHOS domain mutation causes endoplasmic reticulum stress, proteasome dysfunction, and caspase 3 activation. *Am J Respir Cell Mol Biol* 32, 521-530

- Nakamura J, Fujimoto M, Yasuda K, Takeda K, Akira S, Hatayama T, Takagi Y, Nozaki K, Hosokawa N, Nagata K (2008): Targeted disruption of Hsp110/105 gene protects against ischemic stress. *Stroke* 39, 2853-2859
- Nakatsura T, Senju S, Yamada K, Jotsuka T, Ogawa M, Nishimura Y (2001): Gene cloning of immunogenic antigens overexpressed in pancreatic cancer. *Biochem Biophys Res Commun* 281, 936-944
- Nayernia K, Adham IM, Burkhardt-Göttges E, Neesen J, Rieche M, Wolf S, Sancken U, Kleene K, Engel W (2002): Asthenozoospermia in mice with targeted deletion of the sperm mitochondrion-associated cysteine-rich protein (Smcp) gene. *Mol Cell Biol* 22, 3046-3052
- Nogee LM, Garnier G, Dietz HC, Singer L, Murphy AM, deMello DE, Colten HR (1994): A mutation in the surfactant protein B gene responsible for fatal neonatal respiratory disease in multiple kindreds. *J Clin Invest* 93, 1860-1863
- Nogee LM, Wert SE, Proffitt SA, Hull WM, Whitsett JA (2000): Allelic heterogeneity in hereditary surfactant protein B (SP-B) deficiency. *Am J Respir Crit Care Med* 161, 973-981
- Nonoguchi K, Itoh K, Xue JH, Tokuchi H, Nishiyama H, Kaneko Y, Tatsumi K, Okuno H, Tomiwa K, Fujita J (1999): Cloning of human cDNAs for Apg-1 and Apg-2, members of the Hsp110 family, and chromosomal assignment of their genes. *Gene* 237, 21-28
- Nonoguchi K, Tokuchi H, Okuno H, Watanabe H, Egawa H, Saito K, Ogawa O, Fujita J (2001): Expression of Apg-1, a member of the Hsp110 family, in the human testis and sperm. *Int J Urol* 8, 308-314
- Norton N, Li D, Rieder MJ, Siegfried JD, Rampersaud E, Züchner S, Mangos S, Gonzalez-Quintana J, Wang L, McGee S et al. (2011): Genome-wide studies of copy number variation and exome sequencing identify rare variants in BAG3 as a cause of dilated cardiomyopathy. *Am J Hum Genet* 88, 273-282
- Norton PM, Latchman DS (1989): Levels of the 90kd heat shock protein and resistance to glucocorticoid-mediated cell killing in a range of human and murine lymphocyte cell lines. *J Steroid Biochem* 33, 149-154
- Nussbaum RL, Ellis CE (2003): Alzheimer's disease and Parkinson's disease. *N Engl J Med* 348, 1356-1364
- Oh HJ, Easton D, Murawski M, Kaneko Y, Subjeck JR (1999): The chaperoning activity of hsp110. Identification of functional domains by use of targeted deletions. *J Biol Chem* 274, 15712-15718

- Okui M, Ito F, Ogita K, Kuramoto N, Kudoh J, Shimizu N, Ide T (2000): Expression of APG-2 protein, a member of the heat shock protein 110 family, in developing rat brain. *Neurochem Int* 36, 35-43
- Olson EN, Williams RS (2000): Calcineurin signaling and muscle remodeling. *Cell* 101, 689-692
- Passier R, Zeng H, Frey N, Naya FJ, Nicol RL, McKinsey TA, Overbeek P, Richardson JA, Grant SR, Olson EN (2000): CaM kinase signaling induces cardiac hypertrophy and activates the MEF2 transcription factor in vivo. *J Clin Invest* 105, 1395-1406
- Patterson C (2006): Search and destroy: the role of protein quality control in maintaining cardiac function. *J Mol Cell Cardiol* 40, 438-441
- Pearse RV 2nd, Drolet DW, Kalla KA, Hooshmand F, Bermingham JR Jr, Rosenfeld MG (1997): Reduced fertility in mice deficient for the POU protein sperm-1. *Proc Natl Acad Sci USA* 94, 7555-7560
- Peng X, Kraus MS, Wei H, Shen TL, Pariaut R, Alcaraz A, Ji G, Cheng L, Yang Q, Kotlikoff MI et al. (2006): Inactivation of focal adhesion kinase in cardiomyocytes promotes eccentric cardiac hypertrophy and fibrosis in mice. *J Clin Invest* 116, 217-227
- Polier S, Dragovic Z, Hartl FU, Bracher A (2008): Structural basis for the cooperation of Hsp70 and Hsp110 chaperones in protein folding. *Cell* 133, 1068-1079
- Powell SR (2006): The ubiquitin-proteasome system in cardiac physiology and pathology. *Am J Physiol Heart Circ Physiol* 291, H1-19
- Rafiee P, Theriot ME, Nelson VM, Heidemann J, Kanaa Y, Horowitz SA, Rogaczewski A, Johnson CP, Ali I, Shaker R et al. (2006): Human esophageal microvascular endothelial cells respond to acidic pH stress by PI3K/AKT and p38 MAPK-regulated induction of Hsp70 and Hsp27. *Am J Physiol Cell Physiol* 291, C931-945
- Ramalho-Santos M, Yoon S, Matsuzaki Y, Mulligan RC, Melton DA (2002): "Stemness": transcriptional profiling of embryonic and adult stem cells. *Science* 298, 597-600
- Randell SH, Young SL: In *Fetal and Neonatal Physiology* (ed. R. Polin, W. W. Fox and S. H. Abman). Saunders. Philadelphia. 2004, pp. 1034-1040
- Raviol H, Sadlish H, Rodriguez F, Mayer MP, Bukau B (2006): Chaperone network in the yeast cytosol: Hsp110 is revealed as an Hsp70 nucleotide exchange factor. *EMBO J* 25, 2510-2518
- Ridsdale R, Post M (2004): Surfactant lipid synthesis and lamellar body formation in glycogen-laden type II cells. *Am J Physiol Lung Cell Mol Physiol* 287, L743-751

Ritossa F (1962): A new puffing pattern induced and temperature shock and DNP in *Drosophila*. *Cell Mol Life Sci* 18, 571–573

Ritossa F (1996): Discovery of the heat shock response. *Cell Stress Chaperones* 1, 97-98

Robertson KM, O'Donnell L, Jones ME, Meachem SJ, Boon WC, Fisher CR, Graves KH, McLachlan RI, Simpson ER (1999): Impairment of spermatogenesis in mice lacking a functional aromatase (*cyp 19*) gene. *Proc Natl Acad Sci USA* 96, 7986-7991

Rooney SA, Young SL, Mendelson CR (1994): Molecular and cellular processing of lung surfactant. *FASEB J* 8, 957-967

Ross CA (1995): When more is less: pathogenesis of glutamine repeat neurodegenerative diseases. *Neuron* 15, 493-496

Ross CA, Pickart CM (2004): The ubiquitin-proteasome pathway in Parkinson's disease and other neurodegenerative diseases. *Trends Cell Biol* 14, 703-711

Rutkowski DT, Kaufman RJ (2004): A trip to the ER: coping with stress. *Trends Cell Biol* 14, 20-28

Sanbe A, Osinska H, Saffitz JE, Glabe CG, Kaye R, Maloyan A, Robbins J (2004): Desmin-related cardiomyopathy in transgenic mice: a cardiac amyloidosis. *Proc Natl Acad Sci USA* 101, 10132-10136

Scavo LM, Ertsey R, Chapin CJ, Allen L, Kitterman JA (1998): Apoptosis in the development of rat and human fetal lungs. *Am J Respir Cell Mol Biol* 18, 21-31

Schuermann JP, Jiang J, Cuellar J, Llorca O, Wang L, Gimenez LE, Jin S, Taylor AB, Demeler B, Morano KA et al. (2008): Structure of the Hsp110:Hsc70 nucleotide exchange machine. *Mol Cell* 31, 232-243

Schulte U, Thumfart JO, Klöcker N, Sailer CA, Bildl W, Biniossek M, Dehn D, Deller T, Eble S, Abbass K et al. (2006): The epilepsy linked *Lgi1* protein assembles into presynaptic Kv1 channels and inhibits inactivation by Kvbeta1. *Neuron* 49, 697-706

Selkoe DJ (2004): Cell biology of protein misfolding: the examples of Alzheimer's and Parkinson's diseases. *Nat Cell Biol* 6, 1054-1061

Shaner L, Wegele H, Buchner J, Morano KA (2005): The yeast HSP110 SSE1 functionally interacts with the HSP70 chaperones SSA and SSB. *J Biol Chem* 280, 41262–41269

Shaner L, Sousa R, Morano KA (2006): Characterization of Hsp70 binding and nucleotide exchange by the yeast Hsp110 chaperone Sse1. *Biochemistry* 45, 15075-15084

- Shirayama MK, Kawakami Y, Matsui K, Tanaka A, Toh-e (1993): MSI3, a multicopy suppressor of mutants hyperactivated in the RAS-cAMP pathway, encodes a novel HSP70 protein of *Saccharomyces cerevisiae*. *Mol Gen Genet* 240, 323-332
- Shu W, Lu MM, Zhang Y, Tucker PW, Zhou D, Morrissey EE (2007): Foxp2 and Foxp1 cooperatively regulate lung and esophagus development. *Development* 134, 1991-2000
- Shulenin S, Noguee LM, Annilo T, Wert SE, Whitsett JA, Dean M (2004): ABCA3 gene mutations in newborns with fatal surfactant deficiency. *N Engl J Med* 350, 1296-1303
- Son WY, Hwang SH, Han CT, Lee JH, Kim S, Kim YC (1999): Specific expression of heat shock protein HspA2 in human male germ cells. *Mol Hum Reprod* 5, 1122-1126
- Son WY, Han CT, Hwang SH, Lee JH, Kim S, Kim YC (2000): Repression of hspA2 messenger RNA in human testes with abnormal spermatogenesis. *Fertil Steril* 73, 1138-1144
- Steel GJ, Fullerton DM, Tyson JR, Stirling CJ (2004): Coordinated activation of Hsp70 chaperones. *Science* 303, 98-101
- Stiles AD, Chrysis D, Jarvis HW, Brighton B, Moats-Staats BM (2001): Programmed cell death in normal fetal rat lung development. *Exp Lung Res* 27, 569-587
- Storozhenko S, De Pauw P, Kushnir S, Van Montagu M, Inzé D (1996): Identification of an *Arabidopsis thaliana* cDNA encoding a HSP70-related protein belonging to the HSP110/SSE1 subfamily. *FEBS Lett* 390, 113-118
- Sutherland LM, Edwards YS, Murray AW (2001): Alveolar type II cell apoptosis. *Comp Biochem Physiol A Mol Integr Physiol* 129, 267-285
- Takahashi H, Furukawa T, Yano T, Sato N, Takizawa J, Kurasaki T, Abe T, Narita M, Masuko M, Koyama S et al. (2007): Identification of an overexpressed gene, HSPA4L, the product of which can provoke prevalent humoral immune responses in leukemia patients. *Exp Hematol* 35, 1091-1099
- Taylor JP, Hardy J, Fischbeck KH (2002): Toxic proteins in neurodegenerative disease. *Science* 296, 1991-1995
- Terada K, Yomogida K, Imai T, Kiyonari H, Takeda N, Kadomatsu T, Yano M, Aizawa S, Mori M (2005): A type I DnaJ homolog, DjA1, regulates androgen receptor signaling and spermatogenesis. *EMBO J* 24, 611-622
- Thomas M, Massimi P, Jenkins J, Banks L (1995): HPV-18 E6 mediated inhibition of p53 DNA binding activity is independent of E6 induced degradation. *Oncogene* 10, 261-268

Tomasovic SP, Steck PA, Heitzman D (1983): Heat-stress proteins and thermal resistance in rat mammary tumor cells. *Radiat Res* 95, 399-413

Tonkiss J, Calderwood SK (2005): Regulation of heat shock gene transcription in neuronal cells. *Int J Hyperthermia* 21, 433-444

Trott A, Shaner L, Morano KA (2005): The molecular chaperone Sse1 and the growth control protein kinase Sch9 collaborate to regulate protein kinase A activity in *Saccharomyces cerevisiae*. *Genetics* 170, 1009-1021

Tsapara A, Matter K, Balda MS (2006): The heat-shock protein Apg-2 binds to the tight junction protein ZO-1 and regulates transcriptional activity of ZONAB. *Mol Biol Cell* 17, 1322-1330

Tsukamoto M, Hirasaki S, Kuribayashi T, Matsuo A, Matsui H, Sawada T, Nakamura T, Azuma A, Sugihara H, Matsubara H (2006): Systolic outward motion of the left ventricular apical wall as detected by magnetic resonance tagging in patients with apical hypertrophic cardiomyopathy. *J Cardiovasc Magn Reson* 8, 453-460

Tsunekawa N, Matsumoto M, Tone S, Nishida T, Fujimoto H (1999): The Hsp70 homolog gene, Hsc70t, is expressed under translational control during mouse spermiogenesis. *Mol Reprod Dev* 52, 383-391

Verkman AS, Matthay MA, Song Y (2000): Aquaporin water channels and lung physiology. *Am J Physiol Lung Cell Mol Physiol* 278, L867-879

Vos MJ, Hageman J, Carra S, Kampinga HH (2008): Structural and functional diversities between members of the human HSPB, HSPH, HSPA, and DNAJ chaperone families. *Biochemistry* 47, 7001-7011

Wakatsuki T, Hatayama T (1998): Characteristic expression of 105-kDa heat shock protein (HSP105) in various tissues of nonstressed and heat-stressed rats. *Biol Pharm Bull* 21, 905-910

Wan H, Dingle S, Xu Y, Besnard V, Kaestner KH, Ang SL, Wert S, Stahlman MT, Whitsett JA (2005): Compensatory roles of Foxa1 and Foxa2 during lung morphogenesis. *J Biol Chem* 280, 13809-13816

Wang X, Robbins J (2006): Heart failure and protein quality control. *Circ Res* 99, 1315-1328

Wang X, Su H, Ranek MJ (2008): Protein quality control and degradation in cardiomyocytes. *J Mol Cell Cardiol* 45, 11-27

Warburton D, Schwarz M, Tefft D, Flores-Delgado G, Anderson KD, Cardoso WV (2000): The molecular basis of lung morphogenesis. *Mech Dev* 92, 55-81

Weaver M, Dunn NR, Hogan BL (2000): Bmp4 and Fgf10 play opposing roles during lung bud morphogenesis. *Development* 127, 2695-2704

Weaver TE, Conkright JJ (2001): Function of surfactant proteins B and C. *Annu Rev Physiol* 63, 555-578

Weekes J, Morrison K, Mullen A, Wait R, Barton P, Dunn MJ (2003): Hyperubiquitination of proteins in dilated cardiomyopathy. *Proteomics* 3, 208-216

Welch WJ, Garrels JI, Thomas GP, Lin JJ, Feramisco JR (1983): Biochemical characterization of the mammalian stress proteins and identification of two stressproteins as glucose- and Ca²⁺-ionophore-regulated proteins. *J Biol Chem* 258, 7102-7111

Werner A, Meinhardt A, Seitz J, Bergmann M (1997): Distribution of heat-shock protein 60 immunoreactivity in testes of infertile men. *Cell Tissue Res* 288, 539-544

Whitsett JA, Weaver TE (2002): Hydrophobic surfactant proteins in lung function and disease. *N Engl J Med* 347, 2141-2148

Wilkins BJ, Molkentin JD (2002): Calcineurin and cardiac hypertrophy: where have we been? Where are we going? *J Physiol* 541, 1-8

Williams MC (2003): Alveolar type I cells: molecular phenotype and development. *Annu Rev Physiol* 65, 669-695

Williams MC, Mason RJ (1977): Development of the type II cell in the fetal rat lung. *Am Rev Respir Dis* 115, 37-47

Willis MS, Patterson C (2010): Hold me tight: Role of the heat shock protein family of chaperones in cardiac disease. *Circulation* 122, 1740-1751

Wong PC, Cai H, Borchelt DR, Price DL (2002): Genetically engineered mouse models of neurodegenerative diseases. *Nat Neurosci* 5, 633-639

Wu CY, Lin CT, Wu MZ, Wu KJ (2011): Induction of HSPA4 and HSPA14 by NBS1 overexpression contributes to NBS1-induced in vitro metastatic and transformation activity. *J Biomed Sci* 18, 1

Xue JH, Fukuyama H, Nonoguchi K, Kaneko Y, Kido T, Fukumoto M, Fujibayashi Y, Itoh K, Fujita J (1998): Induction of Apg-1, a member of the heat shock protein 110 family, following transient forebrain ischemia in the rat brain. *Biochem Biophys Res Commun* 247, 796 – 801

Yagita Y, Kitagawa K, Taguchi A, Ohtsuki T, Kuwabara K, Mabuchi T, Matsumoto M, Yanagihara T, Hori M (1999): Molecular cloning of a novel member of the HSP110

family of genes, ischemia-responsive protein94 kDa (irp94), expressed in rat brain after transient forebrain ischemia. *J Neurochem* 72, 1544-1551

Yagita Y, Kitagawa K, Ohtsuki T, Tanaka S, Hori M, Matsumoto M (2001): Induction of the HSP110/105 family in the rat hippocampus in cerebral ischemia and ischemic tolerance. *J Cereb Blood Flow Metab* 21, 811-819

Yasuda K, Nakai A, Hatayama T, Nagata K (1995): Cloning and expression of murine high molecular mass heat shock proteins, HSP105. *J Biol Chem* 270, 29718-29723

Yasuda K, Ishihara K, Nakashima K, Hatayama T (1999): Genomic cloning and promoter analysis of the mouse 105-kDa heat shock protein (HSP105) gene. *Biochem Biophys Res Commun* 256, 75-80

Yu YE, Zhang Y, Unni E, Shirley CR, Deng JM, Russell LD, Weil MM, Behringer RR, Meistrich ML (2000): Abnormal spermatogenesis and reduced fertility in transition nuclear protein 1-deficient mice. *Proc Natl Acad Sci USA* 97, 4683-4688

Zakeri ZF, Wolgemuth DJ, Hunt CR (1988): Identification and sequence analysis of a new member of the mouse HSP70 gene family and characterization of its unique cellular and developmental pattern of expression in the male germ line. *Mol Cell Biol* 8, 2925-2932

Zhang Y, Jiang DS, Yan L, Cheng KJ, Bian ZY, Lin GS (2011): HSP75 protects against cardiac hypertrophy and fibrosis. *J Cell Biochem* 112, 1787-1794

Zhu X, Zhao X, Burkholder WF, Gragerov A, Ogata CM, Gottesman ME, Hendrickson WA (1996): Structural analysis of substrate binding by the molecular chaperone DnaK. *Science* 272, 1606-1614

Zou Y, Li J, Ma H, Jiang H, Yuan J, Gong H, Liang Y, Guan A, Wu J, Li L et al. (2011): Heat shock transcription factor 1 protects heart after pressure overload through promoting myocardial angiogenesis in male mice. *J Mol Cell Cardiol* 51, 821-829

5. Publications

Publication I:

Held T, Barakat AZ, **Mohamed BA**, Paprotta I, Meinhardt A, Engel W, Adham IM (2011): Heat-shock protein HSPA4 is required for progression of spermatogenesis. *Reproduction* 142,133-144.

Publication II:

Mohamed BA, Barakat AZ, Zimmermann WH, Bittner RE, Mühlfeld C, Hünlich M, Engel W, Maier LS, Adham IM (2012): Targeted disruption of Hspa4 gene leads to cardiac hypertrophy and fibrosis. *J Mol Cell Cardiol* 53, 459-468.

5.1. Publication I

Heat-shock protein HSPA4 is required for progression of spermatogenesis

DOI: 10.1530/REP-11-0023

Torsten Held, Amal Z Barakat, **Belal A Mohamed**, Ilona Paprotta, Andreas Meinhardt, Wolfgang Engel, Ibrahim M Adham

Status: Published in *Reproduction Journal* (Impact factor 3.049), Volume 142 (2011), pp. 133-144

Author contributions to the work:

1. Torsten Held: Participated in generation of *Hspa4* KO construct, histological and immunohistochemical studies
2. Amal Z Barakat: Participated in histological and immunohistochemical analyses, performed Northern blot analysis and participated in TUNEL assay for detection of apoptotic cells
3. **Belal A Mohamed:** Performed the experiments to identify HSPA4 expression in different murine tissues and in testes of different developmental stages, studied cellular distribution of HSPA4 in the prenatal testes, carried out statistical analysis of the data, participated in data interpretation and was involved in manuscript preparation
4. Ilona Paprotta: Performed genotyping of the mice
5. Andreas Meinhardt: Evaluated the results of histological analyses
6. Wolfgang Engel: Conceived and designed the experiments, interpretation of the data, gave critical comments and recommendations, and financial support
7. Ibrahim M Adham: Conceived and designed the experiments, interpretation of the data and critical review of the manuscript

REPRODUCTION

RESEARCH

Heat-shock protein HSPA4 is required for progression of spermatogenesis

Torsten Held, Amal Z Barakat, Belal A Mohamed, Ilona Paprotta, Andreas Meinhardt¹, Wolfgang Engel and Ibrahim M Adham

Institute of Human Genetics, University of Göttingen, D-37073 Göttingen, Germany and ¹Department of Anatomy and Cell Biology, University of Giessen, D-35378 Giessen, Germany

Correspondence should be addressed to I M Adham; Email: iadham@gwdg.de

T Held and A Z Barakat are contributed equally to this work and should be considered co-first authors

Abstract

Heat-shock protein 110 (HSP110) family members act as nucleotide exchange factors (NEF) of mammalian and yeast HSP70 chaperones during the ATP hydrolysis cycle. In this study, we describe the expression pattern of murine HSPA4, a member of the HSP110 family, during testis development and the consequence of HSPA4 deficiency on male fertility. HSPA4 is ubiquitously expressed in all the examined tissues. During prenatal and postnatal development of gonad, HSPA4 is expressed in both somatic and germ cells; however, expression was much higher in germ cells of prenatal gonads. Analyses of *Hspa4*-deficient mice revealed that all homozygous mice on the hybrid C57BL/6J × 129/Sv genetic background were apparently healthy. Although HSPA4 is expressed as early as E13.5 in male gonad, a lack of histological differences between *Hspa4*^{-/-} and control littermates suggests that *Hspa4* deficiency does not impair the gonocytes or their development to spermatogonia. Remarkably, an increased number of the *Hspa4*-deficient males displayed impaired fertility, whereas females were fertile. The total number of spermatozoa and their motility were drastically reduced in infertile *Hspa4*-deficient mice compared with wild-type littermates. The majority of pachytene spermatocytes in the juvenile *Hspa4*^{-/-} mice failed to complete the first meiotic prophase and became apoptotic. Furthermore, down-regulation of transcription levels of genes known to be expressed in spermatocytes at late stages of prophase I and post-meiotic spermatids leads to suggest that the development of most spermatogenic cells is arrested at late stages of meiotic prophase I. These results provide evidence that HSPA4 is required for normal spermatogenesis.

Reproduction (2011) **142** 133–144

Introduction

Complexes containing heat-shock proteins (HSPs) represent the major components of molecular chaperones that facilitate the folding and assembly of newly synthesized proteins and the selection of unfolded proteins for degradation in different cellular compartments such as cytosol, endoplasmic reticulum, and mitochondria (Hartl 1996). Based on the molecular weight, HSPs are divided into structurally unrelated HSP110, HSP90, HSP70, HSP60, and HSP27 protein families (Vos *et al.* 2008).

The *HSP110* gene family includes two genes in *Saccharomyces cerevisiae* known as *SSE1* and *SSE2* and four genes in the mammalian genome, namely *HSPA4L/APG1*, *HSPA4/APG2*, *HSPH1/HSP105*, and *HYOU1/GRP175/ORP150*. Except *HYOU1*, which is present in the endoplasmic reticulum, all other members of mammalian and yeast HSP110 are found in the cytosolic compartment (Vos *et al.* 2008). Primary structure of HSP110 proteins is highly related to HSP70 and consists of a nucleotide-binding domain (NBD) and

a peptide-binding domain (PBD) that are connected by a flexible linker region (Mayer & Bukau 2005, Liu & Hendrickson 2007). However, biochemical analyses revealed that HSP110 members are co-chaperones of mammalian and yeast HSP70 chaperones and act as nucleotide exchange factors (NEF) during the ATP hydrolysis cycle (Steel *et al.* 2004, Dragovic *et al.* 2006, Raviol *et al.* 2006, Polier *et al.* 2008, Schuermann *et al.* 2008). Binding of newly synthesized polypeptides to HSP70 chaperone and subsequent release of folded proteins is regulated by a continuous cycle of ATP hydrolysis and exchange of ATP to ADP.

Beside HSP110 proteins, there are other unrelated nucleotide exchange factors of BAG and HSPBiP1 protein families. It is believed that the chaperones containing HSP70, HSP40, and HSP110 proteins represent the major protein folding machine of the eukaryotic cytosol (Polier *et al.* 2008).

Male germ cells undergo a dramatic developmental process, which is precisely controlled at the level of transcription and translation. After colonizing the

primordial germ cells in mouse testis, gonocytes proliferate until day 15.5 and arrest in the G1 of cell cycle (Vergouwen *et al.* 1991, Nagano *et al.* 2000). Shortly after birth, gonocytes resume mitotic activity and develop into type A spermatogonia (McLean *et al.* 2003). Primary spermatocytes undergo meiotic division to produce haploid round spermatids that are subsequently differentiated into mature sperm. Chaperone activities are required to mediate folding of *de novo* synthesized proteins and refolding of misfolded proteins during development of male germ cells (Eddy 1999). Mutation in the *Hspa2* gene (*Hsp70-2*), which is highly expressed in pachytene spermatocytes, leads to arrest the spermatogenesis in meiotic prophase I and the majority of late pachytene spermatocytes are eliminated by apoptosis (Dix *et al.* 1997). Loss of DNAJA1, a co-chaperone of HSP70s in protein folding, results in severe defects of spermatogenesis (Terada *et al.* 2005).

To date, relatively little is known about the expression and the physiological function of HSPA4. In adult mouse, *Hspa4* mRNA is detected in most tissues, with the highest expression in testis, ovary, and spleen (Kaneko *et al.* 1997). *In vitro* studies have shown that the expression of *Hspa4* is not inducible by heat shock (Nonoguchi *et al.* 1999). Interestingly, expression of *Hspa4* is up-regulated in some leukemia and solid tumors (Gotoh *et al.* 2004, Li *et al.* 2010).

To determine the expression pattern of HSPA4, we investigated the expression of HSPA4 in different tissues and during prenatal and postnatal testis development. To examine the function of HSPA4 *in vivo*, we generated *Hspa4*-deficient mice and subsequently determined the effect of HSPA4 deficiency on germ cell development.

Results

HSPA4 is highly expressed in embryonic gonocytes and oogenesis

To investigate the expression pattern of HSPA4, northern blot analysis was performed with total RNA from different tissues of adult mice. The 358 bp cDNA probe containing the coding sequence of the C-terminus recognized two *Hspa4* transcripts of 4.8 and 3.2 kb in all studied tissues. Expression levels of the 3.2 kb transcript were relatively higher in testis (Fig. 1A). Analysis of *Hspa4* cDNA sequences in database revealed that a cDNA sequence (GI 60360215; AK 220167) contains two predicted polyadenylation sites that are spanning 1.75 kb region. To confirm that both mRNA isoforms result from alternative splicing of the 3'-untranslated region, an RNA blot was hybridized with the 596 bp cDNA probe containing the sequence between both polyA signals. This probe only detected the 4.8 kb transcript (Fig. 1B). To further confirm these

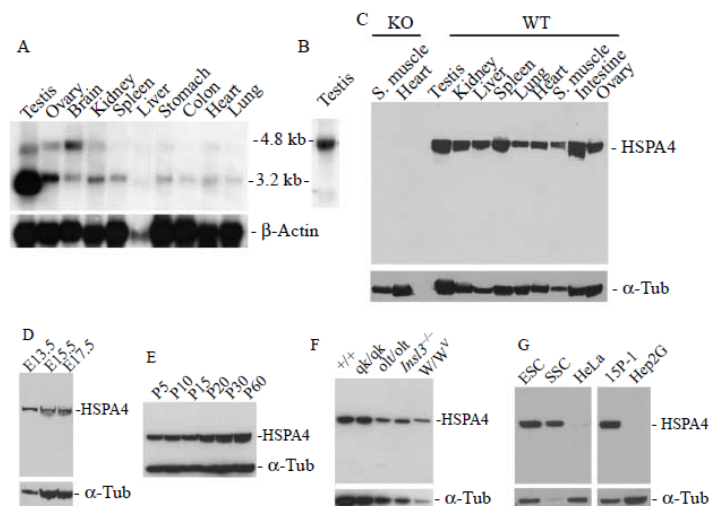


Figure 1 Expression pattern of HSPA4 in different tissues, fetal and postnatal testes, testes of different mutant mice, and different cell lines. (A) Northern blot with total RNA from different tissues of 3-month-old mice was hybridized with the 358 bp *Hspa4* cDNA probe. The same blot was rehybridized with a β -actin cDNA probe. (B) RNA blot with RNA of adult testis was hybridized with the 596 bp *Hspa4* cDNA probe. (C) Immunoblot of HSPA4 expression in cellular extracts from different tissues of 3-month-old wild-type (WT) and mutant mice (KO) revealed that anti-HSPA4 recognized a 96 kDa protein in all wild-type tissue, but not in *Hspa4*-deficient tissues. (D and E) Expression of HSPA4 during prenatal (D) and postnatal testis development (E) was examined by immunoblotting using total lysates obtained from testes of E13.5, E15.5, and E17.5 embryos, and from P5, P10, P15, P20, P30, and P60 mice. The anti- α -tubulin antibody (α -Tub) was used as a control. (F) Western blot with lysates obtained from testes of wild-type (+/+) and different mutant mice was probed with anti-HSPA4 antibody. (G) Immunoblot of HSPA4 expression in cellular extracts from different cell lines. ESC, embryonic stem cells; SSC, spermatogonial stem cells; HeLa, HeLa cells; 15P-1, Sertoli cells; Hep2G, Hepatoma cells.

results, western blot containing protein extracts of different wild-type and *Hspa4*-deficient tissues was probed with the anti-HSPA4 antibody. Immunoblot analysis revealed that the anti-HSPA4 recognized a 96 kDa protein in all wild-type tissues, but not in *Hspa4*-deficient tissues (Fig. 1C). To evaluate the expression pattern of HSPA4 during testis development, immunoblot analysis was performed with testis extracts obtained from mice at the different stages of prenatal and postnatal development. HSPA4 was detected throughout the prenatal and postnatal development of testis as shown in Fig. 1D and E. Expression levels of the HSPA4 are markedly increased in testis after postnatal day 20 suggesting an increased expression of the HSPA4 in haploid spermatids. We also examined the expression of HSPA4 in testes of mouse mutants. HSPA4 was present in testes of *W/W^v* mutant mice that lack most germ cells as well as in testes of *qk/qk*, *olt/olt*, and *Ins13^{-/-}* mutant mice, in which spermatogenesis is arrested at different stages (Fig. 1F; Lyon & Searle 1989, Chubb 1992, Zimmermann *et al.* 1999). Further immunoblot analysis was performed with protein extracts isolating from embryonic stem cells, spermatogonial stem cells (Guan *et al.* 2006), Sertoli cell line 15P-1 (Rassoulzadegan *et al.* 1993), HeLa, and hepatoma Hep2G cell line. HSPA4 was expressed in embryonic, spermatogonial stem, and

Sertoli cell lines, whereas its expression levels were lower in both HeLa and Hep2G (Fig. 1G). These results suggest that HSPA4 is expressed in somatic and germ cells of testis. To determine the cellular localization of HSPA4, immunocytochemical analysis was performed on sections of fetal and newborn testis and ovary after embryonic day 13.5. We observed that HSPA4 is highly enriched in male gonocytes of E13.5, whereas lower levels of HSPA4-immunostaining were seen in somatic cells (Fig. 2A). Expression of HSPA4 remains at high levels in gonocytes throughout fetal stages (Fig. 2B and C). After migration of gonocytes from central to peripheral layer of seminiferous tubules during neonatal development and their start to differentiate to differentiated spermatogonia in 5-day-old testis, HSPA4 still expressed but at lower level than in fetal gonocytes (Fig. 2D). In adult testis, the expression of HSPA4 is slightly increased in post-meiotic germ cells (Fig. 2E). The HSPA4-specific immunostaining was confirmed by the absence of HSPA4-immunostaining in adult *Hspa4*-deficient testis (Fig. 2F). Immunofluorescence with antibodies directed against undifferentiated spermatogonia marker PLZF revealed that HSPA4 and PLZF are expressed in the same population of spermatogonia (Fig. 2G–I). When the preleptotene spermatocytes enter meiosis in 10-day-old testis, differentiated

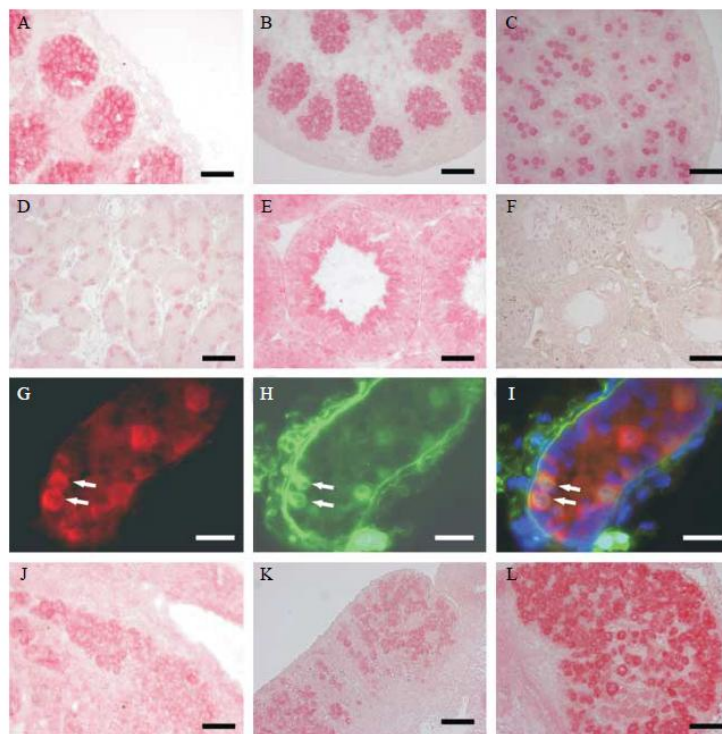


Figure 2 Cellular localization of HSPA4 during testis and ovary development. (A–F) Immunohistochemistry of paraffin sections with anti-HSPA4 shows an abundance of HSPA4 in the gonocytes of wild-type testes at E13.5 (A), E15.5 (B), E18.5 (C), and in spermatogonia at P5 (D). In 3-month-old wild-type testis, expression of the HSPA4 is slightly increased in post-meiotic germ cells (E). A negative control of immunohistochemistry is the absence of HSPA4-specific immunostaining in adult *Hspa4*-deficient testis (F). (G–I) Expression of the HSPA4 in undifferentiated spermatogonia of wild-type mice is confirmed by immunofluorescence of testis at P5 with anti-HSPA4 (G) and anti-PLZF (H). HSPA4 and PLZF are expressed in the same population of spermatogonia (arrows). HSPA4 (red fluorescence) and PLZF (green fluorescence) are shown separately (G and H) and merged (I). DAPI (blue fluorescence) was used for nuclear staining (I). (J–L) Immunohistochemistry with HSPA4 antibody was performed on ovary sections of E13.5 (J), E15.5 (K), and E18.5 (L). Scale bar A–F and J–L = 50 μ m; G–I = 20 μ m.

spermatogonia, leptotene, and zygotene spermatocytes are expressed HSPA4 at very low levels (data not shown). In prenatal ovary, oogonia of E13.5 show weak staining (Fig. 2J), whereas HSPA4 is highly expressed in oogonia of E15.5 and E18.5 (Fig. 2K and L). The high enrichment of HSPA4 in gonocytes and oogonia throughout their embryonic development suggests that the absence of HSPA4 protein might directly affect the development of germ cells in both male and female embryos.

Hspa4 deficiency results in impaired male fertility

To investigate the function of HSPA4, we inactivated the *Hspa4* in mouse ESC. *Hspa4*-targeting vector was designed to replace a 3.0 kb genomic fragment containing exon 1 by neomycin resistance gene (Fig. 3A). Recombinant *Hspa4*^{+/-} ESCs were analyzed by Southern blot hybridization (Fig. 3B) and then used to generate chimeric mice. Chimeric mice were intercrossed with C57BL/6J females to establish the *Hspa4* mutant allele on a C57BL/6J×129/Sv hybrid genetic background. Interbreeding of heterozygous mice yielded a normal Mendelian ratio of *Hspa4*^{+/+}, *Hspa4*^{+/-}, and *Hspa4*^{-/-} offspring. These results indicate that there is no lethality caused by the *Hspa4* mutation. Male and female *Hspa4*-deficient mice developed into apparently normal adults. In *Hspa4*-null allele, exon 1 containing the translation initiation codon ATG is deleted.

Therefore, we expected that the targeted *Hspa4* allele would be transcribed into an untranslated *Hspa4* mRNA. The inactivation of *Hspa4* was confirmed by RT-PCR and northern and western blot analyses. The 596 bp cDNA probe recognized a weak band in RNA from *Hspa4*^{-/-} testis (Fig. 3C). RT-PCR with primers containing sequences of exons 1 and 3 was not able to amplify the *Hspa4* cDNA fragment from testicular RNAs of *Hspa4*-deficient mice (Fig. 3D). At protein level, the HSPA4 antibody recognized the expected 96 kDa HSPA4 protein in testes of wild-type and heterozygous animals, whereas the corresponding protein band was not detected in testes of *Hspa4*-deficient mice (Fig. 3E). These results confirm that the targeted disruption of *Hspa4* generated a null mutation.

To study the consequence of *Hspa4* mutation on female and male fertility, we intercrossed 13 males and seven females from F2 generation with wild-type mice of strain CD1 over a period of 3 months. All mating of *Hspa4*-deficient females were reproductive, and the average litter size (9.2 ± 2.4 , $n=18$) was not significantly different compared to breeding with wild-type females (9.6 ± 1.6 , $n=15$). Breeding of male mutants revealed that fertility was heterogeneous among males. Of the 13 males, eight did not produce a single litter, whereas the remaining five produce litter size (11.1 ± 3.4 , $n=16$) similar to those of their wild-type littermates (14.6 ± 1.2 , $n=15$).

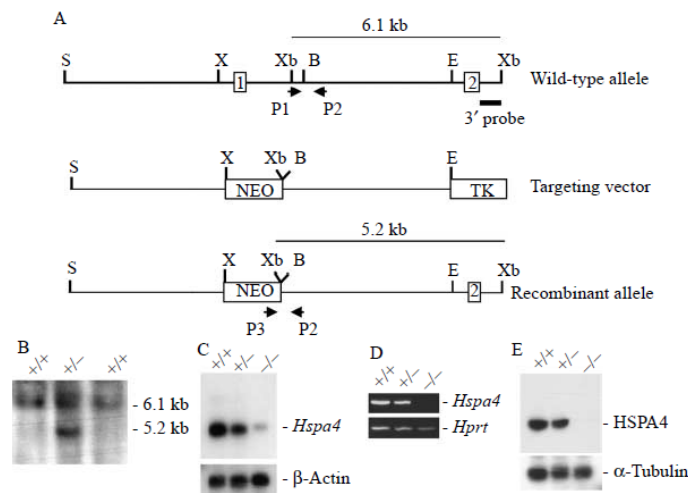


Figure 3 Targeted disruption of the *Hspa4* gene. (A) Schematic representation of wild-type, targeted vector and recombinant allele. Exons are represented as numbered boxes. A 3.0 kb genomic fragment containing exon 1 was replaced by *pgk-neo* selection cassette (NEO). TK box represents thymidine kinase. The 3' external probe used and the predicted length of XbaI restriction fragments in Southern blot analysis are shown. The primers P1, P2, and P3 used to amplify the wild-type and mutant alleles by PCR are also indicated. Restriction sites relevant for generation of knockout vector and for screening strategies are SpeI (S), XhoI (X), XbaI (Xb), BamHI (B) and EcoRI (E). (B) Southern blot analysis of recombinant ES cell (ESC) clones. Genomic DNA from ESC clones was digested with XbaI and probed with the 3'-probe shown in panel A. (C) Northern blot with testicular RNA of *Hspa4*^{+/+}, *Hspa4*^{+/-}, and *Hspa4*^{-/-} mice was hybridized with the 596 bp *Hspa4* and β -actin cDNA probes. (D) RT-PCR analysis using testicular RNA and primers located in exons 1 and 3 of *Hspa4* confirmed the absence of exon 1 in *Hspa4* targeted transcripts. Amplification of *Hprt* cDNA in assays with RNA of three genotypes was used as a control. (E) Western blot with whole protein extracts from testes of *Hspa4*^{+/+}, *Hspa4*^{+/-}, and *Hspa4*^{-/-} mice was probed with HSPA4 and α -tubulin antibodies.

To verify whether the *Hspa4* deficiency results in disruption of spermatogenesis and/or sperm motility, we analyzed the number and the motility of spermatozoa collected from the cauda epididymides of 5-month-old wild-type, fertile, and infertile *Hspa4*^{-/-} males. A significant reduction in the mean number of spermatozoa was found in *Hspa4*^{-/-} males. Analysis of sperm motility and progressive movement showed significant differences only between spermatozoa of wild-type and infertile *Hspa4*^{-/-} mice (Table 1).

Spermatogenesis is arrested at meiotic prophase stage

Testis weights of 5-month-old infertile *Hspa4*-null mice (51.1 ± 12.1 mg, *n* = 5) were significantly reduced than those of control males (125.4 ± 4.2 mg, *n* = 5; Fig. 4A). To elucidate the cause of the reduction in number of spermatozoa, we analyzed cross sections of testes from 5-month-old wild-type and *Hspa4*-deficient mice. Testes of infertile mutant mice exhibited a diverse range of defects, varying in severity among males. Most seminiferous tubules were markedly smaller than those of wild-type controls (Fig. 4B and C). Tubules of testes from infertile mice contained Sertoli and early stages of spermatogenic cells; however, many pachytene spermatocytes have degenerated nuclei, and round and elongated spermatids were absent in most seminiferous tubules (Fig. 4D and E). Many tubules were vacuolated due to spermatocytes loss. Multinucleated spermatids, which may arise by widening of the intercellular bridges after meiotic division (Dym & Fawcett 1971), were frequently observed (Fig. 4B and C). Consequently, the mutant epididymides contained a few number of sperm and immature germ cells with compact chromatin were present (Fig. 4F and G).

To identify the spermatogenic stage, at which spermatogenesis is affected by *Hspa4* deficiency, testicular sections from different postnatal days were histologically and immunohistologically analyzed. No apparent differences were observed in the histological structure of seminiferous tubules between mutant and wild-type mice at postnatal days 5 and 10 (data not shown). Using the HSPH1 antibody to label gonocytes, the *Hspa4*^{-/-} and *Hspa4*^{+/+} tubules were observed to

contain equivalent numbers of gonocytes, suggesting that the *Hspa4* deficiency does not impair gonocytes or development of gonocytes to spermatogonia (Supplementary Figure 1, see section on supplementary data given at the end of this article). At postnatal day 10, the first spermatocytes are formed. The number of germ cells stained with anti-GCNA1, a marker of pre-meiotic and meiotic germ cells, in mutant and wild-type tubules, was not significantly different at postnatal day 10, suggesting that mitotic division in mutant testes is not affected (Supplementary Figure 1). However, a few of the seminiferous tubules of *Hspa4*^{-/-} testes contained meiotic germ cells (pachytene spermatocytes) at postnatal day 15 (Fig. 5A and B). By immunohistological staining with anti-HSPA4L, which is highly expressed in germ cells from pachytene spermatocytes (Held *et al.* 2006), a reduction was observed in the mean number of HSPA4L-immunopositive cells per tubule in *Hspa4*^{-/-} compared with wild-type testes (Supplementary Figure 1). At P20, spermatogenesis has reached the stage of round spermatids in majority of wild-type tubules. In contrast, mutant tubules were almost completely devoid of round spermatids and contained much fewer number of pachytene spermatocytes (Fig. 5C and D). At day 25, when tubules of wild-type littermates showed elongated spermatids, *Hspa4*^{-/-} testes showed a severe depletion of germ cells. In *Hspa4*-deficient testes, very few tubules contained round spermatids as the most advanced germ cells (Fig. 5E and F). To examine whether disrupted spermatogenesis is due to the impairment of chromosomal pairing, we analyzed the formation of the synaptonemal complex in the mutant germ cells. No abnormalities in the chromosome pairing were detected as judged by the proper accumulation of SCPY3 on the synapsed chromosomes during pachytene stage (Supplementary Figure 1). These results suggest that the *Hspa4* deficiency resulted in either developmental delay or partial arrest of the first wave of spermatogenesis.

To investigate whether the observed loss of germ cells is a result of enhanced apoptosis in *Hspa4*-null mice, TUNEL assay was performed on testis section of 10-, 15-, 20-, 25-, and 150-day-old mice. In 5-month-old testes, there were significantly more TUNEL-positive cells in seminiferous tubules of infertile *Hspa4*-null mice than in those of wild-type littermates (Fig. 6G and H). During postnatal development of testis, there were no significant differences in the number of TUNEL-positive cells between *Hspa4*^{+/+} and *Hspa4*^{-/-} testes at P10 (data not shown). A significant increase of TUNEL-positive spermatocytes was found in *Hspa4*-null mice at P15, P20, and P25 (Fig. 6A–F and I). These results indicate that germ cells at meiotic stages appear to be the most affected cells in *Hspa4*-deficient testes.

We then analyzed the expression of different meiotic and post-meiotic marker genes in testes of wild-type, fertile, and infertile mutant mice (Fig. 7A and B).

Table 1 Sperm analysis of *Hspa4*^{+/+} and *Hspa4*^{-/-} mice.

Genotype of mice	No. of sperm in cauda epididymis (10 ⁷)	Sperm motility (%)	Progressive motility (%)
<i>Hspa4</i> ^{+/+}	2.0 ± 0.1 (5)	63.2 ± 4.4 (5)	42.1 ± 5.3 (5)
<i>Hspa4</i> ^{-/-}			
Fertile	1.1 ± 0.4* (4)	57.0 ± 6.5 (4)	33.5 ± 9 (4)
Infertile	0.2 ± 0.3* (5)	18.3 ± 11.4* (4)	9.8 ± 5.9* (4)

Data for sperm analysis represent the mean ± s.d. for the numbers of individual measurements indicated in parentheses. *Value in *Hspa4*^{-/-} mice is significantly different from that in *Hspa4*^{+/+} mice (*P* < 0.01 by Student's *t*-test).

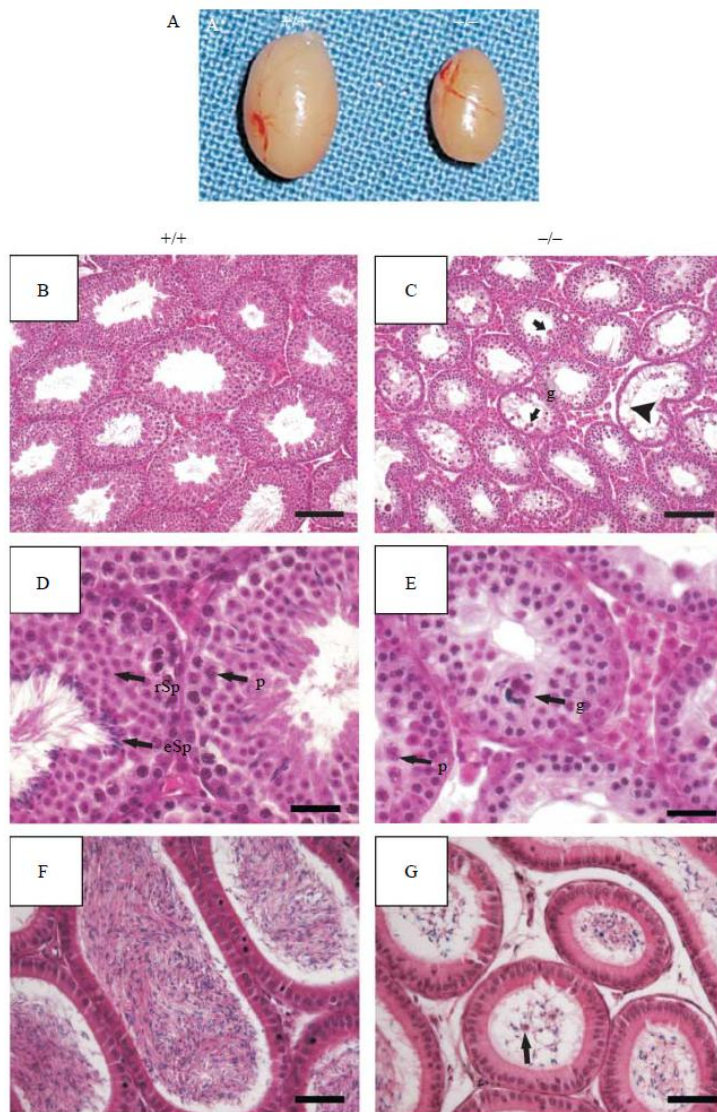


Figure 4 Testes and spermatogenesis of *Hspa4*^{+/+} and infertile *Hspa4*^{-/-} mice. (A) Infertile *Hspa4*^{-/-} mice showed reduced testis size compared with *Hspa4*^{+/+} mice. (B–E) Histological sections from testes of 5-month-old wild-type (+/+) and *Hspa4*^{-/-} mice (-/-) were stained with hematoxylin and eosin (H&E). A strongly reduced number of pachytene spermatocytes and round and elongated spermatids are found in most seminiferous tubules of mutant mice (C and E) compared with wild-type mice (B and D). Furthermore, degenerated germ cells and vacuoles (arrowhead) and presence of multinucleated giant cells (g) are frequently found in testes of infertile *Hspa4*^{-/-} mice. p, pachytene spermatocytes; rSp, round spermatids; eSp, elongated spermatids. (F and G) H&E-stained sections of epididymides of 5-month-old mice. *Hspa4*-deficient epididymides contain a few number of sperm, and immature germ cells with compact chromatin were present (arrow). Scale bar (B and C) = 100 μ m; (D–G) = 50 μ m.

Expression of *Sycp3* gene encoding synaptonemal complex protein-3 is restricted to leptotene and zygotene spermatocytes (Lammers *et al.* 1994). Northern blot analysis revealed that the expression levels of *Sycp3* in testes of fertile and infertile *Hspa4*^{-/-} mice are similar to those in wild-type testes. In contrast, expression of testis-specific genes encoding the phosphoglycerate kinase-2 (*Pgk2*) and acrosin (*Acr*), which were reported to be expressed in pachytene spermatocytes (Goto *et al.* 1990, Kashiwabara *et al.* 1990, Kremling *et al.* 1991), was markedly reduced in testes of infertile *Hspa4*-null mice. Similar results were also obtained for transcript

levels of post-meiotic genes *Hsc70t* (Hsp70 homolog gene) and transition nuclear protein 2 (*Tnp2*; Kleene & Flynn 1987, Tsunekawa *et al.* 1999). These results confirm that the disruption of spermatogenesis in *Hspa4*-deficient mice occurred late in meiotic prophase I.

The mild phenotype in spermatogenesis of *Hspa4*-null mice may be due to overexpression of other members of HSP110 family. Therefore, we analyzed the expression of HSPA4L and HSPH1 in testes of fertile *Hspa4*^{-/-} mice. Western blot analysis did not reveal a marked increase in the expression of HSPA4L and HSPH1 in testes of *Hspa4*-null mice (Fig. 7C).

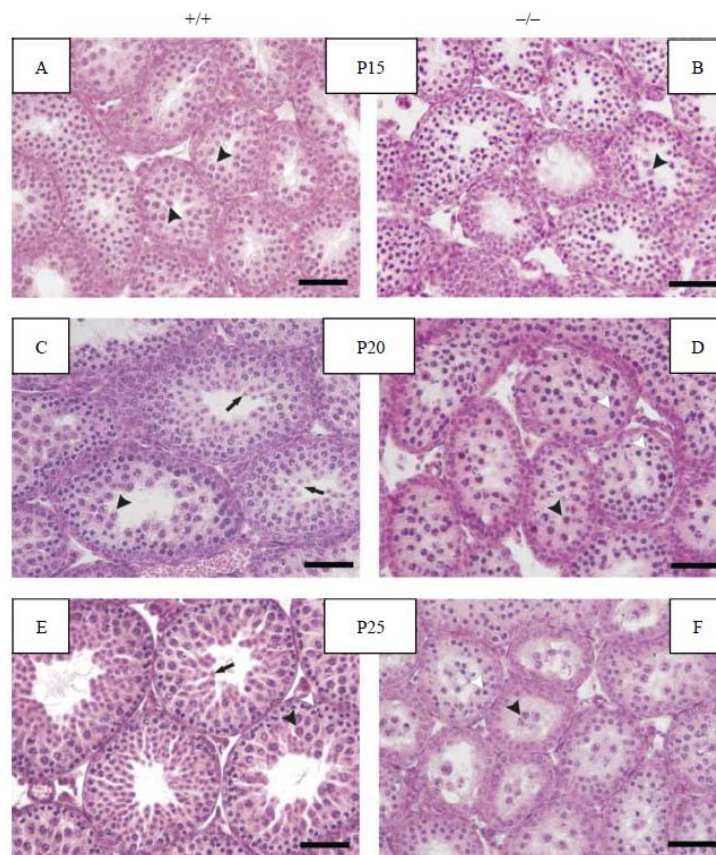


Figure 5 Delayed and disrupted first wave of spermatogenesis in *Hspa4* mutant mice. (A–F) Testicular sections from wild-type (+/+) and *Hspa4*-null mice (-/-) at postnatal days 15 (P15), 20 (P20), and 25 (P25) were stained with H&E. Arrowheads and arrows indicate pachytene spermatocytes and spermatids, respectively. Scale bar = 50 μm.

Discussion

This research describes the expression and physiological function of HSPA4 in germ cell development. Expression of HSPA4 is ubiquitously expressed in both somatic and germ cells of testis. However, the expression is highly enriched in male and female germ cells of prenatal gonads. Expression of HSPA4 in male gonocytes is gradually decreased after migration to the basal layers of seminiferous tubules and differentiation to spermatogonia. This preferential expression leads us to study the specific role of HSPA4 in germ cell development. Analyses of *Hspa4*-deficient mice revealed that all *Hspa4*-null mice on the hybrid C57BL/6J×129/Sv genetic background were born at Mendelian ratio and were apparently normal. Although expression of HSPA4 can be detected in all tissues of wild-type mice, male infertility was the most apparent phenotype for *Hspa4*-deficient mice of the second generation. Male infertility is histologically characterized by a decreased number of the post-meiotic germ cells and an increased number of germ cells undergoing apoptosis. *Hspa4* mutants display a disruption of the first wave of spermatogenesis in

juvenile testes by postnatal day 15, when the most advanced germ cells in the testes remain at the late pachytene spermatocyte stage. The histological results were confirmed by immunohistological and RNA analyses. These results showed the presence of an equivalent number of gonocytes in neonatal *Hspa4*-null testes and a lower percentage of mature spermatids. Expression of early meiosis-specific genes was not affected in *Hspa4*-deficient testes. In contrast, expression of marker genes for later stages of meiotic prophase I and for post-meiotic germ cells was downregulated in the absence of HSPA4. These results indicate that the *Hspa4* deficiency impairs the development of most germ cells in late prophase I.

Numerous proteins that are required for the development of male germ cells through meiotic and post-meiotic stages are mostly translated in the pachytene spermatocyte stage (Eddy & O'Brien 1998). Failure of molecular chaperones to direct correct folding of newly synthesized proteins might lead to accumulation of misfolded and damaged proteins in pachytene spermatocytes, which could prompt spermatocytes to undergo

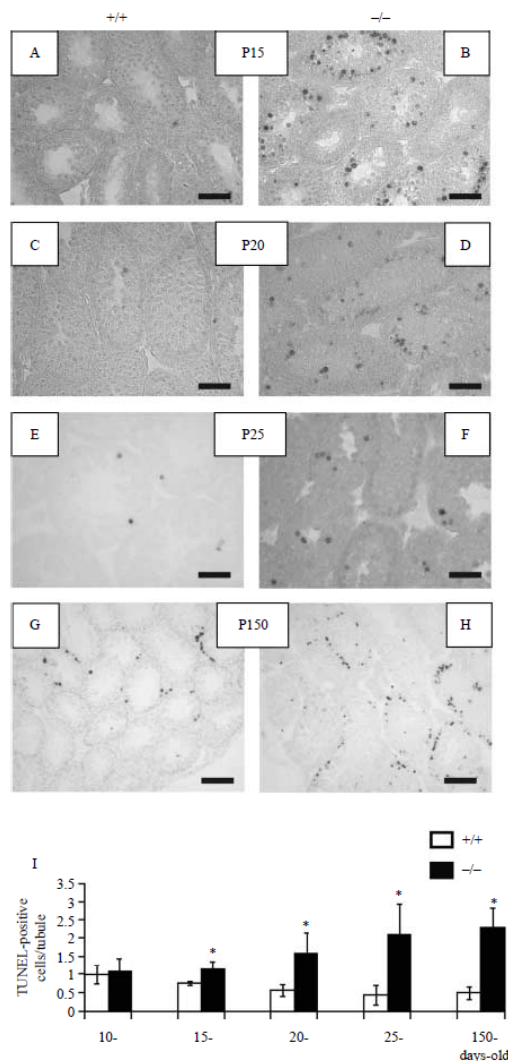


Figure 6 Enhanced apoptosis during germ cell development of *Hspa4*-null mice. (A–H) Histological sections of *Hspa4*^{+/+} (+/+) and *Hspa4*^{-/-} mice (-/-) at postnatal days 15 (P15), 20 (P20), 25 (P25), and 150 (P150) were subjected to TUNEL staining. TUNEL-positive cells are mainly pachytene spermatocytes as indicated by their nuclear size and their position in the seminiferous tubules. Scale bar (A–F) = 50 μ m; (G and H) = 100 μ m. (I) For quantification of TUNEL-positive cells/seminiferous tubule, sections of testes derived from two mice per genotype per stage were microscopically analyzed. Number of the TUNEL-positive cells per tubule in each microscopic field was determined. An average of 10–20 randomly microscopic fields were scored for each genotype and developmental stage ($n=100$ –150 tubules). Then, the mean number of TUNEL-positive cells per tubule and standard deviation were calculated for the examined fields. Paired comparisons of the TUNEL-positive cells/tubule in testis among *Hspa4*^{+/+} and *Hspa4*^{-/-} mice in each stage were performed to determine the statistical significance by using Student's *t*-test. Bar graph represents mean \pm S.D. * $P < 0.05$.

apoptosis, rather carry on with meiotic division. Based on the high similarity of HSP110 family members, we expected that the molecular chaperones, which also include the NEF members of HSP110 family, would be abnormally or partially affected in *Hspa4*^{-/-} mice. The relatively leaky phenotype of *Hspa4*-deficient mice led us to suggest that other members of HSP110 family can partially compensate for the loss of HSPA4 function. HSPA4L and HSPH1 are possible candidates, because both proteins are widely expressed and localized in the cytoplasm like HSPA4. Therefore, the possibility of functional compensation between these proteins would be the cause that *Hspa4*^{-/-} mice are viable and display normal development except for disruption of spermatogenesis. This phenotype is also not completely penetrant, because some *Hspa4*-deficient germ cells were able to progress through spermatogenesis. To check this possibility, we intercrossed *Hspa4*-deficient mice with previously described *Hspa4l* mutant mice to produce mice lacking both genes. We found that *Hspa4*^{-/-} *Hspa4l*^{-/-} double knockout mice developed pulmonary hypoplasia that subsequently caused neonatal death during the first day of life (unpublished data). These results suggest a redundant function for HSPA4 and HSPA4L in lung maturation.

Expression of some HSP proteins is inducible by environmental stress, but expression of others can be either constitutive or developmentally regulated (Dix *et al.* 1997). HSPA4 and HSPH1 are ubiquitously expressed proteins and become relatively enriched in gonocytes after colonization of gonads by primordial germ cells (Fig. 2 and our unpublished data). The enrichment of both proteins in germ stem cells suggests their significant role for male and female germ stem cells. The results showed that the gonocytes are not affected in *Hspa4*-deficient mice, suggesting a redundant function of both proteins in germ cell development. To our knowledge, there is no report describing abnormal spermatogenesis in *Hsph1*-deficient mice. In one study, *Hsph1*-null mice were normally fertile (Nakamura *et al.* 2008). We are, therefore, interested in determining the impact of deleting both HSPA4 and HSPH1 on germ cell development by generation and characterization of *Hspa4*^{-/-} *Hsph1*^{-/-} double knockout mice.

Several reports, which used microarray analysis to identify preferentially expressed genes in different stem cells, revealed that the *Hspa4* is highly expressed in embryonic and different tissue-specific stem cells, and its expression is downregulated in their differentiated counterparts (Ramalho-Santos *et al.* 2002, Bhattacharya *et al.* 2004). *Hspa4* was one of the 216 enriched genes that were found to be expressed at high levels in embryonic, neural, and hematopoietic stem cells. Our results showing HSPA4 expression in germ stem cells further confirm the requirement of HSPA4 function for germ cell development. Although the physiological role of molecular chaperones for self-renewal of stem cells is

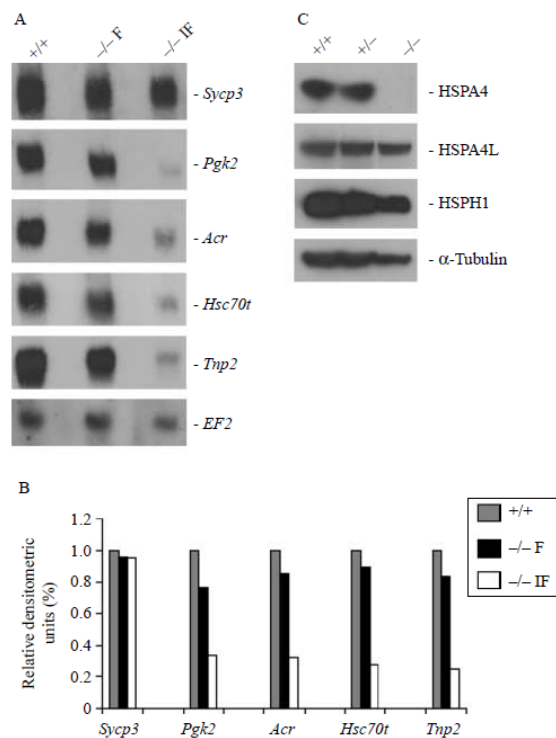


Figure 7 Expression profile of different germ cell markers and members of HSP110 family in *Hspa4*^{-/-} testes. (A) Northern blot with total RNA from testes of *Hspa4*^{+/+} (+/+), fertile (-/-F), and infertile *Hspa4*^{-/-} (-/-IF) mice was sequentially hybridized with cDNA probes for the indicated genes. (B) Densitometry analysis for the expression levels of different spermatogenic markers showing in Fig. 7A was determined. Expression level was expressed as relative percentage, with 1.0 given as the expression of spermatogenic marker in wild-type testis. Expression level of *EF2* gene was used for normalization. (C) Expression patterns of other members of HSP110 family in testes of wild-type and *Hspa4*-null mice. Immunoblots were probed with the antibodies shown at the right margin.

not known, it is believed that molecular chaperones may protect stem cells from aging due to oxidative stress (Ramalho-Santos *et al.* 2002). *Caenorhabditis elegans* that have an extended life span have elevated levels of molecular chaperones and enzymes that process oxidative free radicals and appear to be resistant to environmental stresses (Finkel & Holbrook 2000).

The partial penetrance of male infertility among *Hspa4*-null mice on the hybrid C57BL/6J×129/Sv genetic background may be reflected by the segregation of genetic modifiers on the hybrid genetic background. Background-related differences in male infertility phenotype have been reported in other mutations (Pearse *et al.* 1997, Yu *et al.* 2000, Adham *et al.* 2001). We have observed increased incidence of male infertility among *Hspa4*-null mice in F2 generation, which contain a high level of inter-individual genetic variability. The

decreased incidence of male infertility observed in the subsequent generation suggests that *Hspa4*-null males in different genetic background differ in fertility and would impose a selection bias against that genotype of infertile male. The decreased incidence of spermatogenic phenotypes in the following generations has also been described in different knockout mouse lines (Anderson *et al.* 2008, Burnicka-Turek *et al.* 2009).

The generation of *Hspa4*-, *Hspa4L*- and *Hsph1*-deficient mice constitutes an initial step in the understanding of the physiological role of HSP110 family members in mammals.

Materials and Methods

Generation of HSPA4-null mice

The PAC clone (RPCIP711P18115Q2) containing the *Hspa4* locus was isolated from the 129/Sv genomic library (RZPD, Berlin, Germany). The targeting vector was designed by replacement of exon 1 containing the start codon ATG with the *Pgk-neo* cassette. The 6 kb *SpeI/XhoI* and 4.5 kb *BamHI/EcoRI* genomic fragments containing the sequences of 5'-flanking region and intron 1 of *Hspa4*, respectively, were isolated from the PAC clone and inserted on either side of *Pgk-neo* cassette of pPNT vector (Fig. 3A). The targeting vector was linearized with *NotI* and used for transfection of RI ES cells. Recombined ES-cells were checked for homologous recombination by Southern blot analysis. Genomic DNA was isolated from ES cells, digested with *XbaI*, separated in 0.8% (w/v) agarose gels, and transferred onto nylon membrane (Amersham Pharmacia). A 0.7 kb fragment located at 3' of targeting vector was amplified, radioactive labeled, and used as probe for the Southern blot analysis. Correctly targeted ES cell clones were injected into blastocysts derived from C57BL/6J mice and transferred into pseudo pregnant DBA/BL6 females to generate chimeric mice. The chimeric founders were mated with C57BL/6J to generate heterozygous *Hspa4*^{+/-} mice, which were intercrossed to produce homozygous *Hspa4*^{-/-} mice. Genotyping of mice was carried out by PCR amplification of tail DNA. A 535 bp PCR product from the wild-type allele was detected using primer F1: 5'-GATCACGGGAAGT-GAGTGGT-3' and R1: 5'-GAGCGGGAG TGAGACAGTTC-3'. The targeted allele yielded a 274 bp product with primer F1: and primer PGK 5'-GGATGTGGAATGTGTGCGAGG-3'. The thermal cycling was carried out for 35 cycles of denaturation at 94 °C for 30 s, annealing at 55 °C for 30 s, and extension at 72 °C for 30 s. All animal experiments were reviewed and approved by the Institutional Animal Care and Use Committee of the University of Göttingen.

Northern blot analysis and RT-PCR

Total RNA was extracted using RNAeasy mini-kit (Qiagen) and resolved (10 µg/line) on an agarose gel containing 2.2 M formaldehyde and transferred onto nylon membrane. Blots were hybridized with 358 and 596 bp cDNA fragments containing the sequences of the C-terminal coding and the 3'-untranslated regions of *Hspa4*, respectively. The followed

primers were used to amplify the 358 and the 596 bp cDNA probes: 5'-GAAGAAGTGGGAAGCAAATCC-3' and 5'-TCAATGTCCATCTCAGGAAGC-3'; 5'-GTCCTGTTTAAAGAGCCAGCTA-3' and 5'-ATTATACCAT GCCTACACCCAAC-3'.

RT-PCR assay was performed using 2 µg total RNA and a one step RT-PCR kit (Qiagen). Primers to amplify *Hspa4* and *Hprt* transcripts were 5'-GTCGGTGGTGGGCATAGAC-3' and 5'-TTTATGCCCGTTAATCCAGTG; 5'-GTCAAGGGCATATCCAACAA-CAAAC-3' and 5'-CCTGCTGGATTACATTAAAGCACTG-3', respectively.

Densitometry analysis was performed using the ImageJ Software (NIH, Bethesda, MD, USA); optic density for expression levels of *EF2* in northern blot analysis was used for normalization.

Fertility test and spermatozoa quality

To examine the fertility of *Hspa4*-deficient males on a hybrid 129/Sv×C57BL/6J genetic background, mature *Hspa4*^{-/-} males from the second generation were intercrossed, each with two wild-type CD1 females, for at least 3 months. The number and size of litters sired by each male were determined in a 3-month mating period.

Epididymides of ten *Hspa4*^{-/-} and four wild-type males were collected and dissected in IVF medium (MediCult, Jyllinge, Denmark). Sperm number in cauda epididymides was determined using the Neubauer cell chamber. To determine the sperm motility, spermatozoa were incubated for 1.5 h at 37 °C, 5% CO₂. Sperm suspension (10 µl) was transferred to the incubation chamber, which was set to 37 °C. Sperm movement was quantified using the CEROS computer-assisted semen analysis system (version 10, Hamilton Thorne Research, Beverly, MA, USA).

Histological and immunohistochemical methods

For histological analysis, tissues were fixed in Bouin's solution and embedded in paraffin. Sections (6 µm) were stained with hematoxylin and eosin (H&E). For immunohistochemistry, sections were preincubated for 1 h with 5% normal goat serum in 0.05% (v/v) Triton-X-100-PBS; incubated overnight at 4 °C with either rabbit anti-HSPA4 (N-60; Santa Cruz Biotechnology, Santa Cruz, CA, USA) at 1:200 dilution, anti-HSPA4 (N-96; Santa Cruz) at 1:200 dilution, mouse anti-germ cell nuclear protein (GCNA1) at 1:50 dilution, or anti-HSPH1 (Sigma) at 1:200 dilution; washed with PBS; and then incubated with alkaline phosphate-conjugated goat anti-rabbit antibody or anti-mouse (Sigma) at 1:500 dilution for 1 h at room temperature. After washing with PBS, immunoreactivity was detected by incubation of the sections in a solution containing Fast Red TR/naphthol AS-MX phosphate tablets (Sigma). For PLZF and HSPA4 double immunofluorescent staining, sections of 5-day-old testes were incubated overnight at 4 °C with rabbit anti-HSPA4 and mouse anti-PLZF (D-9, Santa Cruz) antibodies. Sections were washed and then incubated with Cy3-conjugated goat anti-rabbit and FITC-conjugated goat anti-mouse antibodies (Sigma) for 1 h at room temperature. After washing, sections were mounted with Vectashield

mounting reagent (Vector, Burlingame, CA, USA) prior to fluorescence microscopy (Olympus, Hamburg, Germany).

TUNEL-positive cells were detected using an ApopTag peroxidase *in situ* apoptosis kit (Obiogene, Heidelberg, Germany) according to the manufacturer's instruction.

Western blot analysis

Tissues were sonicated in RIPA buffer (Santa Cruz). Protein lysates were cleared by centrifugation at 16 000 g at 4 °C for 20 min, and protein concentration was measured by the Bradford assay (Bio-Rad). Total cell lysate (20 µg) was then resolved in 15% (w/v) SDS-PAGE gel and electroblotted onto nitrocellulose membrane. After blocking with 5% (w/v) skimmed milk in PBS, blots were incubated with either the primary antibodies rabbit anti-HSPA4 (1:500, Santa Cruz), rabbit anti-HSPA4L (1:500, Santa Cruz), rabbit anti-HSPH1 (1:1000, Sigma), or monoclonal anti-α-tubulin (1:10000, Sigma) with skimmed milk in PBS overnight at 4 °C. After a washing step, blots were incubated with HRP-conjugated anti-rabbit or anti-mouse IgG (1:2000, Sigma). The detection of immunoreactivity was performed using enhanced chemiluminescence (Pierce Chemical, Rockford, IL, USA).

Statistical analysis

Paired comparisons of the different sperm parameters and the number of apoptotic cells/tubule in testis among *Hspa4*^{-/-} and *Hspa4*^{+/+} mice were performed for statistical significance by calculating means ± s.d. and Student's *t*-test.

Supplementary data

This is linked to the online version of the paper at <http://dx.doi.org/10.1530/REP-11-0023>.

Declaration of interest

The authors declare that there is no conflict of interest that could be perceived as prejudicing the impartiality of the research reported.

Funding

B A Mohamed is supported by the DAAD through grant A/07/80490.

Acknowledgements

We thank M Schindler, S Wolf and U Fünfschilling for their help in the generation and breeding of knockout mice; A Nagy (Mount Sinai Hospital, Toronto, Canada) for providing RI ES cells; and G C Enders (Kansas University, Medical Center, Kansas City, USA) for providing the GCNA1 antibody. Parts of this research are components of the PhD thesis of T Held: 'Zur Strukturellen und Funktionellen Analyse der Murinen Gene der HSP110 Familie'.

References

- Adham IM, Nayernia K, Burkhardt-Göttges E, Topaloglu O, Dixkens C, Holstein AF & Engel W 2001 Teratozoospermia in mice lacking the transition protein 2 (Tnp2). *Molecular Human Reproduction* 7 513–520. (doi:10.1093/molehr/7.6.513)
- Anderson EL, Baltus AE, Roepers-Gajadien HL, Hassold TJ, de Rooij DG, van Pelt AM & Page DC 2008 Stra8 and its inducer, retinoic acid, regulate meiotic initiation in both spermatogenesis and oogenesis in mice. *PNAS* 105 14976–14980. (doi:10.1073/pnas.0807297105)
- Bhattacharya B, Miura T, Brandenberger R, Mejido J, Luo Y, Yang AX, Joshi BH, Ginis I, Thies RS, Amit M *et al.* 2004 Gene expression in human embryonic stem cell lines: unique molecular signature. *Blood* 103 2956–2964. (doi:10.1182/blood-2003-09-3314)
- Burnicka-Turek O, Shimeshan K, Paprotta I, Grzmil P, Meinhardt A, Engel W & Adham IM 2009 Inactivation of insulin-like factor 6 disrupts the progression of spermatogenesis at late meiotic prophase. *Endocrinology* 150 4348–4357. (doi:10.1210/en.2009-0201)
- Chubb C 1992 Oligotriche and quaking gene mutations. Phenotypic effects on mouse spermatogenesis and testicular steroidogenesis. *Journal of Andrology* 13 312–317.
- Dix DJ, Allen JW, Collins BW, Poorman-Allen P, Mori C, Blizard DR, Brown PR, Goulding EH, Strong BD & Eddy EM 1997 HSP70-2 is required for desynapsis of synaptonemal complexes during meiotic prophase in juvenile and adult mouse spermatocytes. *Development* 124 4595–4603.
- Dragovic Z, Broadley SA, Shomura Y, Bracher A & Hartl FU 2006 Molecular chaperones of the Hsp110 family act as nucleotide exchange factors of Hsp70s. *EMBO Journal* 25 2519–2528. (doi:10.1038/sj.emboj.7601138)
- Dym M & Fawcett DW 1971 Further observations on the numbers of spermatogonia, spermatocytes, and spermatids connected by intercellular bridges in the mammalian testis. *Biology of Reproduction* 4 195–215.
- Eddy EM 1999 Role of heat shock protein HSP70-2 in spermatogenesis. *Reviews of Reproduction* 4 23–30. (doi:10.1530/ror.0.0040023)
- Eddy EM & O'Brien DA 1998 Gene expression during mammalian meiosis. *Current Topics in Developmental Biology* 37 141–200.
- Finkel T & Holbrook NJ 2000 Oxidants, oxidative stress and the biology of ageing. *Nature* 408 239–247. (doi:10.1038/35041687)
- Goto M, Koji T, Mizuno K, Tamaru M, Koikeda S, Nakane PK, Mori N, Masamune Y & Nakanishi Y 1990 Transcription switch of two phosphoglycerate kinase genes during spermatogenesis as determined with mouse testis sections *in situ*. *Experimental Cell Research* 183 273–278. (doi:10.1016/0014-4827(90)90306-U)
- Gotoh K, Nonoguchi K, Higashitsuji H, Kaneko Y, Sakurai T, Sumitomo Y, Itoh K, Subjeck JR & Fujita J 2004 Apg-2 has a chaperone-like activity similar to Hsp110 and is overexpressed in hepatocellular carcinomas. *FEBS Letters* 560 19–24. (doi:10.1016/S0014-5793(04)00034-1)
- Guan K, Nayernia K, Maier LS, Wagner S, Dressel R, Lee JH, Nolte J, Wolf F, Li M, Engel W *et al.* 2006 Pluripotency of spermatogonial stem cells from adult mouse testis. *Nature* 440 1199–1203. (doi:10.1038/nature04697)
- Hartl FU 1996 Molecular chaperones in cellular protein folding. *Nature* 381 571–579. (doi:10.1038/381571a0)
- Held T, Paprotta I, Khulan J, Hemmerlein B, Binder L, Wolf S, Schubert S, Meinhardt A, Engel W & Adham IM 2006 Hspa4l-deficient mice display increased incidence of male infertility and hydronephrosis development. *Molecular and Cellular Endocrinology* 26 8099–8108. (doi:10.1128/MCB.01332-06)
- Kaneko Y, Kimura T, Kishishita M, Noda Y & Fujita J 1997 Cloning of apg-2 encoding a novel member of heat shock protein 110 family. *Gene* 189 19–24. (doi:10.1016/S0378-1119(96)00807-4)
- Kashiwabara S, Arai Y, Kodaira K & Baba T 1990 Acrosin biosynthesis in meiotic and postmeiotic spermatogenic cells. *Biochemical and Biophysical Research Communications* 173 240–245. (doi:10.1016/S0006-291X(05)81047-2)
- Kleene KC & Flynn JF 1987 Characterization of a cDNA clone encoding a basic protein, TP2, involved in chromatin condensation during spermatogenesis in the mouse. *Journal of Biological Chemistry* 262 17272–17277.
- Krempling H, Keime S, Wilhelm K, Adham IM, Hameister H & Engel W 1991 Mouse proacrosin gene: nucleotide sequence, diploid expression, and chromosomal localization. *Genomics* 11 828–834. (doi:10.1016/0888-7543(91)90005-Y)
- Lammers JH, Offenberg HH, van Aalderen M, Vink AC, Dietrich AJ & Heyting C 1994 The gene encoding a major component of the lateral elements of synaptonemal complexes of the rat is related to X-linked lymphocyte-regulated genes. *Molecular and Cellular Endocrinology* 14 1137–1146.
- Li C, Liu D, Yuan Y, Huang S, Shi M, Tao K & Feng W 2010 Overexpression of Apg-2 increases cell proliferation and protects from oxidative damage in BaF3-BCR/ABL cells. *International Journal of Oncology* 36 899–904. (doi:10.3892/ijco.00000568)
- Liu Q & Hendrickson WA 2007 Insights into Hsp70 chaperone activity from a crystal structure of the yeast Hsp110 Sse1. *Cell* 131 106–120. (doi:10.1016/j.cell.2007.08.039)
- Lyon MF, Searle AG 1989 *Genetic Variants and Strains of the Laboratory Mouse*, 2nd edn. Oxford: Oxford University Press.
- Mayer MP & Bukau B 2005 Hsp70 chaperones: cellular functions and molecular mechanism. *Cellular and Molecular Life Sciences* 62 670–684. (doi:10.1007/s00018-004-4464-6)
- McLean DJ, Friel PJ, Johnston DS & Griswold MD 2003 Characterization of spermatogonial stem cell maturation and differentiation in neonatal mice. *Biology of Reproduction* 69 2085–2091. (doi:10.1095/biolreprod.103.017020)
- Nagano R, Tabata S, Nakanishi Y, Ohsako S, Kurohmaru M & Hayashi Y 2000 Reproliferation and relocation of mouse male germ cells (gonocytes) during prespermatogenesis. *Anatomical Record* 258 210–220. (doi:10.1002/(SICI)1097-0185(20000201)258:2<210::AID-AR10>3.0.CO;2-X)
- Nakamura J, Fujimoto M, Yasuda K, Takeda K, Akira S, Hatayama T, Takagi Y, Nozaki K, Hosokawa N & Nagata K 2008 Targeted disruption of Hsp110/105 gene protects against ischemic stress. *Stroke* 39 2853–2859. (doi:10.1161/STROKEAHA.107.506188)
- Nonoguchi K, Itoh K, Xue JH, Tokuchi H, Nishiyama H, Kaneko Y, Tsumi K, Okuno H, Tomiwa K & Fujita J 1999 Cloning of human cDNAs for Apg-1 and Apg-2, members of the Hsp110 family, and chromosomal assignment of their genes. *Gene* 37 21–28. (doi:10.1016/S0378-1119(99)00325-X)
- Pearse RV, Drolet DW, Kalla KA, Hooshmand F, Bermingham JR Jr & Rosenfield MG 1997 Reduced fertility in mice deficient for the POU protein sperm-1. *PNAS* 94 7555–7560. (doi:10.1073/pnas.94.14.7555)
- Polier S, Dragovic Z, Hartl FU & Bracher A 2008 Structural basis for the cooperation of Hsp70 and Hsp110 chaperones in protein folding. *Cell* 133 1068–1079. (doi:10.1016/j.cell.2008.05.022)
- Ramalho-Santos M, Yoon S, Matsuzaki Y, Mulligan RC & Melton DA 2002 "Stemness": transcriptional profiling of embryonic and adult stem cells. *Science* 298 597–600. (doi:10.1126/science.1072530)
- Rassoulzadegan M, Paquis-Flucklinger V, Bertino B, Sage J, Jasin M, Miyagawa K, van Heyningen V, Besmer P & Cuzin F 1993 Transmeiotic differentiation of male germ cells in culture. *Cell* 75 997–1006. (doi:10.1016/0092-8674(93)90543-Y)
- Raviol H, Sadlish H, Rodriguez F, Mayer MP & Bukau B 2006 Chaperone network in the yeast cytosol: Hsp110 is revealed as an Hsp70 nucleotide exchange factor. *EMBO Journal* 25 2510–2518. (doi:10.1038/sj.emboj.7601139)
- Schuemann JP, Jiang J, Cuellar J, Llorca O, Wang L, Gimenez LE, Jin S, Taylor AB, Demeler B, Morano KA *et al.* 2008 Structure of the Hsp110:Hsc70 nucleotide exchange machine. *Molecular Cell* 31 232–243. (doi:10.1016/j.molcel.2008.05.006)
- Steel GJ, Fullerton DM, Tyson JR & Stirling CJ 2004 Coordinated activation of Hsp70 chaperones. *Science* 303 98–101. (doi:10.1126/science.1092287)
- Terada K, Yomogida K, Imai T, Kiyonari H, Takeda N, Kadomatsu T, Yano M, Aizawa S & Mori M 2005 A type I DnaJ homolog, DjA1, regulates androgen receptor signaling and spermatogenesis. *EMBO Journal* 24 611–622. (doi:10.1038/sj.emboj.7600549)
- Tsunekawa N, Matsumoto M, Tone S, Nishida T & Fujimoto H 1999 The Hsp70 homolog gene, Hsc70t, is expressed under translational control during mouse spermiogenesis. *Molecular Reproduction and Development* 52 383–391. (doi:10.1002/(SICI)1098-2795(199904)52:4<383::AID-MRD7>3.0.CO;2-Z)

144 T Held, A Z Barakat and others

Vergouwen RP, Jacobs SG, Huiskamp R, Davids JA & de Rooij DG 1991 Proliferative activity of gonocytes, Sertoli cells and interstitial cells during testicular development in mice. *Journal of Reproduction and Fertility* **93** 233–243. (doi:10.1530/jrf.0.0930233)

Vos MJ, Hageman J, Carra S & Kampinga HH 2008 Structural and functional diversities between members of the human HSPB, HSPH, HSPA, and DNAJ chaperone families. *Biochemistry* **47** 7001–7011. (doi:10.1021/bi800639z)

Yu YE, Zhang Y, Unni E, Shirley CR, Deng JM, Russell LD, Weil MM, Behringer RR & Meistrich ML 2000 Abnormal spermatogenesis and reduced fertility in transition nuclear protein 1-deficient mice. *PNAS* **79** 4683–4688. (doi:10.1073/pnas.97.9.4683)

Zimmermann S, Steding G, Emmen JM, Brinkmann AO, Nayernia K, Holstein AF, Engel W & Adham IM 1999 Targeted disruption of the *Ins13* gene causes bilateral cryptorchidism. *Molecular Endocrinology* **13** 681–691. (doi:10.1210/me.13.5.681)

Received 26 January 2011

First decision 21 February 2011

Accepted 12 April 2011

5.2. Publication II

Targeted disruption of Hspa4 gene leads to cardiac hypertrophy and fibrosis

DOI: 10.1016/j.yjmcc.2012.07.014

Belal A Mohamed, Amal Z Barakat, Wolfram-Hubertus Zimmermann, Reginald E Bittner, Christian Mühlfeld, Mark Hünlich, Wolfgang Engel, Lars S Maier, Ibrahim M Adham

Status: Published in *Journal of Molecular and Cellular Cardiology* (Impact factor 5.50), Volume 53 (2012), pp. 459-468

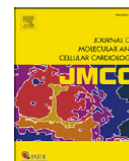
Author contributions to the work:

1. **Belal A Mohamed:** Participated in designing of the experiments, performed the experiments including screening of HSPA4 expression in human and murine heart, analysis of the cardiac hypertrophy and fibrosis induced in *Hspa4* KO mice after TAC, microarray data analysis and verification, molecular studies to identify the affected signaling pathways, neonatal mice cardiomyocyte culture and probing of the ubiquitination status, carried out statistical analysis of the data, participated in data interpretation and was involved in manuscript preparation
2. Amal Z Barakat: Participated in analysis of the baseline cardiac hypertrophy and fibrosis seen in *Hspa4* KO mice, participated in microarray data analysis and verification
3. Wolfram-Hubertus Zimmermann: Helped in establishment of neonatal mouse cardiomyocyte culture, interpretation of the data and gave critical comments and recommendations
4. Reginald E Bittner: Interpreted the data of histological studies
5. Christian Mühlfeld: Carried out electron microscopy analysis
6. Mark Hünlich: Performed echocardiogram analysis and TAC operation in mice
7. Wolfgang Engel: Conceived and designed the experiments, gave critical comments and recommendations, and financial support
8. Lars S Maier: Provided the heart samples from human patients with aortic stenosis, interpreted the data and gave critical comments and recommendations
9. Ibrahim M Adham: Conceived and designed the experiments, interpretation of the data and critical review of the manuscript



Contents lists available at SciVerse ScienceDirect

Journal of Molecular and Cellular Cardiology

journal homepage: www.elsevier.com/locate/yjmcc

Original article

Targeted disruption of *Hspa4* gene leads to cardiac hypertrophy and fibrosisBelal A. Mohamed^a, Amal Z. Barakat^a, Wolfram-Hubertus Zimmermann^b, Reginald E. Bittner^c, Christian Mühlfeld^d, Mark Hünlich^e, Wolfgang Engel^a, Lars S. Maier^e, Ibrahim M. Adham^{a,*}^a Institute of Human Genetics, University of Göttingen, Germany^b Department of Pharmacology/Heart Research Center, University of Göttingen, Germany^c Department of Neuromuscular Research/Center of Anatomy & Cell Biology, University of Vienna, Austria^d Institute of Anatomy and Cell Biology, University of Gießen, Germany^e Department of Cardiology and Pneumology/Heart Research Center, University of Göttingen, Germany

ARTICLE INFO

Article history:

Received 24 October 2011

Received in revised form 12 July 2012

Accepted 24 July 2012

Available online 1 August 2012

Keywords:

HSPA4

Hypertrophy

Fibrosis

Pressure overload

Polyubiquitination

ABSTRACT

Failure of molecular chaperones to direct the correct folding of newly synthesized proteins leads to the accumulation of misfolded proteins in cells. HSPA4 is a member of the heat shock protein 110 family (HSP110) that acts as a nucleotide exchange factor of HSP70 chaperones. We found that the expression of HSPA4 is upregulated in murine hearts subjected to pressure overload and in failing human hearts. To investigate the cardiac function of HSPA4, *Hspa4* knockout (KO) mice were generated and exhibited cardiac hypertrophy and fibrosis. *Hspa4* KO hearts were characterized by a significant increase in heart weight/body weight ratio, elevated expression of hypertrophic and fibrotic gene markers, and concentric hypertrophy with preserved contractile function. In response to pressure overload, cardiac hypertrophy and remodeling were further aggravated in the *Hspa4* KO compared to wild type (WT) mice. Cardiac hypertrophy in *Hspa4* KO hearts was associated with enhanced activation of gp130-STAT3, CaMKII, and calcineurin-NFAT signaling. Protein blot and immunofluorescent analyses showed a significant accumulation of polyubiquitinated proteins in cardiac cells of *Hspa4* KO mice. These results suggest that the myocardial remodeling of *Hspa4* KO mice is due to accumulation of misfolded proteins resulting from impaired chaperone activity. Further analyses revealed a significant increase in cross sectional area of cardiomyocytes, and in expression levels of hypertrophic markers in cultured neonatal *Hspa4* KO cardiomyocytes suggesting that the hypertrophy of mutant mice was a result of primary defects in cardiomyocytes. Gene expression profile in hearts of 3.5-week-old mice revealed a differentially expressed gene sets related to ion channels, muscle-specific contractile proteins and stress response. Taken together, our *in vivo* data demonstrate that *Hspa4* gene ablation results in cardiac hypertrophy and fibrosis, possibly, through its role in protein quality control mechanism.

© 2012 Elsevier Ltd. All rights reserved.

1. Introduction

Heat shock proteins (HSPs) are the major components of molecular chaperones that facilitate the folding of newly synthesized proteins, prevent the aggregation of misfolded proteins, and promote their refolding in different cellular compartments such as the cytosol or endoplasmic reticulum [1]. HSPs are subdivided according to their molecular weight into the following groups: HSPH (HSP110), HSPC (HSP90), HSPA (HSP70), DNAJ (HSP40), HSPD (HSP60), and HSPB (HSP27) [2]. Binding of newly synthesized polypeptides to HSP chaperones and the subsequent release of folded proteins are regulated by continuous cycles of adenosine triphosphate (ATP) hydrolysis and the exchange of ATP for adenosine diphosphate (ADP). The HSP70 chaperone represents

the major protein folding machinery in the eukaryotic cytosol, and it complexes with two co-chaperones, HSP40 and HSP110. HSP40 stimulates ATP hydrolysis, whereas HSP110 acts as a nucleotide exchange factor that accelerates ADP dissociation from the HSP70 [3–6].

Several reports have shown that some HSPs have cardioprotective effects against ischemic injury, while others are induced in response to hypertrophy [7,8]. The cardioprotective role of HSPs was confirmed by the results showing the development of cardiac hypertrophy and dilated cardiomyopathy in HSP70-1/HSP70-3 double mutants and in mice null for mitochondrial HSP40, respectively [9,10]. Moreover, mutations in human BAG3, encoding a co-chaperone of Hsc70, were found in family members with dilated cardiomyopathy [11].

The mammalian genome encodes three cytosolic HSP110 proteins, HSPA4 (APG2), HSPA4L (APG1), and HSPH1 (HSP110), and the endoplasmic reticulum-located protein HYOU1 (GRP175/ORP150). *Hspa4* is widely expressed and not inducible by heat shock [12]. Except for impaired male fertility, analyses of *Hspa4* KO mice did not reveal other overt abnormalities [13].

* Corresponding author at: Institute of Human Genetics, University of Göttingen, Heinrich-Düker-Weg 12, D-37073, Göttingen, Germany. Tel.: +49 551 397522.
E-mail address: iadham@gwdg.de (I.M. Adham).

In the present study, we found that the expression levels of HSPA4 were significantly elevated in hearts of pressure overloaded mice subjected to transaortic constriction (TAC) and in human hearts with aortic stenosis. Loss of HSPA4 in mutant mice resulted in the development of cardiac hypertrophy and fibrosis. These phenotypes were accompanied by accumulation of polyubiquitinated proteins in cardiomyocytes. Furthermore, we studied the effect of stress-response signaling, which might mediate the development of cardiac hypertrophy.

2. Materials and methods

2.1. Mice

Hspa4 KO mice were generated previously [13]. In this study, we analyzed *Hspa4* KO on 129/Sv genetic background. All animal experiments were reviewed and approved by the Institutional Animal Care and Use Committee of the University of Göttingen.

2.2. Histological analysis and immunohistochemistry

Excised hearts were rinsed in phosphate buffered saline (PBS) and incubated in Krebs-Hanseleit solution lacking Ca^{+2} to relax the cardiac muscle before fixation. Heart weight and its respective ratio to body weight were calculated as an index of cardiac hypertrophy. Ventricular tissues were fixed in 4% paraformaldehyde solution for 16 h at 4 °C, embedded in paraffin, and sectioned into 5- μm sections. Sections were stained with hematoxylin and eosin (H&E). Myocyte diameter and area were assessed from images taken at 600 \times from 2 random fields (from 4 sections of each heart of 3 mice per age and genotype) using NIH Image J software. The diameter and area of 500 myocytes were traced in each group. To determine the distribution of fibrosis in heart tissue samples, sections were stained with Masson's trichrome (Sigma-Aldrich) according to the manufacturer's procedures. For immunofluorescence staining, cardiac sections were reacted with primary anti-Ubiquitin (1:500; DakoCytomation), anti- α -Actinin (1:500; Sigma), and anti-HSPA4 (1:300; Santa Cruz Biotechnology) followed by secondary Alexa Fluor 488 IgG antibody (1:500; Invitrogen) and Cy3-conjugated anti-Rabbit IgG antibody (Sigma). DAPI was used for nuclear staining. Sections were analyzed by reverse microscope fluorescence equipped microscope (BX60; Olympus, Hamburg, Germany).

2.3. Quantitative real-time PCR and western blot analyses

For real-time PCR, total RNAs were treated with RNA free DNase (Promega) for 1 h at 37 °C, and reverse transcribed using the Superscript II first strand kit (Invitrogen). Quantitative RT-PCR (qRT-PCR) was performed in triplicate on ABI Prism 7900HT sequence detection system (Applied Biosystems) using QuantiTect SYBR Green PCR Master mix as a double-stranded DNA-specific dye according to manufacturer's instruction (QIAGEN). The mRNA expression levels were normalized to either hypoxanthine guanine phosphoribosyl transferase (*Hprt*) or Succinate dehydrogenase (*Sdh*) mRNA. Data of QRT-PCR analysis are shown as mean \pm standard deviation (SD). Sequences of used primers are shown in Suppl. Table 1.

For extraction of soluble and insoluble protein fractions, the hearts were homogenized in RIPA buffer (Millipore) containing protease inhibitor cocktail (Roche Diagnostics). The homogenates were centrifuged at 12,000 g at 4 °C for 20 min. The supernatants were stored as soluble fraction. The pellet was suspended with 1% SDS detergent homogenization buffer, sonicated and then centrifuged at 12,000 g at 4 °C for 20 min to obtain a detergent insoluble protein fraction. Protein samples were resolved on 4–12% SDS-PAGE and transferred onto nitrocellulose membrane (Amersham Pharmacia). Membranes were then blocked for 1 h with 5% non-fat milk in 0.1% Tween 20 in TBS. Blots were probed at 4 °C overnight with antibodies against total and phosphorylated ERK1/

2, STAT3 (1:1000; Cell Signaling Technology), CaMKII (1:1000; gift from Dr. Bers) [14], P-CaMKII (1:1000; Affinity BioReagents), HSPA4, HSPA4L (1:2000; Santa Cruz), Ubiquitin (1:4000; DakoCytomation), DAB2 (1:1000; BD Transduction Laboratories), HSPH1, HSP70 and α -tubulin (1:5000; Sigma), and followed by incubation with a secondary peroxidase-conjugated antibody (1:5000; Sigma). Signals were detected using a chemiluminescent kit (Santa Cruz). Signals were quantified by AlphaView software; Version: 3.2.0 (Cell Biosciences, Inc.).

2.4. Calcineurin phosphatase activity assay

Cardiac lysates from 12-week-old *Hspa4* WT and KO mice were isolated, and calcineurin activity was measured as the dephosphorylation rate of a synthetic RII phosphopeptide substrate using a calcineurin phosphatase assay kit (BML-AK804; Enzo Life Sciences International) according to the manufacturer's instructions. The released free phosphate was detected photometrically at 620 nm using a microplate reader.

2.5. Determination of 20S Proteasome activity

Cardiac lysates from 12-week-old *Hspa4* WT and KO mice were isolated, and 20S Proteasome activity was measured using 20S Proteasome Assay Kit (10008041; Biomol) according to the manufacturer's instructions. In short, a synthetic 20S substrate, SUC-LLVY-AMC was used which, upon cleavage by the active enzyme, generates a highly fluorescent product that can be measured using excitation and emission wavelengths of 360 nm and 480 nm, respectively.

2.6. Neonatal cardiomyocyte culture and immunocytochemistry

Cardiac cells were isolated from heart ventricles of 1- to 3-day-old mice by multiple rounds of DNase/trypsin digestion as described previously [15]. Cells were pre-cultured in Dulbecco's modified Eagle medium containing 10% fetal calf serum for 2 h to reduce non-myocyte content. Non-adherent cells were collected by centrifugation and either used for RNA extraction or cultured on laminin-coated 96-well plates in the presence of Ara-C (20 μM) to inhibit proliferation of contaminating fibroblasts. After 96 h, cells were either harvested for RNA isolation or fixed in 4% paraformaldehyde for 30 min at 4 °C, permeabilized with 0.1% triton X-100 in PBS and blocked with 2% bovine serum albumin in PBS for 1 h. Cells were incubated with a monoclonal antibody against sarcomeric α -actinin (Sigma; 1:700) for 2 h at 4 °C, washed and incubated with FITC-conjugated goat anti-mouse IgG antibody (Sigma) for 1 h at 4 °C. After washing, cells were incubated with TRITC-Phalloidin (Sigma) to label f-actin, counterstained with DAPI and examined by reverse microscope fluorescence equipped microscope (BX60; Olympus, Hamburg, Germany). For morphometric analysis, approximately 800 cells costained with both α -actinin and f-actin per each genotype ($n=2$ independent experiment) were randomly chosen, and the cross sectional area (CSA) of cardiomyocytes was measured using NIH Image J software.

2.7. Transthoracic echocardiography

Cardiac dimensions and functions were evaluated by echocardiography (Visual Sonic 770 system, 30-MHz transducer, Toronto, Ontario, Canada) in anesthetized mice. M-mode was recorded (sweep speed, 150 mm/s).

2.8. Induction of hemodynamic overload

To induce cardiac pressure overload in mice, transverse aortic constriction (TAC) was performed on 8-week-old male mice as previously described [16]. Sham control mice underwent the same procedure except for aortic constriction.

Volume overload was induced by creating aortocaval shunt according to the method of García and Diebold [17]. The sham-operated control protocol was identical to shunt induction, except no aortic puncture was performed.

2.9. Human tissue samples

Cardiac biopsies were obtained from aortic stenosis patients and from normal subjects undergoing aortic replacement and bypass surgery, respectively. The study was approved by the Institutional Ethics Committee of the University Medical Center Goettingen and written informed consent was obtained from all patients.

2.10. Transmission electron microscopy

Transmission electronic microscopy analysis was performed as described previously [18] with some modifications. Briefly, a small piece of myocardium was taken from the LV and immediately immersed in fixation solution (3% glutaraldehyde, 1% Paraformaldehyde in 0.1 M sodium cacodylate buffer, pH 7.4) for 8–12 h at 4 °C. Tissues were then washed in washing buffer (3.4% Saccharose in 0.1 M Cacodylate buffer, pH 7.4) for 2 h. After aldehyde fixation, the pieces were subsequently postfixed with osmium tetroxide, stained en bloc with uranyl acetate and dehydrated in an ascending ethanol series. After epoxy resin embedding and polymerization 50- to 80-nm-thick sections were cut with an ultramicrotome, stained with uranyl acetate and lead citrate and then observed with a transmission electron microscope (EM 902, Zeiss, Oberkochen, Germany).

2.11. Microarray analysis

Total RNA was extracted from heart ventricles of 3.5-week-old *Hspa4* WT and KO males ($n = 3$ mice for each genotype). Using the WT Target Labeling Kit (Affymetrix), cDNA was synthesized according to the manufacturer's recommendations. Global gene expression analysis was applied using the GeneChip® Mouse Gene 1.0 ST arrays (Affymetrix). Hybridization was performed for 18 h at 60 rpm and 45 °C in the GeneChip® Hybridization Oven 640. After washing and staining in Gene Chip® Fluidics Station 450 (Affymetrix), the arrays were scanned using the GeneChip® scanner 3000 7G (Affymetrix). Intensity data were extracted using R (Version 2.13.0) and Bioconductor using the *rma*-function of package *Affy* (*affy_1.30.0*) and the *CDF*-package *mogene10sttranscriptcluster* 14.1.0 from Brainarray (<http://brainarray.mbi.med.umich.edu>) and analyzed using the *Limma* package of Bioconductor [19,20].

The microarray data analysis consists of the following steps: 1. quantile normalization, 2. global clustering, 3. fitting the data to a linear model, and 4. detection of differential gene expression. For cluster analysis, we used a hierarchical approach with the average linkage-method. Distances were measured as 1-Pearson's Correlation Coefficient. To estimate the average group values for each gene and assess differential gene expression, a simple linear model was fit to the data, and group-value averages and standard deviations for each gene were obtained. To find genes with significant expression changes between groups, empirical Bayes statistics were applied to the data by moderating the standard errors of the estimated values [19]. P-values were obtained from the moderated t-statistic and corrected for multiple testing with the Benjamini-Hochberg method [21]. Classification of the differentially expressed genes was performed according to the gene ontology (GO) listing found in the DAVID (the database for annotation, visualization and integrated discovery) bioinformatics resources [22,23].

The data discussed in this paper are generated conforming to the MIAME guidelines and have been deposited in NCBI's Gene Expression Omnibus and are accessible through GEO Series accession number GSE32885 (<http://www.ncbi.nlm.nih.gov/geo/query/acc.cgi?acc=GSE32885>).

2.12. Statistical analysis

Data were expressed as mean \pm SD or mean \pm SEM where appropriate. Differences among groups were tested by Student's *t* test or 2-way ANOVA where appropriate. A *P* value < 0.05 was considered to be significantly different.

3. Results

3.1. HSPA4 is up-regulated in pressure overloaded hearts

To investigate whether myocardial expression of *Hspa4* in heart is induced in response to hemodynamic stress, we examined the expression levels of HSPA4 in WT mice subjected to pressure overload by transverse aortic constriction (TAC) and volume overload (Shunt). HSPA4 was significantly upregulated after TAC (Fig. 1A). In contrast, no difference in HSPA4 expression was observed in sham- and shunt-operated mice (Fig. 1B). To substantiate the relevance of this finding in light of a human disease equivalent, we examined the expression of HSPA4 in hearts of human patients with aortic stenosis and normal subjects. In agreement with our mouse data, we observed in patient samples with aortic stenosis profoundly enhanced levels of HSPA4 protein levels (Fig. 1C). These results suggest that afterload is the main stressor inducing the HSPA4 expression in the heart.

To elucidate the cellular distribution of HSPA4 protein, cryosections of hearts isolated from sham- and TAC-operated mice were subjected to immunofluorescent analysis. We observed that the subcellular localization of HSPA4 in the WT cardiac cells of sham- and TAC-operated WT hearts was restricted to the cytosolic compartments (Fig. 1D) with marked increase of fluorescent signals in hearts subjected to TAC surgery. The HSPA4-specific immunoreaction was confirmed by the absence of HSPA4 immunostaining in KO hearts (Fig. 1D).

3.2. Development of cardiac hypertrophy and fibrosis in *Hspa4* KO mice

To determine the consequences of HSPA4 deficiency in the heart, we determined the heart weight to body weight ratio (HW/BW) and studied histology of the hearts from 2-, 12-, and 24-week-old *Hspa4* WT and KO littermates. No significant changes in HW/BW ratio could be observed between 2-week-old WT and KO mice (Fig. 2B). *Hspa4* KO at 12- and 24-weeks showed a significant increase in HW/BW ratios (Figs. 2A, B). H&E staining showed an increase in cardiomyocyte diameter in 12- and 24-week-old *Hspa4* KO mice (Figs. 2C; upper panels, D). Ultrastructural analysis of sections from left ventricular myocardium of 8-week-old mice revealed peculiar structural abnormalities in *Hspa4* KO cardiomyocytes (i.e. myofibrillar disassembly and nuclear vacuolation; Suppl Fig. 1).

To confirm the development of cardiac hypertrophy at molecular level, expression of hypertrophy response genes, atrial natriuretic peptide (*Nppa/Anp*), brain natriuretic peptide (*Nppb/Bnp*), β -myosin heavy chain (*Myh7/ β -MHC*) and α 1-skeletal actin (*Acta1/ α -SA*) were determined by quantitative RT-PCR. Expression levels of these hypertrophic markers were significantly elevated in *Hspa4* KO hearts (Fig. 2E). These results demonstrate that the depletion of HSPA4 in mice causes baseline cardiac hypertrophy.

To check whether cardiac hypertrophy was associated with the development of cardiac fibrosis, microscopic analysis of Masson's trichrome-stained histological sections was performed. Increased interstitial fibrosis was observed in hearts of 12-week-old *Hspa4* KO mice compared with age-matched WT (Fig. 2C; lower panels). Further analysis of mRNA expression levels of fibrosis markers collagen III (*Col3a1*) and *Tgfb1* revealed enhanced expression in KO hearts (Fig. 2F).

To evaluate heart dimensions and functions, echocardiogram on 16-week-old mice was performed. *Hspa4* KO mice exhibited significant hypertrophy with increased interventricular septum thickness (IVSD) compared to WT (Fig. 2G). Left ventricular mass (LVM) as well as the

462

BA Mohamed et al. / Journal of Molecular and Cellular Cardiology 53 (2012) 459–468

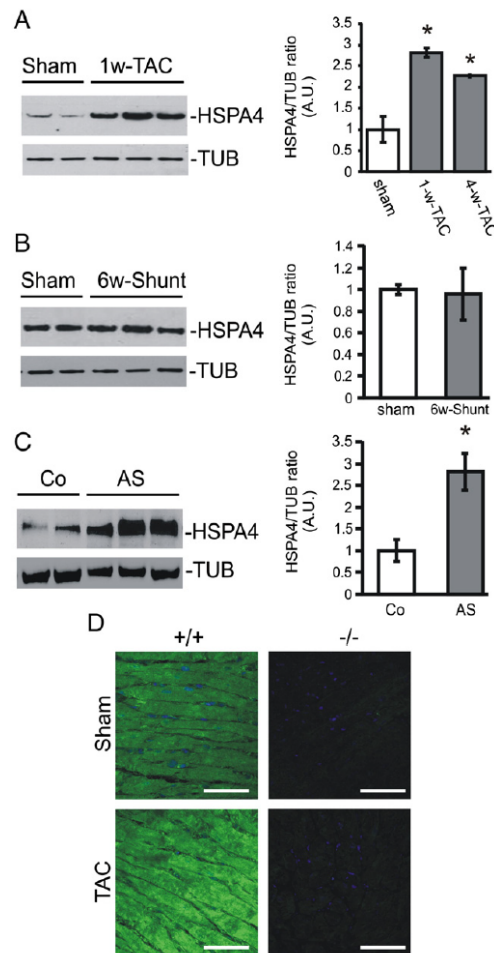


Fig. 1. Upregulation of HSPA4 in response to pressure overload. Heart protein extracts were isolated from mice subjected to transverse aortic constriction (TAC) for 1- or 4-weeks (A), from mice subjected to aorticaval shunt operation for 6 weeks (shunt) (B), or from patients with aortic stenosis (AS) (C). Western blots were probed with antibodies directed against HSPA4 and α -tubulin (TUB). In the bar graph presenting in the right panels, expression levels of HSPA4 were normalized to that of α -tubulin. Values are expressed as mean \pm SD. HSPA4 protein levels in hearts of sham-operated mice or human control hearts (Co) samples served as reference. * $P < 0.05$ vs control, $n = 4-6$ per group. A.U. indicates arbitrary units. (D) Subcellular distribution of HSPA4 in the hearts. Immunofluorescence of HSPA4 (green) in cardiac sections from *Hspa4* WT (+/+) and KO (-/-) mice 2 wk after sham and TAC operation. Nuclei were stained blue with DAPI. Bar = 30 μ m.

left ventricular mass to body weight ratios (LVM/BW) were higher in *Hspa4* KO mice (Figs. 2H, I). However, the increased ratio of LVM/BW was not significant (Fig. 2I). Furthermore, the calculated ratio of wall thickness to heart radius (h/r) at diastole was significantly increased compared to that of WT mice (Fig. 2J), suggesting concentric hypertrophy. Remarkably, echocardiography showed that left ventricle end diastolic dimension and left ventricle end systolic dimension were both maintained in *Hspa4* KO mice at levels comparable with those of WT excluding the development of dilated cardiomyopathy (Suppl. Table 2). Furthermore, left ventricle fractional shortening (FS), reflecting left

ventricular contractile functions, was preserved in *Hspa4* KO mice at a level comparable with that of WT (Fig. 2K), denoting the preservation of LV function.

To rule out any relevant compensation exerted by other members of HSP110 and HSP70 families in *Hspa4* KO hearts, we have determined the protein levels of HSPA4L, HSPH1 and HSP70 in the myocardium of *Hspa4* WT and KO mice. HSPA4 immunoreactivity was absent in *Hspa4* KO heart tissues. Protein levels of HSPA4L, HSPH1 and HSP70 were not markedly different in KO compared with WT hearts, suggesting that the depletion of HSPA4 is not compensated by increased expression of studied HSP proteins in KO hearts (Suppl. Fig. 2).

3.3. Loss of HSPA4 led to an exaggerated hypertrophic response to pressure overload

To examine the role of HSPA4 in modulating the response to cardiac pressure overload, we exposed *Hspa4* KO and WT mice to TAC. In response to TAC for 2 weeks, *Hspa4* KO mice developed significant increase in the ratio of HW/BW than WT mice (Figs. 3A, D). Histological analysis demonstrated that TAC resulted in a significant increase in cardiac myocyte cross-sectional area (Figs. 3B, E) and ventricular fibrosis (Figs. 3C, F) in KO mice compared with WT mice. Consistent with the enhanced hypertrophy and remodeling in KO mice, myocardial expression levels of *Nppa*, *Nppb* and β -Myh7 were significantly higher in KO mice than in WT mice after TAC (Fig. 3G). In line with the observed enhanced remodeling, myocardial expression levels of fibrosis markers *Col1a1*, *Col3a1* and *Tgfb β 1* were higher in TAC-operated KO hearts compared with TAC-operated WT hearts (Fig. 3H). Compared with the WT TAC group, echocardiogram showed statistically increased IVSD, LVM/BW, LVM and h/r in the KO TAC hearts (Figs. 3I–L). FS showed significant reduction in KO group after TAC but was not significantly different from that of TAC-operated WT mice (Fig. 3M). These results suggest that HSPA4 ablation aggravates pathological cardiac hypertrophy and remodeling in response to pressure overload.

3.4. Alteration in activity of signaling pathways contributing to the development of cardiac hypertrophy in *Hspa4* KO mice

Several molecular pathways are implicated in the molecular response of cardiomyocytes to external stimuli. Alterations in the activity of gp130/STAT3, MAPK, CaMKII, or calcineurin-NFAT signaling can lead to the development of cardiac hypertrophy [24]. To determine the signaling pathway that is affected in the heart of *Hspa4* KO mice and which might be responsible for development of the observed cardiomyopathy, we studied the expression levels of some of the genes and proteins involved in these pathways. Western blot analysis did not reveal detectable differences in activated mitogen-activated protein kinases pERK1/2 (Fig. 4A). In contrast, expression levels of phosphorylated STAT3 were elevated in KO hearts, suggesting enhanced activation of gp130-STAT3 signaling (Fig. 4A). We also found a significant increase in the levels of phosphorylated CaMKII (Fig. 4B). In addition, the expression levels of *Rcan 1.4/Mcpl-4*, which is a gene directly targeted by the activated transcription factor (NFAT), was elevated 14-fold in KO hearts (Fig. 4C). Examination of total calcineurin phosphatase activity from KO hearts revealed a significant increase compared with that of WT (Fig. 4D). These results confirm the activation of calcineurin-NFAT signaling in *Hspa4* KO heart. These findings suggest that elevated gp130-STAT3 activity, phosphorylated CaMKII, and the calcineurin-NFAT-dependent signaling pathway are all intimately involved in the cardiac remodeling of *Hspa4* KO mice.

3.5. Increased accumulation of polyubiquitinated proteins in the heart of *Hspa4* KO mice

Molecular chaperones mediate the proper folding of newly synthesized proteins and refolding of misfolded proteins. Impaired chaperone functions lead to increased misfolded proteins and subsequent

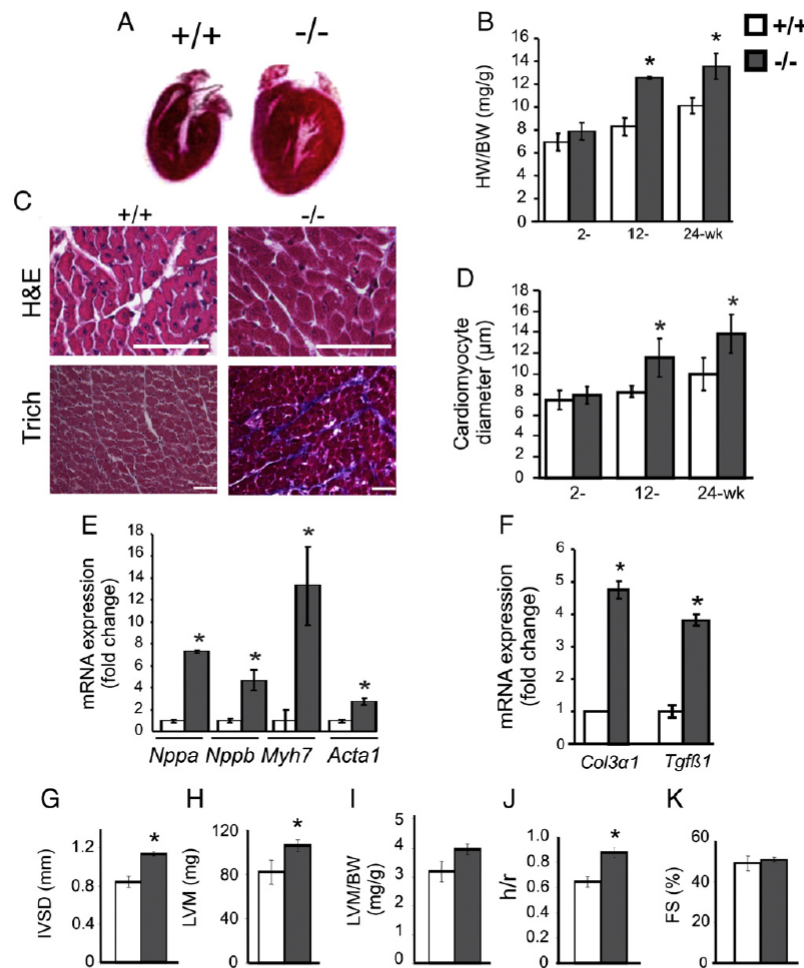


Fig. 2. Development of cardiac hypertrophy in *Hspa4* KO mice. (A) Representative longitudinal sections of hearts from 24-week-old *Hspa4* WT (+/+) and KO (-/-) mice. (B) HW/BW ratio of 2-, 12-, and 24-week-old WT and KO mice. Seven to ten animals per age, stage and genotype were used in this analysis. Ratio is presented as mean \pm SD. * $P < 0.05$ vs WT. (C) Representative H&E- (upper panels) and Masson's trichrome-staining (Trich, lower panels) of transverse myocardial sections of 12-week-old mice showing enlarged *Hspa4* KO cardiomyocytes and marked increased interstitial fibrosis. Bar = 20 μ m in upper panels; 50 μ m in lower panels. (D) Quantitative analysis of cardiomyocytes diameters in 2-, 12- and 24-week-old *Hspa4* WT and KO mice. * $P < 0.05$ vs WT, $n = 3$ hearts per group and stage. (E, F) RNA isolated from heart ventricles of 12-week-old mice was used to determine the expression levels of hypertrophic markers *Nppa*, *Nppb*, *Myh7*, and *Acta1* (E) and fibrosis markers *Col3a1* and *Tgfb1* (F) by qRT-PCR. Values of expression levels normalized by *Sdh* are presented as mean \pm SD. Transcript levels in hearts of WT mice were expressed as 1.0. * $P < 0.05$ vs WT, $n = 3$ per age and genotype. (G–K) Mean echocardiographic parameters of 16-week-old WT and KO mice. (G) Interventricular septum dimension (IVSD); (H) left ventricular mass (LVM); (I) ratios of left ventricular mass to body weight (LVM/BW); (J) ratios of wall thickness to heart radius (h/r) and (K) fractional shortening (FS). Data are mean \pm SEM. * $P < 0.05$ vs WT, $n = 6–8$ per group.

accumulation of ubiquitinated proteins [25]. To determine whether the HSPA4 depletion results in an increased polyubiquitinated protein level, soluble and insoluble protein fractions of myocardial extracts isolated from 4- and 12-week-old *Hspa4* WT and KO mice were probed with anti-ubiquitin. As shown in Fig. 5A, levels of polyubiquitinated proteins in soluble and insoluble fractions were markedly increased in KO hearts compared with WT controls at both ages. Further analysis did not show elevated levels of ubiquitinated proteins in skeletal muscle and brain of KO mice (Fig. 5B and data not shown). Immunofluorescent analysis revealed a prominent accumulation of ubiquitin conjugates in cardiac sections of KO mice. In contrast, microscopic analysis failed to detect any ubiquitin aggregates in WT cardiac tissues (Fig. 5C). Ubiquitinated proteins are proteolytically degraded by enzymatic activities of proteasome

[26]. We determined the chymotrypsin-like activity in crude protein extracts of KO and WT hearts using a synthetic fluorogenic substrate to compare proteasome activity. No significant differences could be observed in KO hearts compared with WT hearts (Fig. 5D).

3.6. *Hspa4* KO neonatal cardiac cells exhibited hypertrophy

Hspa4 is ubiquitously expressed in different tissues [12,13]. To prove whether the hypertrophic cardiomyocyte phenotype is due to an intrinsic heart defect, cardiac cells were isolated from newborn *Hspa4* WT and KO mice and cultured (Fig. 6A). After 4 days of culture, the CSA of cardiomyocytes was measured and the ratios of cardiomyocytes with CSA of 100–200, 200–300, and 300–400 μ m²

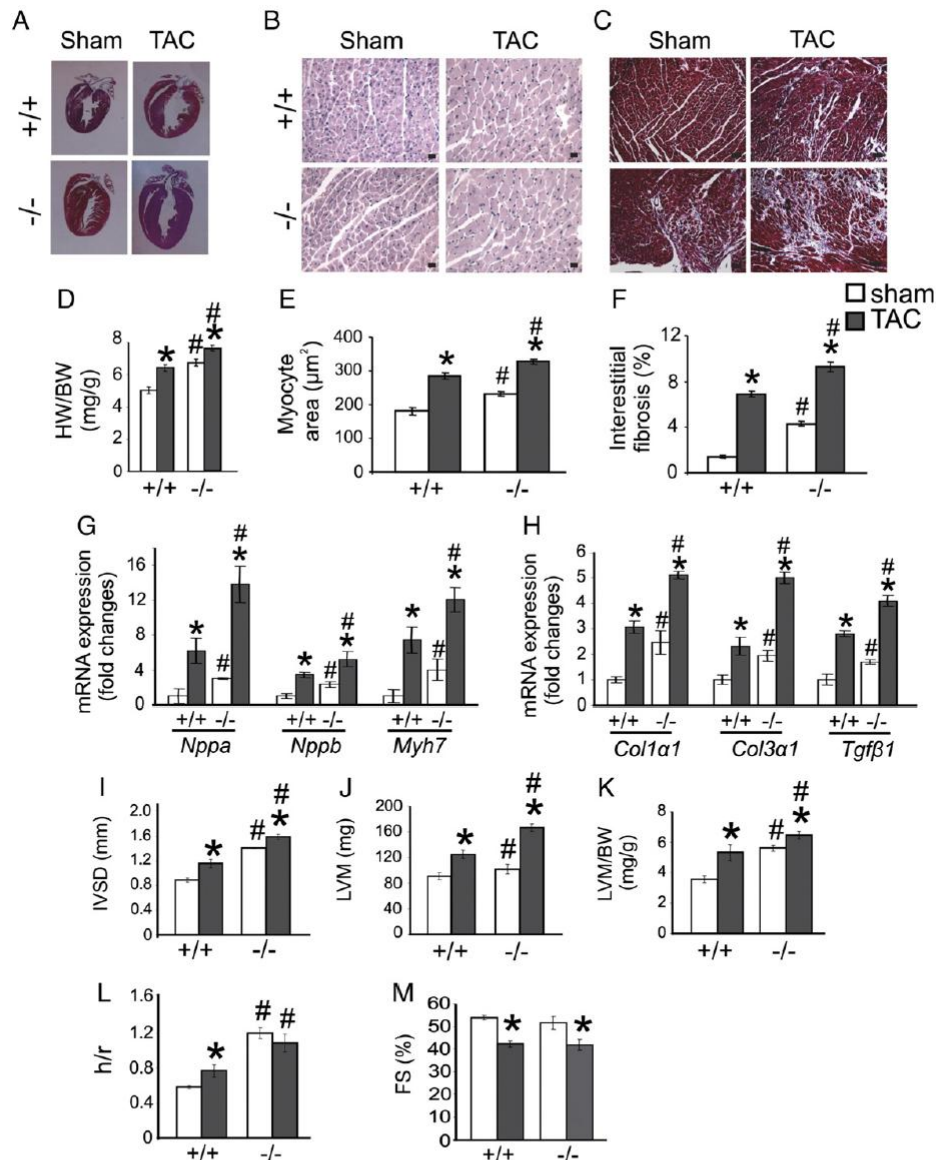


Fig. 3. Aggravation of cardiac hypertrophy and fibrosis in *Hspa4* KO mice after TAC operation. (A) Representative longitudinal sections of hearts from 10-week-old *Hspa4* WT (+/+) and KO (-/-) mice following 2 weeks of sham and TAC surgery. (B, C) H&E- (B) and Masson's trichrome-stained (C) myocardial sections of sham- and TAC-operated WT and KO hearts. Bar = 20 μ m in B; 50 μ m in C. (D–F) Mean HW/BW ratio (D), quantification of mean area of cardiomyocytes (E) and volume of interstitial fibrosis (F) of *Hspa4* WT and KO hearts after 2 weeks of operation. Data were obtained from 4 hearts per group. Data are mean \pm SD. * P < 0.05 versus sham of the same genotype. # P < 0.05 versus WT of the same treatment. (G, H) Quantitative RT-PCR analysis of mRNA levels of hypertrophic marker genes (G) and fibrosis marker genes (H). Expression levels normalized by *Hprt* are presented as mean \pm SD. Transcript levels in hearts of sham WT mice were expressed as 1.0. * P < 0.05 versus sham of the same genotype. # P < 0.05 versus WT of the same treatment, n = 3–4 per genotype. (I–M) Mean echocardiographic parameters of WT and KO mice after 2 week of TAC. (I) Interventricular septum dimension (IVSD); (J) left ventricular mass (LVM); (K) ratios of left ventricular mass to body weight (LVM/BW); (L) ratios of wall thickness to heart radius (h/r) and (M) fractional shortening (FS). Data are mean \pm SEM. * P < 0.05 versus sham of the same genotype. # P < 0.05 versus WT of the same treatment.

were determined. As shown in Fig. 6B, the ratio of cardiomyocytes with a CSA of less than 200 μ m² was significantly lower in cultures of *Hspa4* KO cells than that of WT. In contrast, the ratio of mutant cardiomyocytes with a CSA of more than 300 μ m² was significantly

increased in cultured KO cells compared with WT. The increased size of *Hspa4* KO myocytes in culture suggests strongly that the cardiac hypertrophy of KO mice is a result of primary alterations in cardiomyocytes. At the molecular level, significantly elevated expression levels of

hypertrophic markers, *Nppa* and *Nppb*, were found in neonatal *Hspa4* KO cardiomyocytes (Fig. 6C).

3.7. Differential gene expression in hearts of *Hspa4* KO mice

In an attempt to identify potential molecular targets, which are involved in the initiation of cardiac remodeling, we compared the global gene expression profiles of 3.5-week-old *Hspa4* WT and KO hearts by microarray analysis. We selected 3.5 weeks for generation of RNA because this time largely precedes any pathological manifestations in the deficient heart and therefore secondary alterations are excluded.

The cDNA generated from three independent ventricles isolated from *Hspa4* WT and KO hearts were used to screen Affymetrix Mouse Genome 1.0 ST Arrays. Between both genotypes, approximately 97 sequences were differentially expressed (≥ 1.4 -fold with *P* values of < 0.05 ; Fig. 7A; Suppl. Tables 4 and 5). Notably, results of microarray analysis revealed increased expression of fetal genes, *Nppa*, *Nppb*, *Myh7* and *Acta1* that are associated with the cardiac stress response. Among the differentially expressed genes, several encode for proteins that are involved in ion channel signaling, including the voltage-gated potassium channels *KCNE1* and *KCND2*, the potassium/sodium hyperpolarization-activated cyclic nucleotide-gated channel 1 (*HCN1*), sodium channel-gated, type IV, alpha subunit (*SCN4A*) and leucine glioma inactivation 1 (*LG11*) that regulates the activity of voltage-gated potassium channels [27]. Furthermore, *Hspa4* KO hearts also had significant alterations in expression of transcriptional factors such as iroquois related homeobox 4 (*IRX4*) and *GATA6* [28,29]. Noteworthy, membrane metalloendopeptidase (*MME/NEF*), monoamine oxidase B (*MAOB*) and guanine nucleotide binding protein, alpha O (*GNAO1*) genes known to be involved in molecular pathways related to oxidative response, were also differentially expressed [30–32]. Quantitative RT-PCR was performed to verify changes in the transcription levels of ion channel-related genes and some other differentially expressed genes in hearts of 3.5-week-old *Hspa4* WT and KO mice (Fig. 7B).

Moreover, we verified the expression of some differentially expressed gene by Western blot analysis. Connective tissue growth factor (CTGF) plays an important role in the development of fibrosis in different tissues, including the heart [33]. Adapter molecule *DAB2* (*DOC-2*) inhibits collagen synthesis in cardiac fibroblasts [34]. In the microarray analysis, *Ctgf* mRNA was found to be up-regulated in the *Hspa4* KO hearts (Suppl. Table 4). On the other hand, *Dab2* mRNA was down-regulated (Suppl. Table 5). In agreement with the microarray data, Western blot analyses showed significant increase and decrease in protein levels of CTGF and *DAB2* in *Hspa4* KO hearts, respectively (Fig. 7C).

Further classification of the differentially expressed genes according to the gene ontology illustrated the biggest sector of the differentially expressed genes were those related to the ions transport and binding (38/97), cytoskeleton and structural proteins (32/97), nucleotide binding and transcription related factors (26/97) and nucleotide binding proteins (25/97) (Fig. 7D).

4. Discussion

Under physiological conditions, the heart is constantly subjected to a variety of stresses that progressively increase with age. One way the heart overcomes stress-induced damage is to increase cardiomyocyte size in order to adapt to an increased workload. Increased protein synthesis in hypertrophic cardiomyocytes requires the elevated expression of molecular chaperones to repair misfolded proteins. Failure of molecular chaperones to correctly fold newly synthesized polypeptides might lead to the accumulation of misfolded and damaged proteins, triggering cardiomyocytes to initiate cell death [35]. Enhanced expression of HSPA4 in response to pressure overload suggests that HSPA4 may either be involved in disease progression or plays a protective role against mechanical stress-induced pathological hypertrophy. The induction of

HSPA4 expression in hearts of patients with aortic stenosis provides evidence for a similar function of this protein in human heart. The elevated expression of HSPA4 in response to hypertrophic stress is in line with the expression pattern of some HSPs, which are induced by hypertrophic stimuli [7,36,37].

The cardioprotective effect of HSPA4 is supported by the studies investigating the effects of *Hspa4* deficiency on heart development. Analysis of *Hspa4* KO hearts demonstrates the development of cardiac hypertrophy and fibrosis, characterized by increases in the expression of hypertrophic and fibrosis markers, LVM, IVSD and LVPWT, along with histological changes. In response to pressure-overload, the *Hspa4* KO mice developed a further exaggeration in the degree of cardiac hypertrophy and fibrosis compared with their littermate controls.

The development of hypertrophic cardiomyopathy in KO mice was accompanied by alterations in the activity of numerous signaling pathways involved in the protection of the heart against a variety of stressors. Our results reveal that the transcriptional activity of NFAT and the expression levels of activated CaMKII are significantly elevated in *Hspa4* KO hearts. Both proteins participate in signaling pathways that play critical roles in regulating hypertrophic growth of the heart [38]. Activated NFAT in collaboration with *GATA4* induces the expression of fetal genes [39,40]. Similarly, activated CaMKII promotes MEF2 transcriptional activity, which induces the expression of prohypertrophic genes [41].

The increased activity of gp130-STAT3 signaling in response to extracellular stress was reported to induce myocardial hypertrophy [42,43].

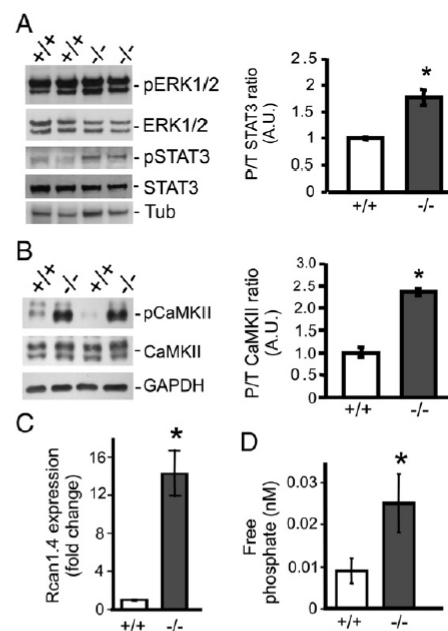


Fig. 4. Effect of *Hspa4* deficiency on the activity of ERK1/2, STAT3, CaMKII, and Calcineurin/NFAT signaling. (A and B) Western blot analysis for the expression of total and phosphorylated ERK1/2, STAT3 (A), and CaMKII (B) in 12-week-old *Hspa4* WT (+/+) and KO (-/-) hearts (left panels). Histograms show relative intensity of phosphorylated to total protein levels of STAT3, ERK1/2, and CaMKII (right panels). α -tubulin (Tub) was used as a loading control. Phosphorylated protein ratio in hearts of WT mice was expressed as 1.0. * $P < 0.05$ vs WT, $n = 3$ animals per genotype. A.U. indicates arbitrary units. (C) Expression levels of *Rcan1.4* mRNA in hearts of 12-week-old mice were determined by qRT-PCR. Values of expression levels normalized to *Sdh* are presented as mean \pm SD. Transcript levels in hearts of WT mice were expressed as 1.0. * $P < 0.05$ vs WT, $n = 3$ animals per genotype. (D) Bar graphs showing calcineurin phosphatase activity in the hearts of 12-week-old mice. Data are expressed as the mean \pm SD, $n = 4$ –6 per group. * $P < 0.05$ vs. WT.

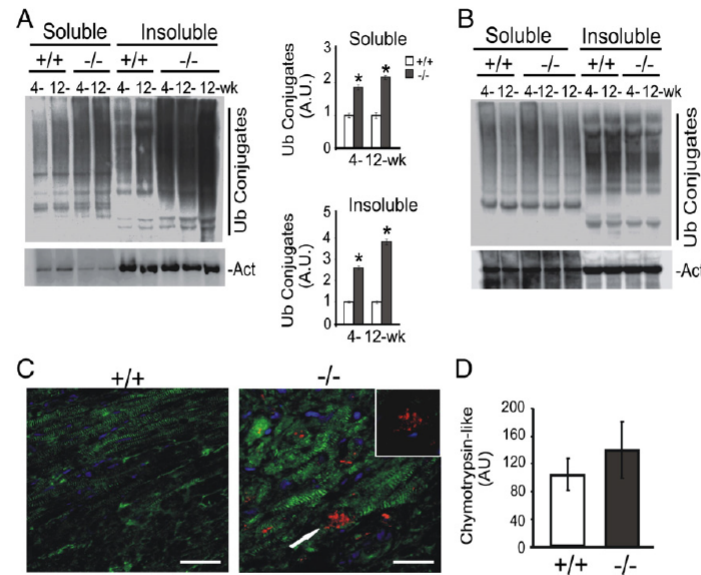


Fig. 5. Increased accumulation of ubiquitinated proteins in *Hspa4* KO hearts. (A) Total ubiquitinated proteins in ventricular soluble and insoluble protein extracts from 4- and 12-week-old *Hspa4* WT (+/+) and KO (-/-) mice were analyzed by immunoblots (left panels). Histograms show relative abundance of ubiquitinated proteins in soluble and insoluble protein extracts (right panels). α -actinin (Act) was used as a loading control. Values are expressed in mean \pm SD. Ubiquitinated proteins in WT samples were expressed as 1.0. * $P < 0.05$ vs WT, $n = 4$ per group. A.U. indicates arbitrary units. (B) Western blot analysis for the expression of ubiquitinated proteins in the skeletal muscles of 4- and 12-week-old *Hspa4* WT and KO. (C) Cryosections of hearts from 12-week-old *Hspa4* WT and KO mice were double immunolabeled for ubiquitin (red) and α -actinin (green). Nuclei were stained blue with DAPI. Inset is the enlarged images of the arrow-pointed area. Bar = 30 μ m. (D) Bar graph showing myocardial chymotrypsin peptidase activities in *Hspa4* WT and KO mice.

In this study, we also show a marked increase in protein levels of phosphorylated STAT3. These results suggest that the gp130-STAT3 signaling also participates in cardiac remodeling in *Hspa4* KO mice. It remains to be determined whether the observed increase in the activity of these prohypertrophic signaling pathways is, on the one hand, the result of the development of cardiac hypertrophy in *Hspa4* KO hearts. On the other hand, it might also result from an increase of misfolded proteins in cardiomyocytes, causing intracellular stress and the activation of stress-induced signaling pathways.

A noteworthy finding of transcriptional profiles is that many genes related to ion channel signaling are differentially expressed in the mutant heart. It remains to be addressed whether the observed alterations in the expression of these genes could lead to electric remodeling in *Hspa4* KO hearts; and further, if this is responsible for development of cardiac hypertrophy.

Protein quality control in the cells facilitates proper folding of nascent proteins and refolding of misfolded proteins by molecular chaperones and promotes degradation of misfolded and aggregated proteins by ubiquitin-proteasome system (UPS). Functional defects in chaperones result in an increase of misfolded proteins with consequent accumulation of polyubiquitinated proteins, which are removed by proteasome [25]. Consistent with this, we have shown increased levels of ubiquitinated proteins in *Hspa4* KO hearts. These results suggest that the depletion of HSPA4 affects the folding capacity of chaperones. Recent reports demonstrated that increased accumulation of misfolded proteins above the threshold level impairs the functional capacity of the proteasome [44]. Overexpression of mutant desmin or α B-crystallin results in accumulation of misfolded proteins which impairs the proteolytic functions of proteasome. Mice of both mutant lines develop cardiac hypertrophy [45,46]. In human heart with dilated or hypertrophic cardiomyopathies, abnormal protein aggregations and accumulation of ubiquitinated proteins are common phenomenon [47,48].

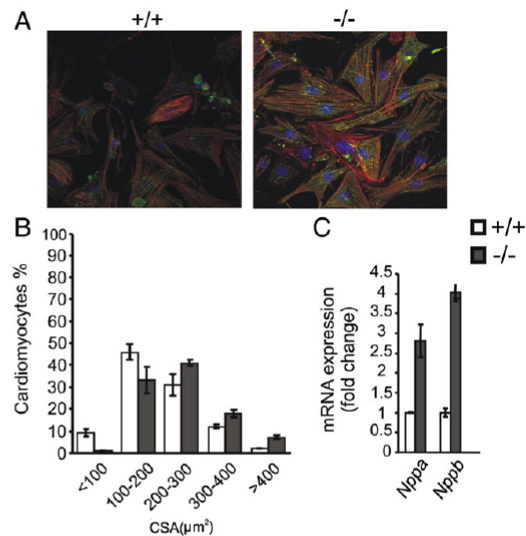


Fig. 6. Neonatal cardiomyocytes of *Hspa4* KO mice display hypertrophic properties. (A) Immunofluorescence analysis of *Hspa4* WT (+/+) and KO (-/-) neonatal cardiomyocyte culture using α -actinin (green) antibody and phalloidin (red). (B) Histogram shows that the ratio of cardiomyocytes with increased CSA in primary culture of neonatal *Hspa4* KO heart is significantly elevated compared with that of WT culture. CSA was measured in cells costained with both α -actinin and phalloidin ($n = 800$ cells per genotype of 2 independent experiments). (C) Expression levels of *Nppa* and *Nppb* in neonatal cardiomyocytes of *Hspa4* WT and KO hearts were determined by qRT-PCR. Values of expression levels normalized by *Hprt* are present as mean \pm SD. Transcript levels in cardiomyocytes of WT mice were expressed as 1.0. * $P < 0.05$ vs WT.

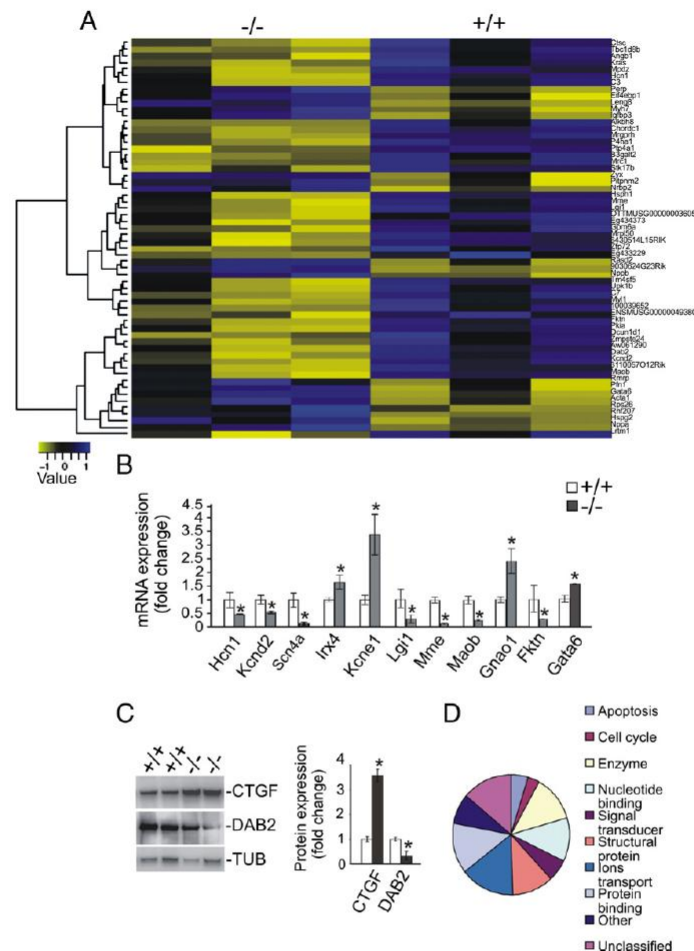


Fig. 7. Assessment of global gene expression in hearts of *Hspa4* KO mice. (A) Heat map of genes showing the significantly altered expression in hearts of 3.5-week-old *Hspa4* WT (+/+) and KO (-/-) mice. Yellow represents increased expression and blue represents diminished expression. (B) Differential expression of the set of genes was validated using qRT-PCR. Values of expression levels normalized by *Sdh* are presented for each gene as mean \pm SD. Transcript levels of each gene in WT hearts were expressed as 1.0. Data are mean \pm SD. * $P < 0.05$ vs WT, $n = 3$ mice/genotype. (C) Western blot analyses for the expression of CTGF and DAB2 in 12-week-old *Hspa4* WT and KO hearts (left panels). Histogram shows relative intensity of CTGF and DAB2 (right panel). α -tubulin (TUB) was used as a loading control. Values are expressed in mean \pm SD. Protein levels in hearts of WT mice samples were expressed as 1.0. * $P < 0.05$ vs control, $n = 4$ per group. (D) Pie diagram illustrating the categorization of differentially expressed genes based on molecular function using Gene Ontology. Note that some genes may have more than one function and be categorized in several groups.

In conclusion, the present study demonstrates that lack of HSPA4 leads to cardiac hypertrophy and fibrosis. Moreover, our data reveal the distinct, non-redundant role of HSPA4 in the protein quality control that maintains the proper protein folding and homeostasis in the cardiomyocytes.

Supplementary data to this article can be found online at <http://dx.doi.org/10.1016/j.jmcc.2012.07.014>.

Disclosures

None declared.

Acknowledgments

B.A.M. was supported by Deutscher Akademischer Austausch Dienst (DAAD) through grant A/07/80490. Dr. Maier (MA 1982/4-1&2-2) is funded by the DFG and by the Foundation Leducq

Transatlantic Network of Excellence on "Redox and Nitrosative Regulation of Cardiac Remodeling: Novel Therapeutic Approaches for Heart Failure" as well as the "Alliance for CaMK Signaling in Heart Disease". Dr. Zimmermann is funded by the DFG (ZI 708/7-1,8-1&10-1) and BMBF (DZHK, 01GN0827, 01GN0957). We are grateful to L. Opitz and G. Salinas-Reister for kindly helping us in Microarray data analysis. We also would like to thank T. Sowa and I. Quentin for their expert technical assistance.

References

- [1] Hartl FU. Molecular chaperones in cellular protein folding. *Nature* 1996;381: 571-9.
- [2] Vos MJ, Hageman J, Carra S, Kampinga HH. Structural and functional diversities between members of the human HSPB, HSPH, HSPA, and DNAJ chaperone families. *Biochemistry* 2008;47:7001-11.
- [3] Dragovic Z, Broadley SA, Shomura Y, Bracher A, Hartl FU. Molecular chaperones of the Hsp110 family act as nucleotide exchange factors of Hsp70s. *EMBO J* 2006;25: 2519-28.

- [4] Ravioli H, Sadlish H, Rodriguez F, Mayer MP, Bukau B. Chaperone network in the yeast cytosol: Hsp110 is revealed as an Hsp70 nucleotide exchange factor. *EMBO J* 2006;25:2510–8.
- [5] Polier S, Dragovic Z, Hartl FU, Bracher A. Structural basis for the cooperation of Hsp70 and Hsp110 chaperones in protein folding. *Cell* 2008;133:1068–79.
- [6] Schuermann JP, Jiang J, Cuellar J, Llorca O, Wang L, Gimenez LE, et al. Structure of the Hsp110:Hsc70 nucleotide exchange machine. *Mol Cell* 2008;31:232–43.
- [7] Kumarapeli AR, Su H, Huang W, Tang M, Zheng H, Horak KM, et al. Alpha B-crystallin suppresses pressure overload cardiac hypertrophy. *Circ Res* 2008;103:1473–82.
- [8] Latchman DS. Heat shock proteins and cardiac protection. *Cardiovasc Res* 2001;51:637–46.
- [9] Kim YK, Suarez J, Hu Y, McDonough PM, Boer C, Dix DJ, et al. Deletion of the inducible 70-kDa heat shock protein genes in mice impairs cardiac contractile function and calcium handling associated with hypertrophy. *Circulation* 2006;113:2589–97.
- [10] Hayashi M, Imanaka-Yoshida K, Yoshida T, Wood M, Feams C, Tataka RJ, et al. A crucial role of mitochondrial Hsp40 in preventing dilated cardiomyopathy. *Nat Med* 2006;12:128–32.
- [11] Norton N, Li D, Rieder MJ, Siegfried JD, Rampersaud E, Züchner S, et al. Genome-wide studies of copy number variation and exome sequencing identify rare variants in BAG3 as a cause of dilated cardiomyopathy. *Am J Hum Genet* 2011;88:273–82.
- [12] Kaneko Y, Kimura T, Kishishita M, Noda Y, Fujita J. Cloning of apg-2 encoding a novel member of heat shock protein 110 family. *Gene* 1997;189:19–24.
- [13] Held T, Barakat AZ, Mohamed BA, Paprotta I, Meinhardt A, Engel W, et al. Heat-shock protein HSPA4 is required for progression of spermatogenesis. *Reproduction* 2011;142:133–44.
- [14] Huke S, Bers DM. Temporal dissociation of frequency-dependent acceleration of relaxation and protein phosphorylation by CAMKII. *J Mol Cell Cardiol* 2007;42:590–9.
- [15] Zimmermann WH, Fink C, Kralisch D, Remmers U, Weil J, Eschenhagen T. Three-dimensional engineered heart tissue from neonatal rat cardiac myocytes. *Biotechnol Bioeng* 2000;68:106–14.
- [16] Müller P, Kazakov A, Semenov A, Böhm M, Laufs U. Pressure-induced cardiac overload induces upregulation of endothelial and myocardial progenitor cells. *Cardiovasc Res* 2008;77:151–9.
- [17] Garcia R, Diebold S. Simple rapid and effective method of producing aorticaval shunts in the rat. *Cardiovasc Res* 1990;24:430–2.
- [18] Peng X, Kraus MS, Wei H, Shen TL, Pariaut R, Alcaraz A, et al. Inactivation of focal adhesion kinase in cardiomyocytes promotes eccentric cardiac hypertrophy and fibrosis in mice. *J Clin Invest* 2006;116:217–27.
- [19] Smyth GK. Linear models and empirical bayes methods for assessing differential expression in microarray experiments. *Stat Appl Genet Mol Biol* 2004;3 (Article 3).
- [20] Gentleman RC, Carey VJ, Bates DM, Bolstad B, Dettling M, Dudoit S, et al. Bioconductor: Open software development for computational biology and bioinformatics. *Genome Biol* 2004;5:R80.
- [21] Benjamini Y, Hochberg Y. Controlling the false discovery rate: A practical and powerful approach to multiple testing. *J R Statist Soc Ser B* 1995;57:289–300.
- [22] Huang da W, Sherman BT, Tan Q, Kir J, Liu D, Bryant D, et al. DAVID Bioinformatics Resources: expanded annotation database and novel algorithms to better extract biology from large gene lists. *Nucleic Acids Res* 2007;35:W169–75.
- [23] Huang da W, Sherman BT, Lempicki RA. Systematic and integrative analysis of large gene lists using DAVID bioinformatics resources. *Nat Protoc* 2009;4:44–57.
- [24] Frey N, Olson EN. Cardiac hypertrophy: the good, the bad, and the ugly. *Annu Rev Physiol* 2003;65:45–79.
- [25] Patterson C. Search and destroy: the role of protein quality control in maintaining cardiac function. *J Mol Cell Cardiol* 2006;40:438–41.
- [26] Glickman MH, Ciechanover A. The Ubiquitin–Proteasome Proteolytic Pathway: Destruction for the Sake of Construction. *Physiol Rev* 2002;82:373–428.
- [27] Schulte U, Thumfart JO, Klöcker N, Sailer CA, Bildl W, Biniossek M, et al. The epilepsy-linked Ig11 protein assembles into presynaptic Kv1 channels and inhibits inactivation by Kvbeta1. *Neuron* 2006;49:697–706.
- [28] He W, Jia Y, Takimoto K. Interaction between transcription factors Iroquois proteins 4 and 5 controls cardiac potassium channel Kv4.2 gene transcription. *Cardiovasc Res* 2009;81:64–71.
- [29] Van Berlo JH, Elrod JW, van den Hoogenhof MM, York AJ, Aronow BJ, Duncan SA, et al. The transcription factor GATA-6 regulates pathological cardiac hypertrophy. *Circ Res* 2010;107:1032–40.
- [30] Wang Z, Yang D, Zhang X, Li T, Li J, Tang Y, et al. Hypoxia-induced down-regulation of neprilysin by histone modification in mouse primary cortical and hippocampal neurons. *PLoS One* 2011;6:e19229.
- [31] Naoi M, Maruyama W, Akao Y, Yi H, Yamaoka Y. Involvement of type A monoamine oxidase in neurodegeneration: regulation of mitochondrial signaling leading to cell death or neuroprotection. *J Neural Transm Suppl* 2006;71:67–77.
- [32] Nishida M, Maruyama Y, Tanaka R, Kontani K, Nagao T, Kurose H. G alpha(i) and G alpha(o) are target proteins of reactive oxygen species. *Nature* 2000;408:492–5.
- [33] Ahmed MS, Øie E, Vinje LE, Yndestad A, Øystein Andersen G, Andersson Y, et al. Connective tissue growth factor: a novel mediator of angiotensin II-stimulated cardiac fibroblast activation in heart failure in rats. *J Mol Cell Cardiol* 2004;36:393–404.
- [34] Kumbar DH, VanBergen A, Ocampo C, Muangmingsuk S, Griffin AJ, Gupta M. Adapter molecule DOC-2 is differentially expressed in pressure and volume overload hypertrophy and inhibits collagen synthesis in cardiac fibroblasts. *J Appl Physiol* 2007;102:2024–32.
- [35] Kumarapeli AR, Wang X. Genetic modification of the heart: chaperones and the cytoskeleton. *J Mol Cell Cardiol* 2004;37:1097–109.
- [36] Osaki J, Haneda T, Kashiwagi Y, Oi S, Fukuzawa J, Sakai H, et al. Pressure-induced expression of heat shock protein 70 mRNA in adult rat heart is coupled both to protein kinase A-dependent and protein kinase C-dependent systems. *J Hypertens* 1998;16:1193–200.
- [37] Kee HJ, Eom GH, Joung H, Shin S, Kim JR, Cho YK, et al. Activation of histone deacetylase 2 by inducible heat shock protein 70 in cardiac hypertrophy. *Circ Res* 2008;103:1259–69.
- [38] Wilkins BJ, Molkentin JD. Calcineurin and cardiac hypertrophy: where have we been? Where are we going? *J Physiol* 2002;541:1–8.
- [39] Molkentin JD, Lu JR, Antos CL, Markham B, Richardson J, Robbins J, et al. A calcineurin-dependent transcriptional pathway for cardiac hypertrophy. *Cell* 1998;93:215–28.
- [40] Olson EN, Williams RS. Calcineurin signaling and muscle remodeling. *Cell* 2000;101:689–92.
- [41] Passier R, Zeng H, Frey N, Naya FJ, Nicol RL, McKinsey TA, et al. CaM kinase signaling induces cardiac hypertrophy and activates the MEF2 transcription factor in vivo. *J Clin Invest* 2000;105:1395–406.
- [42] Kunisada K, Tone E, Fujio Y, Matsui H, Yamauchi-Takahara K, Kishimoto T. Activation of gp130 transduces hypertrophic signals via STAT3 in cardiac myocytes. *Circulation* 1998;98:346–52.
- [43] Kunisada K, Negoro S, Tone E, Funamoto M, Osugi T, Yamada S, et al. Signal transducer and activator of transcription 3 in the heart transduces not only a hypertrophic signal but a protective signal against doxorubicin-induced cardiomyopathy. *Proc Natl Acad Sci USA* 2000;97:315–9.
- [44] Bennett EJ, Bence NF, Jayakumar R, Kopito RR. Global impairment of the ubiquitin–proteasome system by nuclear or cytoplasmic protein aggregates precedes inclusion body formation. *Mol Cell* 2005;17:351–65.
- [45] Liu J, Chen Q, Huang W, Horak KM, Zheng H, Mestrl R, et al. Impairment of the ubiquitin–proteasome system in desminopathy mouse hearts. *FASEB J* 2006;20:362–4.
- [46] Chen Q, Liu JB, Horak KM, Zheng H, Kumarapeli AR, Li J, et al. Intracellular amyloidosis impairs proteolytic function of proteasomes in cardiomyocytes by compromising substrate uptake. *Circ Res* 2005;97:1018–26.
- [47] Heling A, Zimmermann R, Kostin S, Maeno Y, Hein S, Devaux B, et al. Increased expression of cytoskeletal, linkage, and extracellular proteins in failing human myocardium. *Circ Res* 2000;86:846–53.
- [48] Kostin S, Pool L, Elsässer A, Hein S, Drexler HC, Amon E, et al. Myocytes die by multiple mechanisms in failing human hearts. *Circ Res* 2003;92:715–24.

6. List of Publications

- 1) Held T, Barakat AZ, **Mohamed BA**, Paprotta I, Meinhardt A, Engel W, Adham IM (2011): Heat-shock protein HSPA4 is required for progression of spermatogenesis. *Reproduction* 142,133-44
- 2) **Mohamed BA**, Barakat AZ, Zimmermann WH, Bittner RE, Mühlfeld C, Hünlich M, Engel W, Maier LS, Adham IM (2012): Targeted disruption of Hspa4 gene leads to cardiac hypertrophy and fibrosis. *J Mol Cell Cardiol* 53, 459-468
- 3) Burnicka-Turek O*, **Mohamed BA***, Shirneshan K*, Thanasupawat T, Hombach-Klonisch S, Klonisch T, Adham IM (2012): INSL5-Deficient Mice Display an Alteration in Glucose Homeostasis and an Impaired Fertility (*Endocrinology*, In press)
(*) contributed equally to this work

Manuscript in Submission Stage

- 1) **Mohamed BA**, Barakat AZ, Held T, Elkenani MM, Mühlfeld C, Männer J, Adham IM: Simultaneous deletion of *Hspa4l* and *Hspa4* genes causes pulmonary immaturity and early neonatal lethality in mouse

Acknowledgments

To **Prof. Dr. I. M. Adham**, for readily accepting me as a doctoral student in his lab, for closely supervising my thesis through the entire course of my MD study, for helpful comments and insightful conversations, and above all for his constant support such that I could finish my thesis in a “decent” time-frame.

To **Prof. Dr. med. Dr. h. c. Wolfgang Engel**, for taking out his “precious” time to go through my thesis, as well as for those fruitful discussions that lead to the generation of novel ideas, and for encouraging me to participate actively in meetings and seminars, and also for his genuine feedback on various manuscripts.

To **Prof. Dr. W.-H. Zimmermann** for expert guidance and support during the neonatal mice cardiomyocyte culture work as well as for fruitful scientific discussions and suggestions.

To **Prof. Dr. L. S. Maier** for providing us with cardiac samples of human patients with Aortic stenosis, for his help in TAC operation and Echo measurement, as well as for helpful comments.

To **Dr. S. Lutz** for guidance and support during the generation of recombinant Adenovirus work.

To **Xingbo, Christian** and **Dr. Pantakani**, for invaluable help and continuous support throughout the course of my thesis.

To my lab mates and to all my institute colleagues for their friendship, discussions, advices, help.

Curriculum Vitae

I was born in 18.10.1978 as a second child of Mohamed Awd and Nadjia Soliman.

From 1984 till 1994, I visited the Primary and Secondary schools in Mansoura, Egypt. I passed the Secondary school final examination in 1994. From 1994 till 2000, I studied Medicine in the Faculty of Medicine, Mansoura University. In 2000, I got my Bachelor degree in Internal Medicine and General Surgery. From 2001 till 2002, I did training courses as a rotatory internship in the Mansoura University Hospitals. From 2002 till 2003, I did my Military service as a soldier. Since 2003, I studied in the Department of Medical Biochemistry and Molecular Biology as a Demonstrator. In 2006, I finished my Master thesis entitled “Coagulation Profile in chronic liver diseases” and I got my Master degree in the field of Medical Biochemistry and Molecular Biology. From 2006 till now, I am working as an Assistant Lecturer in the Department of Medical Biochemistry and Molecular Biology. In 2008, I got a scholarship from DAAD to do my MD study in Germany. In 2009, I started my MD thesis entitled “The molecular role of the heat shock protein family110 (HSP110)” in the Institute of Human Genetics, University of Göttingen.